PROCESS MONITORING USING A VARIABLE-SPEED DRIVE

Case: Bioproduct mill

Lappeenranta–Lahti University of Technology LUT

Master's Programme in Sustainability Science and Solutions, Master's thesis

2023

Tuomas Anttilainen

Examiners: Professor Risto Soukka

Santeri Pöyhönen, D.Sc. (Tech.)

ABSTRACT

Lappeenranta–Lahti University of Technology LUT

LUT School of Energy Systems

Degree Program in Sustainability Science and Solutions

Tuomas Anttilainen

Process monitoring using a variable-speed drive

Case: Bioproduct mill

Master's thesis

2023

118 pages, 36 figures, and 5 tables

Examiners: Professor Risto Soukka

Santeri Pöyhönen, D.Sc. (Tech.)

Keywords: variable-speed drive, fluid handling, fan, pump, monitoring

Electric motor systems account for more than half of the global electricity consumption. End-use consumption mostly consists of fluid handling systems, which are a major consumer in both the industrial and tertiary sectors. Since a fluid handling systems' life cycle costs and emissions are primarily generated during use, monitoring and ensuring proper operation is vital. Recognizing, and even predicting, phenomena that reduces energy efficiency and increases life cycle costs can make the system operation more economical and sustainable.

This thesis aims to find out the applicability of variable-speed drive monitoring by examining real-life data from a case site. First, a literary review acquaints the reader with the subject by presenting information about the studied industrial fans, VSD monitoring, and the case site. To establish a framework for the case study, the literary review compiles previous studies on VSD-based phenomena monitoring and justifies the used model-based estimation methodology by showcasing their structure and identifying potential accuracy influencing factors. Additionally, the literary review showcases the bioproduct mill operation and its typical fluid handling applications.

The thesis concludes the model-based operation point estimation to be applicable in both the studied systems. Although uncertainty is associated with model-based estimation, they can still be utilized in identifying harmful phenomena from the system. The thesis also discusses, and proposes, potential methods to derive a correction factor to generate estimates with a low relative error compared to realized values. Applicability of VSD-signal-based monitoring could not be evaluated with the received data sets. Therefore, the thesis focuses on outlining the requirements to allow for the applicability testing in future studies.

TIIVISTELMÄ

Lappeenrannan–Lahden teknillinen yliopisto LUT

LUT Energiajärjestelmät

Ympäristötekniikan koulutusohjelma

Tuomas Anttilainen

Prosessin seuranta taajuusmuuttajan avulla

Case: Biotuotetehdas

Ympäristötekniikan diplomityö

2023

118 sivua, 36 kuvaajaa ja 5 taulukkoa

Tarkastajat: Professori Risto Soukka

TkT Santeri Pöyhönen

Avainsanat: taajuusmuuttaja, virtauksen käsittely, puhallin, pumppu, seuranta

Virtausjärjestelmissä käytetyt sähkömoottorijärjestelmät muodostavat suuren osan maailman sähkönkulutuksesta. Koska virtausjärjestelmien elinkaarikustannukset ja -päästöt syntyvät ensisijaisesti käytön aikana, niiden valvonta ja optimaalisen toiminnan varmistaminen ovat tärkeää. Energiatehokkuutta vähentävien sekä elinkaarikustannuksia lisäävien ilmiöiden tunnistaminen, ja ennustaminen, voi tehdä järjestelmien toiminnasta taloudellisempaa ja kestävämpää.

Tämän diplomityön tavoitteena on selvittää taajuusmuuttajapohjaisen valvonnan soveltuvuutta tutkimalla case-tapauksien dataa. Kirjallisuuskatsaus tutustuttaa lukijan aiheeseen esittämällä tietoa teollisista puhaltimista, taajuusmuuttajavalvonnasta sekä case-kohteesta. Case-tutkimuksen rakenteen luomiseksi kirjallisuuskatsauksessa kootaan aiempia tutkimuksia taajuusmuuttajapohjaisesta ilmiöiden seurannasta ja perustellaan valitun mallipohjaisen estimointimenetelmän käyttöä esittelemällä sen rakennetta sekä tunnistamalla mahdollisia tarkkuuteen vaikuttavia tekijöitä.

Diplomityössä havaittiin mallipohjaisen toimintapiste-estimoinnin soveltuvan molempiin case-tapauksiin. Vaikka mallipohjaiseen estimointiin liittyy epävarmuutta, niitä voidaan silti hyödyntää haitallisten ilmiöiden tunnistamisessa. Diplomityössä tarkastellaan sekä ehdotetaan mahdollisia menetelmiä myös arvojen eroavaisuuksien vähentämiseksi. Taajuusmuuttajasignaalipohjaisen valvonnan soveltuvuuden kokeilemista ei voitu suorittaa käsitellyillä dataseteillä. Tämän takia diplomityössä keskitytään hahmottamaan vaatimukset soveltuvuuskokeilun mahdollistamiseksi tulevissa tutkimuksissa.

ACKNOWLEDGEMENTS

I am thankful for everyone at ABB for providing me this opportunity to conduct this thesis.

A special thank you to Santeri Pöyhönen and Markku Niemelä, who guided me greatly throughout the thesis, for providing your expertise, insights, and support. Additionally, my sincerest thank you to Risto Soukka for approving this thesis for examination, as well as providing great guidance regarding the structure and content of the thesis. Also, a huge thank you to Simo Hammo for the ideas and assistance through the writing process, and Heikki Kervinen for evoking my interest in this field. A warm thank you also to the contact persons who had the time to respond to my inquiries about the studied industrial cases, while supplying me the relevant data for the thesis.

I am incredibly grateful for all the unwavering support my parents and family have given me throughout the years, thank you. Similarly, a thank you to all my friends for being you.

Lappeenranta, April 14th, 2023

Tuomas Anttilainen

SYMBOLS AND ABBREVIATIONS

Roman characters

á	Overall	
e	Specific energy consumption	[kWh/Nm^3]
E	Energy	[kWh]
f	Frequency	[Hz]
L	Length	[µm, cm]
n	Rotational speed	[rpm]
N	Adjusted rotational speed	[rpm]
p	Pressure	[Pa, kPa, mbar]
P	Power	[W, kW]
Q	Flow rate	[Nm^3/s]
R	Specific gas constant	[J/(kg·K)]
T	Temperature	[K, °C]

Greek characters

π	Pi	
Π	Adjusted rotational speed	[rpm]
ρ	Density	[µg/Nm^3, g/Nm^3, kg/Nm^3]
τ	Torque	[% of Nominal]

Subscripts

% of Nom.	Percentage of nominal value

0	Curve value
actual	System definition value
curve	Curve definition value
d	Dry gas
est.	Estimated
eq.	Equivalent
f	Fan
meas.	Measured
Nom.	Nominal value
v	Water vapour
VSD	Variable-speed drive

Abbreviations

ADt	Air Dried Tonnes
ASME	American Society of Mechanical Engineering
CNCG	Concentrated Non-Condensable Gases
DNCG	Diluted Non-Condensable Gases
DTC	Direct Torque Control
EPA	United States Environmental Protection Agency
ESP	Electrostatic Precipitator
HVAC	Heating, Ventilation, and Air Conditioning
IEC	International Electrotechnical Commission
IPCC	Intergovernmental Panel on Climate Change
ISO	International Organization for Standardization

LCC	Life Cycle Costs
NCG	Non-Condensable Gases
PWM	Pulse Width Modulation
TRS	Total Reduced Sulphur
VSD	Variable-Speed Drive
VOC	Volatile Organic Compounds

Compounds

CO_2	Carbon dioxide
CO	Carbon monoxide
$CaCO_3$	Calcium carbonate
CaO	Calcium oxide
H_2S	Hydrogen sulphide
H_2SO_4	Sulfuric acid
NaCl	Sodium chloride
HCl	Hydrochloric acid
NaOH	Sodium hydroxide
Na_2S	Sodium sulphide
NO_x	Nitrogen oxides
SO_2	Sulphur oxide

Table of contents

1. Introduction

Human activities, mainly in form of greenhouse gas emissions, have undeniably contributed to climate change, making the Earth's surface temperature 1.1°C higher in 2011–2020 than in the pre-industrial era. Greenhouse gas emissions have constantly increased globally, due to the present, and past, unsustainable energy consumption, land use, lifestyles, consumption, and production patterns in different regions. (IPCC 2023, 4.) Human-caused climate change has generated key climatic changes, which include changes in precipitation, rising sea level, and extreme temperatures (FCCC 2021, 30). These weather and climate extremes already impact all regions around the world. This has led to various harmful effects, along with associated loss and damage to environment and human life. (IPCC 2023, 5.) Today's climate discussion is largely guided by the Paris Climate Agreement, which was ratified in 2016. Its main target is to limit the global average temperature increase to well below 2°C above pre-industrial levels and support endeavours to restrict the temperature increase to 1.5°C above pre-industrial levels. (United Nations 2015, 3.) Still, according to the Intergovernmental Panel on Climate Change (IPCC), the warming level will exceed 1.5°C during the 21st century. To mitigate the effects of climate change and restrain the rising temperatures, immediate reduction of emissions caused by human activity on a global scale is necessary. (IPCC 2023, 10.) According to the United Nations (2022), to curb warming to the 1.5°C, global emissions must decrease by 45 percent by 2030, and reach net zero by 2050.

Objectives at international and regional levels, especially in terms of reducing energy consumption related emissions, as well as increasing the support and transparency of climate actions, have been developed and implemented to reach these targets. (IPCC 2023, 10.) Decarbonizing the energy system and utilizing renewable energy sources are often in the center of attention in this process. For instance, the 2030 European Union’s climate and energy framework obliges all member countries to reduce their greenhouse gas emissions by at least 40% (from the country’s 1990 level), and to utilize at least 32% renewable energy in the total energy generation. (European Commission 2021.) Additionally, member countries can have their own, more ambitious, targets as well. For example, Finland that aims to

decrease its greenhouse gas emissions by 60% by 2030, while aiming for a 95% decrease by 2050. All the values are compared to the level of 1990. Finland also seeks to be carbon neutral by 2035 at the latest. (Ministry of Environment, 2021.)

In addition to these energy source related targets, the European Union obligates all members to also attain at least a 32.5% improvement in energy efficiency by 2030, from the level of 1990. Although transitioning to renewable energy sources reduces the generated emissions, it does not automatically impact the energy consumption. This can be achieved by reducing energy demand by improved energy efficiency. (European Commission 2021.) Along with the legislative motivations, improving energy efficiency generates a variety of benefits, such as reallocation public of budgets, local air pollution reduction, and well-being improvements, thus being dubbed as the first fuel in climate change control. (IEA 2014, 28–31.) Energy efficiency is crucial in controlling energy demand, especially during the early stages of the energy system transformation, when other mitigation strategies are still being established (Almeida et al. 2023, 1).

Electric motor systems are one of the most important technologies whose energy efficiency has improved substantially in recent decades. According to a report by International Energy Agency (2016, 298), electric motors accounted for 53% of the global total final electricity consumption in 2014. This percentage has been since cited by multiple authors. For example, according to Almeida et al. (2023, 1–2), global electricity consumption of electric motor systems in 2016 was 12 100 TWh, which corresponded to 6 gigatonnes of $CO_{2eq.}$ emissions. In 2019, electric motors accounted for about 70% of industrial electricity consumption (6700 TWh), while also being a large consumer in the service sector (more than 40%). The high level of energy consumption means that even a small increase in efficiency can amount to significant absolute savings. Hence, improving the deployment of energy efficient motor systems can be deemed to be notable in achieving the internationally set climate goals. The following figure 1 compiles these global electricity consumption values for 2019.

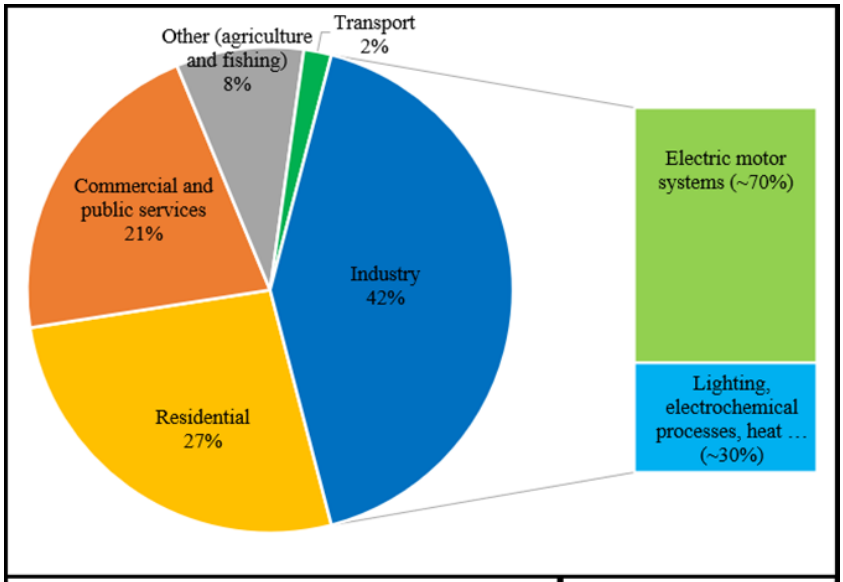

Industry	9566 TWh
Residential	6072 TWh
Commercial and public services	4849 TWh
Other (agriculture and fishing)	1940 TWh
Transport	420 TWh
Total (2019):	22847 TWh

Figure 1. Global electricity consumption in 2019, with industrial electricity categorized to two categories (Almeida et al. 2023, 2, and IEA 2022).

Electric motor systems are utilized in a variety of applications across all municipal, service, and industrial processes. Most substantial of them are fluid handling systems. In this thesis, the terms fluid handling systems, and device, refer to pump, fan, and compressor applications. They are often crucial in ensuring proper operation of the system and contribute a significant portion of the total electricity consumption of electric motor system. Almeida et al. (2003, 564) concludes, as shown in the figure 2 below, fluid handling systems accounted for 56% of the electric motor system electricity consumption in the industrial sector. In the service sector, fans and pumps are responsible for 40% electric motor system electricity consumption.

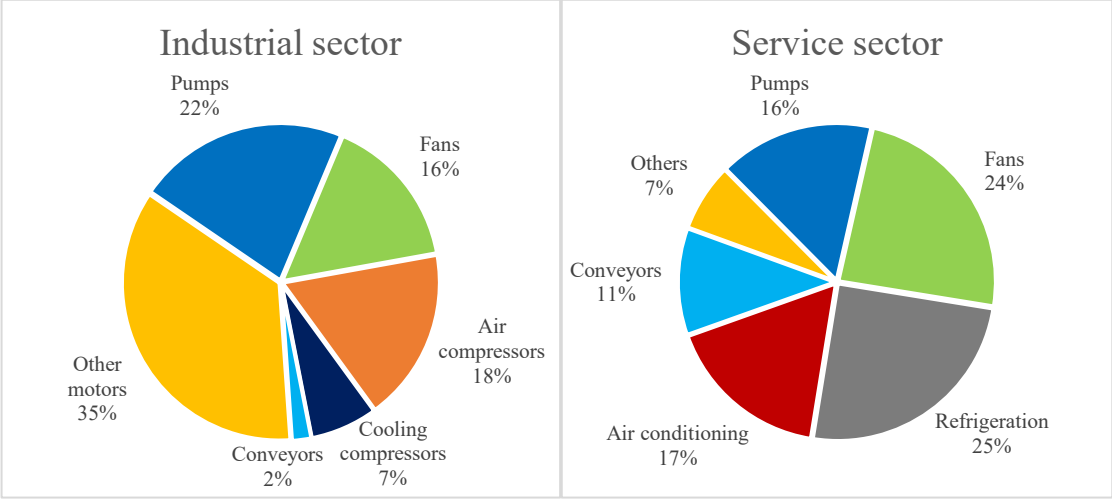

Figure 2. Electric motor system electricity consumption by end-use category, in the industrial and service sectors (Almeida et al. 2003, 564).

Majority of fluid handling system related life cycle costs (LCC) stem from the energy costs. Additionally, production losses and maintenance costs caused by failures influences the LCC. Therefore, reducing and predicting the energy consumption and failure rate can decrease the LCC. (Tamminen 2013, 16.) LCC includes all expenses occurred during a product's life cycle from the initial investment costs to the decommissioning costs (Grundfos 2023). Fluid handling systems often operate as a part of a process which possesses fluctuating loads; thus, the flow requires regulation. The flow can be controlled by restricting it via a damper or valves. Although they possess low investment costs, they are a rather inefficient long-term control method, since restricting the flow results in the system constantly wasting energy to work against the loses generated by them. Another way is to utilize a variable-speed drive (VSD) to adjust the operation point to a desired value by altering the rotational speed of the of fluid handling device. Instead of throttling with control valves, variable-speed drives are increasingly applied to regulate the flow. The use of a VSD allows the adoption of a new pump or blower operating point by changing the rotational speed of the device. (Process Barron 2016.) VSD utilization can help to reach considerable reductions in the LLC. By using a VSD for pumps and fans, a 20 percent reduction in motor speed can decrease the required power by up to 50 percent. Additionally, VSD use can make the process more efficient, and help to better allocate employees' time by, for example, reducing the time spent on manually opening and closing dampers. (ABB 2023.)

Gradual technological development and increasing demand in various industrial sectors often increases their capacity over time, the pulp industry examined in the thesis being one of them. The industry has advanced in leaps and bounds during the last half century since many limiting factors, like recovery boiler capacity which was the main limiting factor until the 1990s, have been overcome. Typical pulp line capacities have increased from the 100 000 ADt/a (air dried tonnes per year) of the 1960s, to the latest bioproduct mills being capable of generating over 1.5 million ADt/a. (Salmenoja 2019, 2 and Metsä Group 2023.) Processes of bioproduct mills require a lot of regulation and numerous applications for fluid handling systems can be found. Fluid handling systems function as part of the mill in accordance with the needs of the unit processes. Examples of these are showcased in the subchapter 3.2.

While regulating the process could be conducted via damping, it would not be an energy efficient nor cost effective decision. Instead, the process control is nowadays conducted via VSDs. For instance, introduction of a VSD in a Swedish cardboard mill attained 80% annual energy savings. This generated the VSD a payback period of less than two years. (ABB 2023.) While the main function a VSD to control the rotational speed of a motor, research (Tamminen et al. 2012, Tamminen 2013, Pöyhönen et al. 2021) has demonstrated the usability of VSDs in process monitoring and estimation. Studies have concluded the VSD signals to be sufficiently precise in calculating motor's rotational speed and torque which enables defining the operation point of a fluid handling device though calculations. Information on the operation point can subsequently be applied in detecting different phenomena or calculating system related values, like specific energy consumption.

1.1 Objective of the thesis

In various industrial fluid handling systems, process monitoring is at the heart of ensuring energy efficiency and reliability. The monitoring is mainly done by installing physical instruments, which measures or calculates a certain quantity, or applying model-based

estimations, which makes use of different mathematical models alongside with the process information calculated by a VSD. This master thesis focuses on gaining insight on the latter.

The literary review investigates the case site operation and validates the monitoring method utilization by showcasing relevant theory and examining previous examples of cases where monitoring had been proven applicable. In the case study, real-life data, acquired from industry contacts, is utilized to generate estimations used to monitor the system behaviour.

The aim is to find out the applicability of the model-based estimations as a process monitoring method. Additionally, thesis studies the applicability of using a VSD to monitor and recognize different phenomena. Potential causes of unreliability or inaccuracy of related calculations are discussed. Observations about the studied case data sets are presented and unusual activity visible in the data is reviewed. Based on the case study results, the thesis presents an opinion on whether if monitoring various phenomena could be utilized at these types of sites. Additionally, feasibility of applying these methods in other similar applications is considered. These results can then be utilized to justify certain simplifications and decisions in future research.

Research questions can be formulated as follows:

1. Are model-based estimations an applicable process monitoring method in the studied industrial case or similar systems?

2. Can VSD signals be utilized to monitor and recognize different phenomena in the studied industrial case or similar systems?

1.2 Outline of the thesis

A literary review is conducted as the first part of this thesis. Its first chapter lays a foundation for the model-based fan operation estimation. VSD electrical operation is discussed only superficially as the chapter's focus is more on the VSD monitoring. Previous research on

VSD-based phenomena monitoring is showcased and compiled. The second subchapter takes a more in-depth look into the types, characteristics, and operation of industrial fans, which are the analysed fluid handling device of the empirical case part. Finally, the utilization of the estimation methods is justified by showcasing their structure and identifying factors that potentially influence their accuracy. The second literary review chapter describes the studied case by presenting an overview of a bioproduct mill. Since the data utilized in the empirical case study chapter was acquired from a bioproduct mill, a review of the practices is in place. Initially, the mill operations and unit processes are showcased. The following subchapter showcases typical fluid handling applications of a bioproduct mill. Common applications, magnitude of their power, and energy consumption values are discussed.

The second part of the thesis is the empirical case study. Two different applications, flue gas and odorous gas treatment fans, are analysed. The surrounding system and received data sets of both applications are described in their own subchapters. The estimations are presented and the applicability of model-based monitoring in these cases is reviewed. Review about the estimations is provided, for example if distinguishing potential phenomena, such as leaks and unknown excess flow or restraints, can be conducted via the estimations.

Conclusions are drawn from the empirical case study and presented in the third part of the thesis. The sections discuss the applicability of the model-based monitoring for these cases, the possibility of utilizing these VSD-based methods in other similar applications, and potential recommendations for future studies, for example. Last, the summary chapter concludes the thesis while giving a brief overview of the main points.

2. VSD-signal-based estimation

In this thesis, operation point estimation calculations are conducted with signals provided by the VSD, manufacturer-provided fan information, and real-life measurement data. Operation point refers to the relation between the pressure or power of the fluid handling device and achieved flow rate. The operation point is affected by two key components: rotational speed of the motor, and flow restrictions in the surrounding system. Flow can be restricted in the system, for instance by damping, to achieve a desired flow rate. The same effect can be achieved by adjusting the rotation speed. Keeping the rotational speed constant while changing the flow restrictions generates a device curve, which is depending on the device often referred to as fan or pump curves. In the following figure 3, they are represented by the dark blue, light blue, grey, and orange curves. An operation where the rotational speed changed, and system restrictions remain unchanged, produces the system curve. In the figure 3, system curves are represented with purple, green, and yellow curves. The operation point is found in the intersection of these two curves, which the following figure 3 showcases with two example curves. (Robinson 2018, 31.)

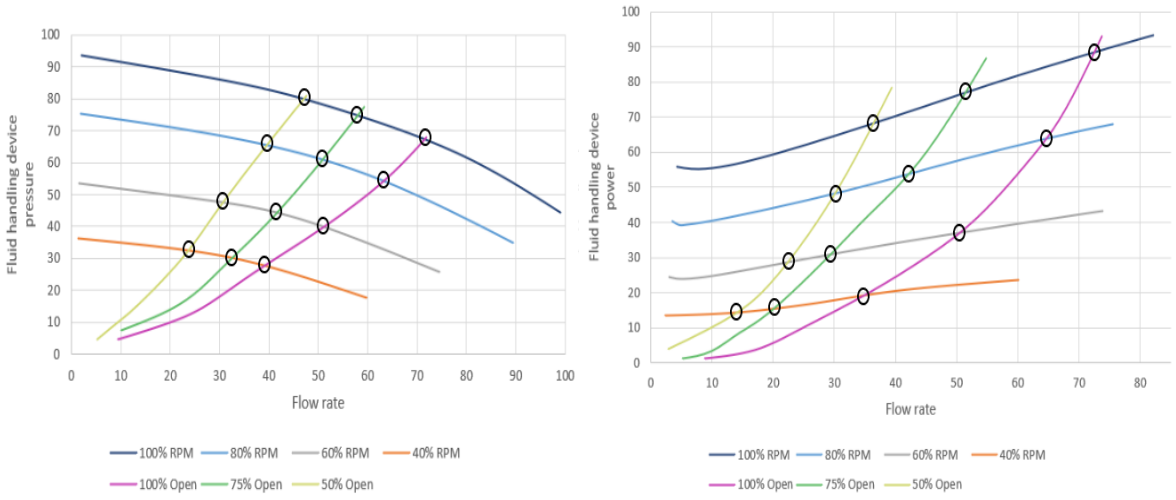

Figure 3. Operation points, depicted with circles, are located at the intersection of the system and fan curves.

For example, if a flow rate of 55 is desired in a system like the one depicted in the figure 3, an operator could reach it by throttling the system to 75% and setting rotational speed to

close to 90% of nominal speed. But as seen in the rightmost figure, this would require more power than a fully open system, running at 60% of the nominal speed. Benefits of rotational speed control provided by a VSD are showcased in the following subchapter. It is important to note that the figure 3 afore is only an example aiming to offer the reader the overall picture of the operation point definition, instead of reflecting real behaviour of a particular fluid handling device.

The following subchapters provide information on the VSD and its utilization as a flow controlling and monitoring device. The prevalence and reasons for the VSD use in different industries are examined. Phenomena in fluid handling systems that could be monitored using a VSD are identified. The later subchapter takes a closer look into the industrial fan operations. This is done to gain insight on them to better understand the systems analysed in the case study chapter. After this, the model-based operation point estimation utilized in this thesis is showcased. Formulae and uncertainties associated to them are presented in their own subchapters.

2.1 Variable-speed drives

In fan, pump, and compressors systems, VSDs are utilized to control the rotational speed of the fluid handling device. A VSD is positioned between the electricity grid and the motor (ABB 2022), from where it can influence the magnetising flux and torque of the motor. It conducts calculations based on the signals it receives to produce information, which can then be used to monitor or control the system. (ABB 2011, 14.)

VSD implementation can help to reach major savings in operational costs as the motor's speed and torque can be accurately matched with the system requirements. This reduces the electricity consumption, which allows for energy savings and faster investment payback. Matching the system's needs can also decrease the need for operating in conditions that can damage the different parts and equipment. This can extend the system's service life, lower the ambient noise levels, reduce the need for maintenance, and shorten the consequent

downtime. (ABB 2022.) Energy consumption is alluded to account for around 90 percent of a motor life cycle carbon footprint. (Zawya 2023.)

Since VSD investment costs have dropped considerably, knowledge of the field has increased along with government assistance programs, VSD implementation has been on the rise. A detailed assessment report from 2021 about the United States industrial and commercial motor system market by Rao et al. (2021) suggests that the implementation of VSDs is highly dependent on the industry and its scale. According to the study, only 16% of the industrial motor system capacity utilizes a VSD, while 74% of them have no load control technology installed, and 10% utilizes other methods, such as dampers or inlet vanes. VSD implementation varies throughout different industries. Beverage, chemical, plastic, and rubber production are examples of industries where VSD use is higher than average, 31–37 percent. Primary metal and non-metallic mineral handling are industries where VSD applications are not common, only 7 to 8 percent of facilities use them. Also as mentioned before, the scale of the operation can affect the VSD integration rate. According to the study, the VSD implementation rate in small facilities is about half of the industrial average, while in medium and large-scale productions it is a little bit higher than the average. (Rao 2021, 84–86.) These differences between industries could be explained by nature of the operations. In industries with constant outputs and rarely changing operation conditions, it can be determined that motor usage in an on/off manner is sufficient, thus a VSD is deemed to be unnecessary. Also, the location of the data set collection can influence the results. Low energy prices discourage facilities from investing on energy efficiency improvements. But still, the preceding assessment from 2002 concluded that only 9% of industrial motor systems in the United States utilized a VSD. This demonstrates that the number is steadily rising in that region as well. (Rao 2021, 116.)

In an interview conducted in 2023, Ahmed Hassan, ABB's Motion Business Area Manager for Egypt, North & Central Africa, evaluates that 23% of motors in-use today are linked with a VSD (Zawya 2023). This number is expected to rise globally as stakeholder consciousness of the potential benefits of VSDs increases. Already in 2011, VSD was technology being introduced in 30–40 percent of all newly installed motors. (Lendenmann et al. 2011, 1.)

Variable-speed drive technology has undergone multiple years of research and development optimizing its operation and reliability. Since this thesis is not a technical study of the technology, the technology development and history are not explored in this study. Instead, the following subchapters focus on VSD as a monitoring device, model-based estimations, and the uncertainties related to them.

2.1.1 Variable-speed drive as a monitoring device

The primary task of a VSD is to control the rotational speed, and consequently fluid system. Traditionally, different devices are implemented in the system to measure aspects like pressure, temperature, and flow rate. These quantities can be employed in calculating the system output, which can then be used in determining the system's energy efficiency. Modern VSD technology estimates the motor shaft's torque and rotational speed (ABB 2011, 14). This information can then be used further calculations, which can provide information about the system without additional metering. However, it is important to note that all the methods may not be suitable or adequately accurate in the whole operation range of the fluid handling device. (Tamminen et al. 2014, 1.)

The calculations can also be used to recognize and minimize phenomena that could affect the operation conditions negatively, such as fan surge (Tamminen et al. 2012) or impeller contamination build-up (Tamminen 2013). In this thesis, these calculation methods are referred to as VSD-based. For example, detection of fan impeller contamination build-up in fan systems, pictured in figure 4, and the consequent fan imbalance it can cause, is traditionally conducted by vibration measurements. If the vibrations increase to high enough level, an impromptu pause in the process maybe required. The study by Tamminen (2013) presents a VSD-based method which can be used to identify the contamination build-up on the fan impeller before it causes an imbalance. Information is gathered during a start-up where the impeller is known to be clean. Those values are then compared with a regular start up during use. If certain limit values are reached, impeller cleaning must take place to avoid utilizing a too fouled system. This information can then be applied to match the fan

maintenance in accordance with other events in the location. (Tamminen 2013, 57–59.) Similar to stalling, a fan surge is a phenomenon in which the fluid flow through the fan impeller is not sufficient, causing the flow to detach from the impeller blade surfaces. This leads to substantial swings in the fan pressure and flow outputs. Typically, the surges are detected via monitoring the pressure and its fluctuation with additional measurement instrumentation. The fan surge causes fluctuation in the power requirement of the fan which can be detected without additional instrumentation. (Tamminen et al. 2012, 2.) The study by Tamminen et al. (2012) demonstrates and concludes that a VSD-based surge detection is possible, and it produces similar results as methods based on physical metering. The method is based on comparison of the low-frequency fluctuation of the torque and speed estimates. First, a steady state run is conducted, where fan is operated with a constant speed and torque. The generated values are the compared with the values generated during use. (Tamminen et al. 2012, 3.)

Since the flow direction in centrifugal fan and pump application does not depend on the rotational direction of the impeller, the system can be operated while rotating the impeller in a reverse direction. While it does not prevent the system from working, rotation direction has a detrimental effect on the efficiency and outputs of the system. The impeller blades, system housing, and outlet are often designed for only one direction of rotation, which results in losses. (Tamminen 2013, 61.) A patent showcased by Tamminen (2013) predicts the fan or pump rotation direction by using the VSD-signal-based torque and rotational speed estimates to calculate their low-frequency fluctuation and deduce the rotation direction. The centrifugal fan or a pump is rotated in both directions, after which the calculated values are compared. The method can determine the rotational direction correctly in most cases, regardless of whether the application is a pump or a fan. (Tamminen 2013, 62–63.)

VSDs are also a great tool at detecting other events. Cavitation is a phenomenon where small vapour-filled cavities are generated in the handled liquid resulting from a static pressure drop in the liquid. Cavitation causes considerable erosion of the impeller blades, erratic flow rate changes, reduced the efficiency, and additional noise. (Britannica 2023.) Erosion of the impeller is showcased in the following figure 4. Ahonen (2011) presents a novel method for

cavitation detection with a VSD. In the method, typical operation values are first determined in conditions where system is pumping without cavitation. Root mean square formulae are used to determine the time-domain variations of the VSD-provided rotational speed and torque estimate values. Then the pump is operated, and the scale of the variation is compared with the scale calculated for conditions where cavitation is absent. If the time-domain values exceed the reference values, cavitation may occur during operation. (Ahonen et al. 2017, 5–6.)

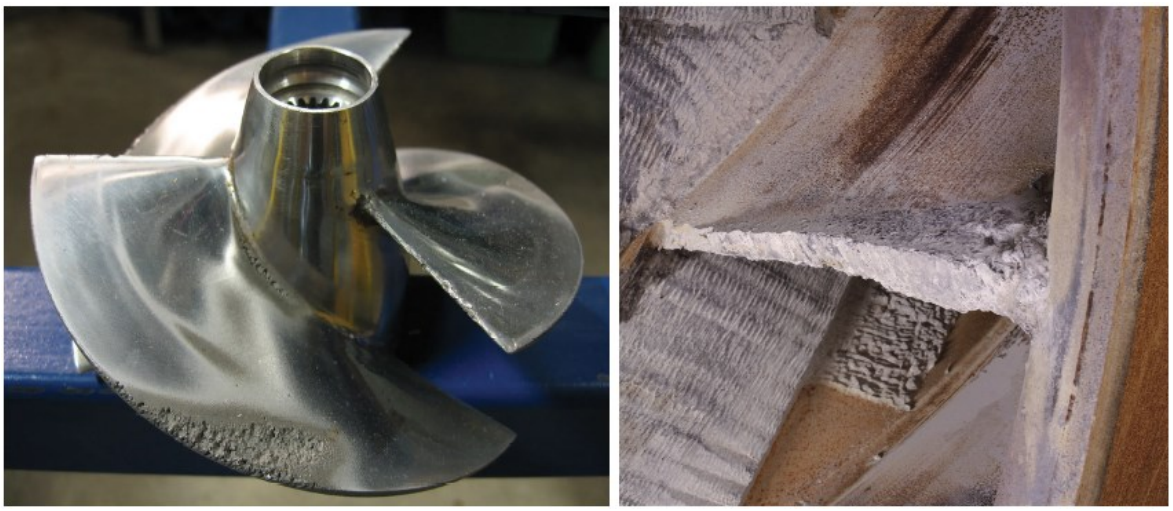

Figure 4. From the left: pump impeller with cavitation damage and fan impeller used in the cement industry, with critical wear and particle accumulation (Britannica 2023 and Venti Oelde 2023a).

Operation point can be utilized in calculating several system parameters, such as specific energy consumption, which can be used in assessing the operation efficiency. Traditionally, the system operation point is obtained with physical instruments measuring flow rate and pressure. But all systems do not have this type of instrumentation installed, or it cannot be installed. Also, they can malfunction or be replaced at certain intervals, which might make them not be able to provide constant measurements. (Tamminen 2013, 31.) The operation point can also be estimated via the VSD-provided signals. One of the methods to conduct this is model-based estimation. In it, manufacturer's curves of the fluid handling device characteristics are used to model the application. Those values used in conjunction with the VSD-estimated rotational speed and shaft power values can be utilized to estimate the

operation point. (Tamminen 2013, 25.) One method of model-based operation point estimation is explained in more detail in the following subchapter 2.3.

Reviewing the operation point estimate made using a VSD in conjunction with physical instrumentation can also be effective in locating different malfunctions in the system. For example, if the values differ greatly from each other, this could indicate that the system has a leak or the fluid is directed to a wrong place, or if there is excess flow, fluid is flowing to an unwanted direction, i.e., back to the ductwork. Operation point estimation by itself can also be indicative of many phenomena. Some components, like a heat exchanger or a cleaner, could have started to dirty, which can then generate pressure losses or gas flow restrictions thus causing the operation point to steadily change. Functions preceding the fluid handling device might also not work as expected. For example, the prior combustion process behaves differently causing the cleaner or heat exchanger to perform poorly that affects the system operation.

VSDs can also be utilized in detecting fouling of the system. Fouling refers to the accumulation of undesirable material on a surface (Shah and Dušan 2003, 863). Fouling of filters, heat exchangers, and other components increases the pressure loss of the system. Pöyhönen et al. (2021) presents a method to optimize air filter replacement schedule via a VSD. Utilizing the VSD signals and manufacturer-provided curves, pressure loss of the system can be calculated to model the effects fouling has over time. This information can then be used to cost effectively replace the system filters when the pressure drop has not become too high, but the filter is not replaced while it is still in working order. (Pöyhönen et al. 2021, 2–3.) Fouling increases the flow resistance in the system in form of added friction resistance, and in worst cases it can prevent the fluid flow altogether. In friction type resistance, the resistance increases as the momentum transfer to the ducting rises. Other type of flow resistance includes local resistances that are generated when the direction of flow changes abruptly, causing vortexes and non-laminar flow, for example. This type of flow resistance is often generated by adapters, nozzles, and other components, but can be intensified by additional friction resistance generated by accumulation of material on the

surfaces. (Kurganov and Ibragimov 2011.) Flow rate restrictions influence the system characteristics and power requirements, which can be recognized from the VSD signals.

Estimations conducted based on VSD signals are a viable alternative in systems where traditional measurements are prone to break, malfunction, or produce unreliable results. Moving away from physical metering can also reduce LCC, as the related investment and maintenance costs can be circumvented. But utilization of VSD-based monitoring does not mean that traditional measuring devices could not be used. Especially if metering infrastructure already exists, utilization of multiple monitoring methods in conjunction with each other can corroborate the achieved results, and verify their applicability, or non-applicability. (Tamminen et al. 2014, 1.) This is a great technique to create redundancy in the system. VSD continues to provide information independent from the physical instrumentation, which ensures reliable monitoring even if a measuring device malfunctions. The following table 1 lists the discussed fluid handling system VSD monitoring applications.

Table 1. VSD monitoring applications of fluid handling systems.

Fluid handling system monitoring application enabled by VSDs

Phenomena monitoring via standalone calculations:
Fan surge
Cavitation
Fan or pump rotation direction
Impeller contamination build-up

Phenomena monitoring via operation point monitoring:
Specific energy consumption
Leakage or surplus flow
Fouling

2.2 Fan operation

Fan systems are utilized in most industrial and municipal applications to circulate fluid in a gaseous form. In municipal applications, they are frequently utilized in heating, ventilation,

and air conditioning (HVAC) purposes to control factors, like temperature and humidity of an enclosed area. In industry, they can be utilized to move generated gases, like flue gas, transfer process heat, or to maintain pressure in the process. According to a review study of the European Commission's Ecodesign regulation, in 2015, industrial fans used up to 300 TWh of electricity annually. This made it the third largest electricity consumer, within the current Ecodesign scope, after industrial motors and lighting sources. (Van Holsteijn en Kemna B.V. 2015, 7). It was also cited that fans account for 11% of industrial sector's and 9% of service sector's total electricity consumption in the European Union. (Almeida et al. 2003, 563–564.)

While some studies use the words fan and blower interchangeably, the American Society of Mechanical Engineering (ASME) has presented commonly accepted definition for fans and blowers, which distinguishes the devices with the ratio of the discharge pressure over the suction pressure. This ratio known as specific ratio. Devices operating with a specific ratio up to 1.11 are classified as fans and devices with a specific ratio between 1.11 and 1.20 as blowers. Devices that have a specific ratio higher than 1.20 are classified as compressors. (BEE 2015, 145). This classification is utilized by many manufacturers and regulators, like the European Commission (European Commission 2011, 13 and Funkhouser 2021a). In this study, the term fan refers to both blowers and fans.

As some fans are better suited for certain conditions than others, choosing a proper casing, impeller, and motor size are important factors in ensuring a safe and continuous operation process. Hence being aware of the system requirements already in the planning phase is crucial. It is vital to examine the technical and nontechnical aspects of the process while determining the most suitable fan for the process. Examples of these technical aspects can include pressure and flow requirements, or space and noise constraints. Nontechnical aspects include matters like costs, availability, and user friendliness. (LBNL 2003, 19.)

Fans can be categorized by their use case and working current mode, but industrial fans are usually categorized by the path of the fluid flow in the fan (Dongguan Wanhang Electronic Technology Co. 2022). Utilizing this methodology, fans can be classified into two primary

categories: centrifugal and axial fans. There are also other types of fans, like mixed fans, which combine features from both axial and centrifugal fans (Air Control Industries 2015), and tangential fans, which are revised versions of the industrial axial fans (Funkhouser 2021b). The bioproduct mill fans examined in the case chapter are all centrifugal fans, thus other fan types are not discussed in this thesis. The following figure 5 showcases the gas flow path in these four types of fans.

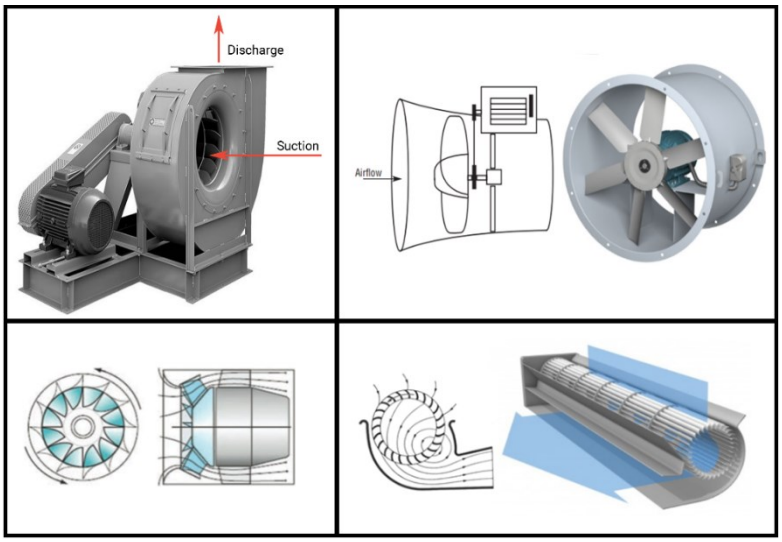

Figure 5. Classification of fan types according to their gas flow path. Clockwise from top left: centrifugal (Trocel 2021), axial (LBNL 2003, 22 and Aerovent 2022), mixed (Cibse Journal 2011), and tangential fans (Radgen et al. 2008, 189, and LTG 2022).

Centrifugal fans are the most common industrial fan type. As seen in the figure 5, they intake gas at an angle and spin it outwards from the impeller hub to the tip of blades. This causes the gas to gain kinetic energy that gets converted to a static pressure increase as the gas slows down before entering the output. (LBNL 2003, 3.) Due to their ability to generate high pressures with high efficiencies, they are often used to move gases in ductworks, while axial fans are often used in applications where pressure generation is not required, such as an exhaust fans between two different spaces.

Shape of the impeller blades is the main factor influencing the properties of the fan. Effects of the blade shape from the perspective of the operation point estimation are discussed more

in the subchapter 2.3.1. Depending on the impeller shape, centrifugal fans can be utilized in an extensive variety of operating conditions. For example, centrifugal fans with forward-curved blades are not suitable for dirty or high-pressure applications, while fans with radial blades are capable of handling heavily contaminated gas flow, containing large particles such as scrap metal and dust. Still, forward-curved blades are a common choice in HVAC applications as they can operate at relatively low speeds, which translates to low levels of noise. The simple shape of the radial blade is great at limiting material build-up and makes coating the blades, for additional resistance to corrosive and erosive elements, inexpensive. Its distinctive durability has made this blade type favoured by many different size industrial facilities, like metalworking shops and factories. Backward-inclined blades are available in different forms, which are showcased in the following figure 6 along with other blade types. Curved backward-inclined blade fans tend to be more efficient while fans with flat blades are more robust. Airfoil type blades possess a high efficiency, but often suffer from erosion issues resulting from the thinness of the blades. This can then have major impacts on the fan's performance. Since they do not perform well in volatile operating conditions, backward-inclined blades are commonly utilized in forced-draft services, where they can operate in relatively steady gas flows with high efficiencies. (LBNL 2003, 19–21.)

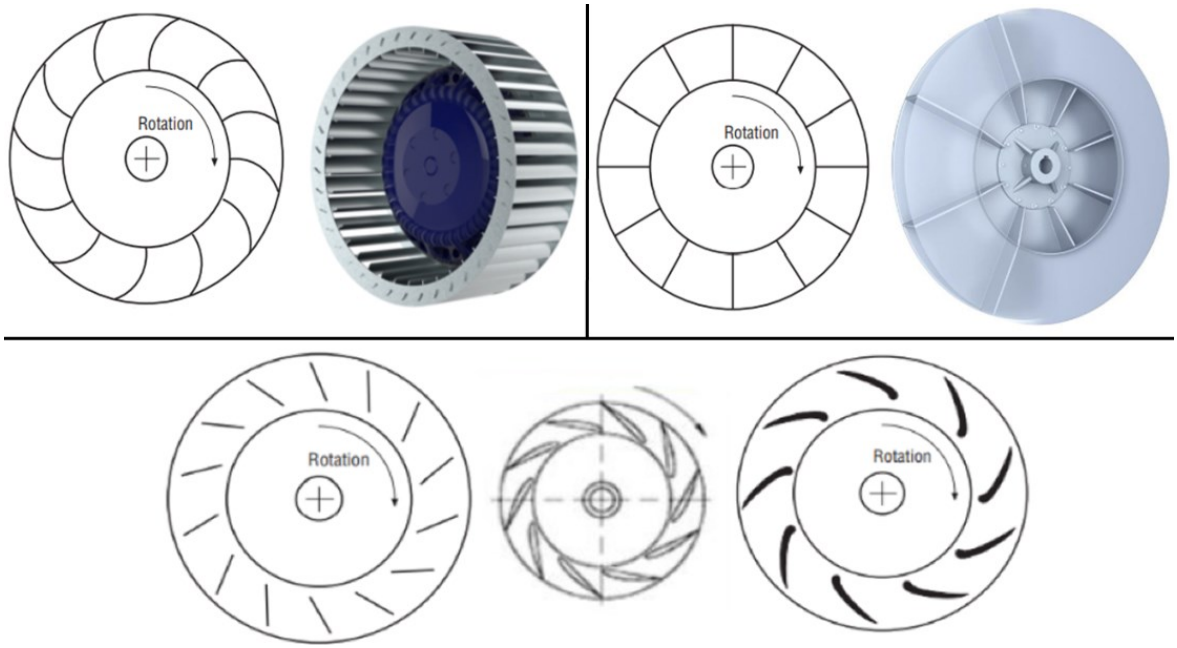

Figure 6. Top row from left: a schematic and a 3-dimensional rendering of a forward-curved (LBNL 2003, 19 and Blauberg Motoren 2022) and radial (LBNL 2003, 20 and Twin City Fan 2020) blade designs. The bottom

row present schematics of backward-inclined centrifugal fans. From left to right the blade types are flat, curved, and airfoil (LBNL 2003, 21 and Aerotech Fans 2019).

2.3 Fan operation point estimation

As the methodology and theory of the estimation calculations are discussed in many publications, this thesis focuses on only outlining the main formulae related to the estimations. For example, Tamminen (2013) studies the VSD usage in fan system monitoring in his doctoral thesis extensively. The study thoroughly showcases the different model-based operation point estimation methods, while discussing their applicability in different fields.

In this thesis, model-based operation point estimation refers to estimations that utilizes fan curves as a model of fan or pump, in conjunction with the VSD signals. VSD-based methods, showcased in the subchapter 2.1.1, rely solely on the signals. While in these sections the thesis showcases the VSD model-based operation point estimation for fan, similar methodology has been proven to be accurate in estimating the operating point of a pump (Tamminen 2013, 18). Compiled by the fan manufacturer, the fan curves provide information on the fan operation at a certain rotational speed, with certain fluid properties. There were two types of fan curves provided by the fan manufacturer. Pressure curves, sometimes referred to as Qp_f curves, provide information on the pressure change as a function of flow rate. And power curves, alternatively QP curves, which depict the fan power as a function of flow rate. In this thesis, only the power curves are utilized in the model-based estimations. As demonstrated by the following figure 7, the power curve shape can differentiate depending on the fan type and its blade shape. Their shape can cause issues in estimation and lead to re-evaluation of the scope. For example, if one power value corresponds to two flow rate values, like seen on the left in the following figure 7, the flow rate region must be known to prevent the estimation calculations from utilizing the incorrect starting values. With the curves on the right, such thinking is not necessary. This phenomenon is discussed more in the following subchapter, along with other factors influencing the estimation accuracy.

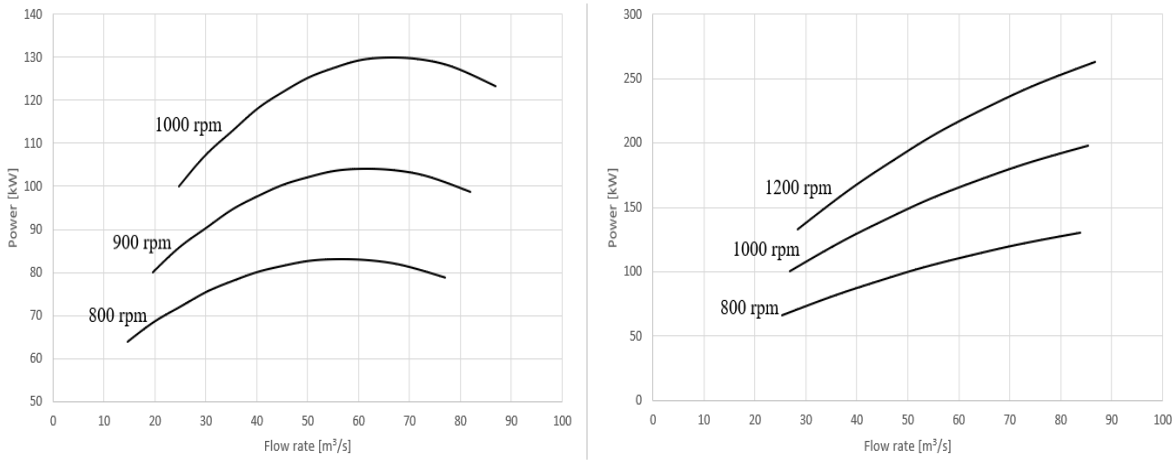

Figure 7. Examples of two different power curve set shapes.

Estimation calculations are based on the affinity laws. The three laws, showcased below, are used to estimate the operation point at different rotational speeds. According to the first law, showcased as the formula (1), flow rate at a certain rotational speed can be determined by first dividing the reviewed rotational speed value with the rotational speed value in which the curve value has been defined in. This value is then multiplied with the manufacturer-provided flow rate value, i.e., fan curve value. As seen below in the formula (2), pressure at certain rotational speed can be determined similarly. The difference being that the rotational speed quotient is squared and multiplied with the manufacturer-provided pressure value. Determining the power follows the same pattern. In the formula (3), the rotational speed quotient is cubed and multiplied with the manufacturer-provided power value. It should be additionally mentioned that the actual power consumption is also dependent on the surrounding system.

$$Q = \left(\frac{n}{n_0}\right) * Q_0 \tag{1}$$

$$p = \left(\frac{n}{n_0}\right)^2 * p_0 \tag{2}$$

$$P = \left(\frac{n}{n_0}\right)^3 * P_0 \tag{3}$$

In the formulae, the subscript "0" indicates the value found from the manufacturer-provided curves. In this study those values are digitized from manufacturer-provided fan curves. Q denotes the fan flow rate, p the fan pressure, and P the fan shaft power. (Tamminen 2013, 17–18.)

These laws are utilized in making a third-degree polynomial formula that is used in MATLAB to estimate the flow rate. Before using it, a third-degree polynomial (4) is fit to the power curve data. As seen in the following figure 8, the fitted curve aims to match the shape of the power curve. The polynomial fit generates four coefficients that ensure the curve made with the polynomial estimation formula (8) has a similar shape and range as the power curve data.

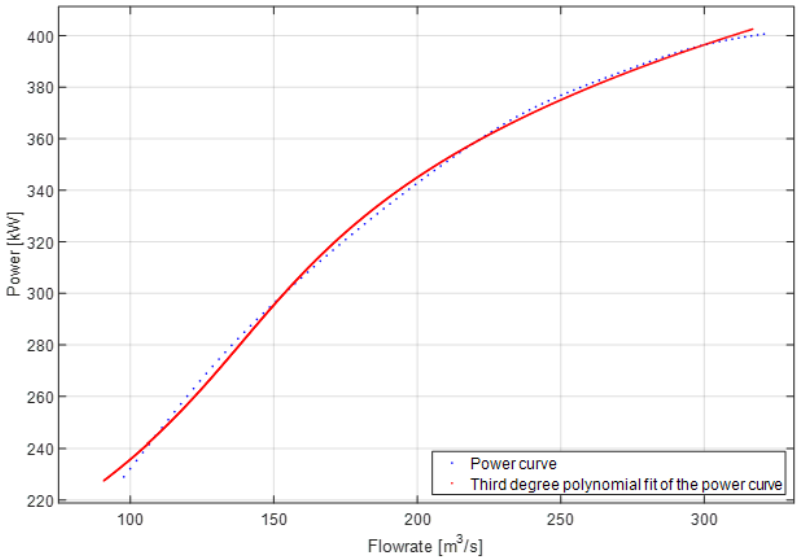

Figure 8. Power curve and a 3rd degree polynomial curve fit.

Also, the fan rotational speed and gas density will not stay constant in real-life scenarios, hence some adjustments need to be made. Rotational speed received from the VSD signals is used to adjust the values to the desired level, in accordance with the formula (5). While optional, density adjustment has an impact on the estimation accuracy. If actual density (ρ_{actual}) is not measured it can be calculated by using measured temperature and pressure

values, as seen in the formula (6), and then adjusted via formula (7). In this thesis, all these calculation operations were conducted by using MATLAB.

$$Q(P_0) = aP_0{}^3 + bP_0{}^2 + cP_0 + d \tag{4}$$

$$N = \frac{n_{\text{curve}}}{n_{\text{VSD}}} \tag{5}$$

$$\rho = \left(\frac{p_d}{R_d * T}\right) + \left(\frac{p_v}{R_v * T}\right) \tag{6}$$

$$\Pi = \frac{\rho_{\text{curve}}}{\rho_{\text{actual}}} \tag{7}$$

In the formula (4), *a*, *b*, *c*, and *d* denote the coefficients solved by MATLAB, which are then utilized in the polynomial formula (8) below. Subscript "curve" refers to values in which the curve has been defined, while "actual" refers to the system's values. Subscript "VSD" refers to the signals received from the VSD. (LUT University 2022.) In the formula (6), the subscripts "d" and "v" indicate that the values are for dry gas and water vapour, respectively. Variable ρ notes density, *T* temperature, and *R* the specific gas constants, which is 287.058 J/(kg·K) for dry air and 461.495 J/(kg·K) for water vapour. (Czernia and Szyk 2022).

By utilizing the values mentioned before, the estimation procedure can be conducted. Essentially, the power curve is shifted to the wanted rotational speed (and density) by applying the affinity laws. The flow rate equivalent to the shaft power estimate (calculated from the VSD signals) is then located from the shifted curve. A visual presentation of this is given in the following figure 9.

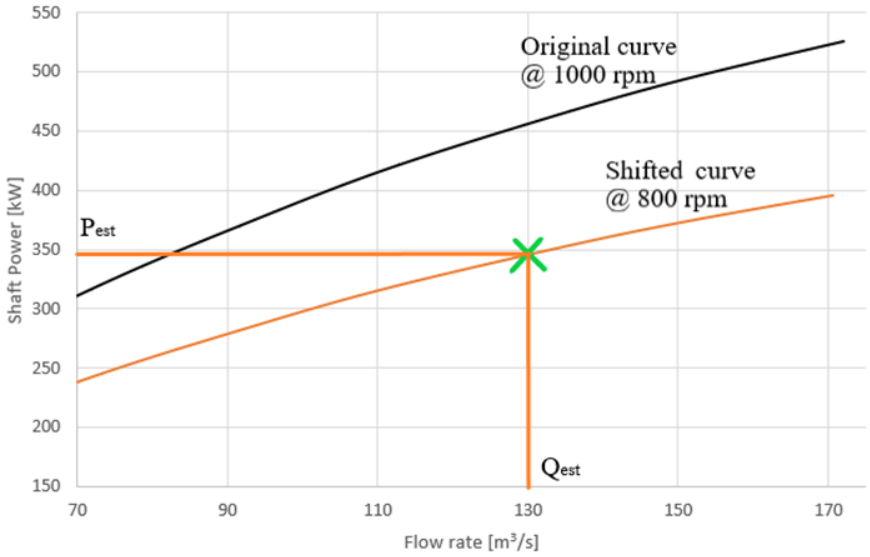

Figure 9. Visual illustration of the estimation process (modified from Tamminen 2013, 32).

When implemented in MATLAB, the polynomial formula (9) can do this shifting process and calculate flow rate estimations for selected time periods. Before that, the utilized power value must be calculated. In some cases, this value is provided by VSD automatically, but it can also be calculated from the torque and rotational speed estimates recorded by the VSD. Power calculation is done in the following formula (8), which is then utilized in the polynomial formula (9) to determine the flow rate:

$$P_{VSD} = \tau_{\%\ of\ Nom.} * \tau_{Nom.} * \frac{2 * \pi * n_{VSD}}{60} \tag{8}$$

$$Q_{\text{est.}}(P_{\text{VSD}},\ N, \Pi) = a\Pi^3 N^8 P_{\text{VSD}}^3 + b\Pi^2 N^5 P_{\text{VSD}}^2 + c\Pi N^2 P_{\text{VSD}} + \frac{d}{N} \tag{9}$$

Subscript “est.” refers to the value being an estimation, and “VSD” refers the value being provided from the VSD signals. “% of Nom.” subscript refers to the value being a percentage of the nominal value, and “Nom.” refers to the value being a nominal value. Torque value is denoted by the Greek character τ. Meanings of all other characters remain same as in the prior formulae.

This estimation method was chosen due to its applicability to the initial data. Rotational speed and torque values received from the VSD are used as inputs, which can be used in conjunction with measured temperature and pressure values to estimate the flow rate. Another major advantage of the polynomial method compared other estimation methods, which use the same inputs, is that its calculation processes are simple and not that time consuming. Other methods include interpolation, which is estimation of a value between two known values present in a series of values, can be used in operation point estimation (Awati 2022). Via the power curve values and affinity laws, a calculation that interpolates the flow rate value can be conducted. After initial processing of the received data sets, the polynomial estimation was determined to perform the necessary operations faster. Thus, polynomial estimation was chosen as the sole method in this thesis.

2.3.1 Factors influencing estimation accuracy

The following sections showcase the different factors that can affect the VSD model-based fan operating point estimation accuracy. As these estimations utilize different calculation processes and simplifications, they are prone to making erroneous estimations under certain conditions. Potential factors influencing estimation accuracy showcased in this thesis include condition changes, such as temperature, pressure, density, and humidity variation, wear of the system over time, signals provided by the VSD, numerical methods applied in converting visual data into numerical data sets, and initial data suitability, i.e., curve accuracy and shape.

Density, temperature, and pressure

As showcased in the subchapter 2.3, temperature and pressure have a direct effect on gas density. This density value is subsequently utilized in generation of the flow rate estimates. The following figure 10 showcases the how the density change impacts the estimated flow rate values. In the figure, values calculated from the received fan data set sets are presented in two forms: one uses unaltered a density values, while other applies density values that have been increased by a fifth.

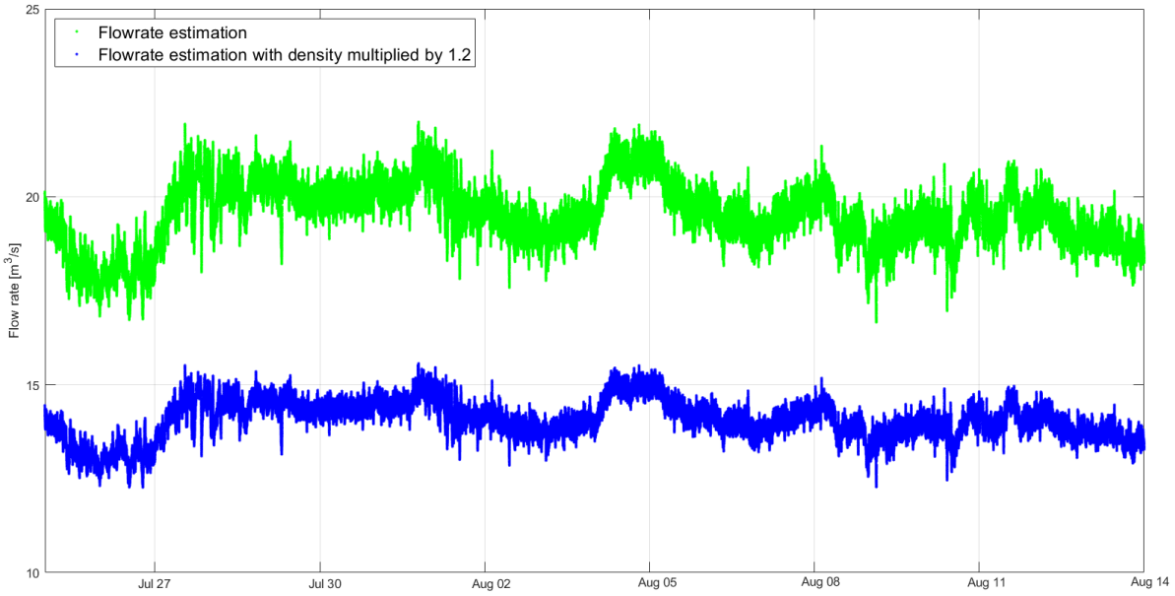

Figure 10. Effect of density on the flow rate estimation. If the density value is changed uniformly at all points in time, the flow rate change is also consistent. Green curve values are unaltered, and blue ones have a density multiplied by 1.2.

As seen in the figure 10, a constant change in the gas density affects all flow rate estimation values similarly. Still, determining the density value can be considered optional. Since, depending on the application, estimating the flow rate can be more about identifying various phenomena from the flow rate estimation values, thus aiming generate an estimate that imitates the realized flow rate is not always necessary. In some cases, the objective is to match the estimation values to certain measured ones, correction factors can be applied manually afterwards to achieve this. Temperature and pressure values can also be used in understanding different abnormal operating conditions or malfunctions in the system. Overall, if the initial data enables the density calculation, it is recommended to apply it.

Humidity

Changes in gas composition and humidity can affect the estimation accuracy. Humid gases often weigh less than dry gases due to the lower weight of the water molecules that often displace oxygen and nitrogen molecules from the gas. This change in weight influences the gas density, which can then affect the flow rate. (University of Georgia 2020, 1.) The formula

(6), showcased in the subchapter 2.3, can be used in calculating an example to illustrate the effect of relative humidity on the gas density. When temperature and pressure are set to be constantly at 20 °C and 101 325 Pa, it can be observed in the following figure 11 that a shift in relative humidity from 10% to 90% changes the density by less than a percent.

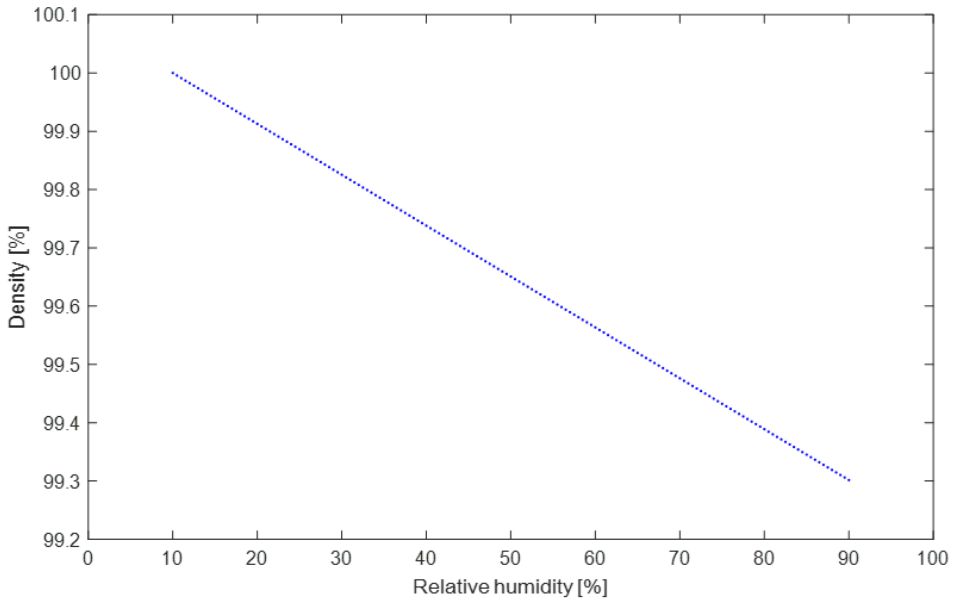

Figure 11. Density as a function of relative humidity in constant temperature and pressure conditions.

As seen in the figure 11, effect of relative humidity change on density is minute. Thus, in this thesis, humidity is not considered to be major point of importance. In the estimation calculations, the gas flows are assumed to be dry. However, it should still be noted that outliers exist, and if the gas flow composition differs significantly from air, humidity variation can have a greater effect. Humidity can also cause other issues, such as moisture accumulation on the impeller surfaces, which can increase malfunction probability and the estimation inaccuracy.

Wear of the system over time

Some fan systems are subjected to wear during operation. This wear often results from the conditions in which the system operates. For instance, in sugar mill plants, smelting, mining, and minerals processing the fan systems are subjected to harsh abrasive materials transported

in the gas flow. If not properly protected, the impeller blades, seen in the following figure 12, and other parts, like bearings, and housing, can be prone to being damaged. Wearing decreases the impeller thickness and shortens service life of the device. It also reduces performance and can cause imbalances that lead to a malfunction. (Venti Oelde 2023b, 2.)

Figure 12. From the left: a worn-down impeller without protective coating and a fan impeller, used in the timber industry, with critical wear and some broken and cracked blades (Venti Oelde 2023b, 2 and Venti Oelde 2023a).

Fan impeller wear can be minimized by coating and choosing an impeller type that is suitable for more rugged conditions. This is discussed further in the subchapter 3.2. For example, blade shapes in which the air moves through the blade more slowly are more vulnerable to contamination, while some blade shapes, with larger clearances for instance, are less likely abraded. (LBNL 2003, 5, 20.) The fan impeller wear can also influence the model-based estimation accuracy. If the fan impeller is badly worn, bent, or damaged, it might not be able to attain values defined in its power and fan curves. This would mean that running the fan at a specified certain speed would not yield the calculated amount of flow rate. Thus, making the accurate model-based estimation trickier. In this thesis, the fan system is presumed to be operating without defects to simplify the estimation. If there are unusual estimation results, the case chapter discusses whether they could be due to wear.

Signals provided by the variable-speed drive

The fan operating point estimation utilizes data recorded and automatically calculated by the VSD, such as actual rotational speed and output power, making its impact on the estimation accuracy major. One of the most prevalent modern-day VSD control method is direct torque control (DTC), which conducts the motor operating by controlling two variables, which are motor magnetising flux and motor torque. (ABB 2011, 14.) All the fans examined in this thesis are controlled by DTC, which ensures the fact that the VSD data is as accurate as possible to effectively control, maintain, and analyse the process.

According to ABB's Technical Guide, from 2011, when examining values within a speed range of 2–100 percent and a load range of 10–100 percent, the static speed estimation accuracy is 10 percent of the motor slip, and the torque estimation accuracy is 2 percent. For example, a motor slip of a 37-kW motor is close to 2 percent which corresponds to a speed accuracy of 0.2 percent. As the static speed accuracy of a frequency-controlled pulse width modulation (PWM) drive is usually between 1–3 percent. (ABB 2011, 19, 27.) International Electrotechnical Commission (IEC) 60034-2-1:2007 standard on rotating electrical machines insist that the instrumentation used to measure the rotational speed should have an accuracy of ±0,1 percent full scale, while the accuracy torque measurement of should be ±0.2% of full scale. (IEC 60034-2-1:2007).

Numerical methods applied in converting visual data into numerical data sets

Different numerical methods are frequently utilized in fan operating point estimation. Methods, like interpolation and extrapolation, are often used by different digitization software in assembling numerical data sets from fan curve figures. In this thesis, digitization of the fan curves was conducted with Engauge Digitizer tool, screenshot of which is shown in the following figure 13. Engauge Digitizer is an open-source tool that can convert a visual presentation of data in form of a graph into a set of data points in accordance with the user defined parameters. These user-set parameters include coordinate definition and other

optional aspects that will affect the number of data points, like interpolation interval length. (Mitchell et al. 2022.)

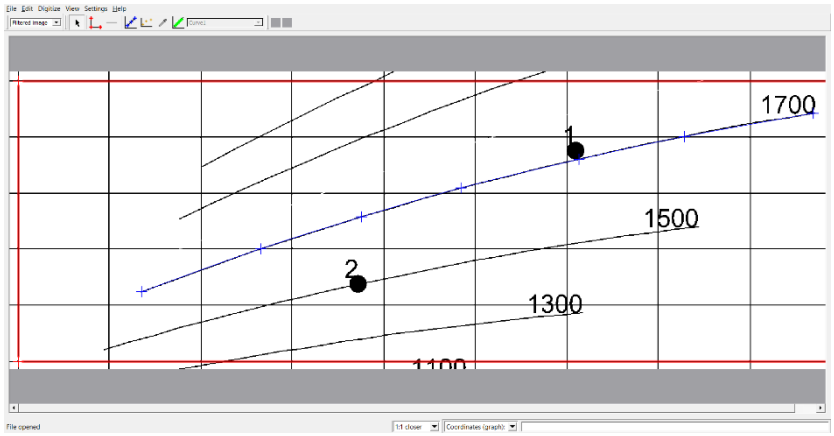

Figure 13. Engauge Digitizer converts fan curve figures into numerical data with provided user-defined y- and x-axes and curve information.

If the digitized data set has been inaccurately digitized due to an insufficient amount of data points or other user errors, the use of the aforementioned methods may render the estimation results inaccurate. But usually, large enough data sets can be constructed from the curves without errors, making the effect of numerical method usage on estimation accuracy be less significant than the other potential factors.

Initial data accuracy and suitability

The fan curves provided by manufacturers are normally measured to match the accuracy criteria defined in the ISO 13348:2007 standard. The standard states that the flow rate and pressure values must be within a ±5% margin of the given fan curve, while the shaft power must be within a +8% margin of the curve. (ISO 2007.) Since the shaft power accuracy does not have a negative limit value, the actual device efficiency cannot be lower than the manufacturer-provided value. Since it only has positive tolerance, the difference between the actual and manufacturer-provided efficiency values is limited to an improvement of 8 percent when tolerances in flow rate and pressure are not taken into account.

The shape of the fan curve, affected by the fan type and blade selection, can cause limitations in model-based estimation. The shape of the blade is known to affect the performance of a fan, thus making two same design category fans with differing blades be suitable for unique applications. (BEE 2015, 146.) The shape of the curve can create problems if one shaft power or pressure value corresponds to two different flow rate values. Curves like this are referred as nonmonotonic. Estimations can still be conducted using nonmonotonic curves, but the estimation process scope needs to be modified. For example, certain flow rate regions can be excluded and only the dominantly used monotonic curve regions are utilized in the estimations. Excluding certain part of the curve will lead to information loss, thus it is very important to ensure that the fan's actual operation region matches the assumed one. (Tamminen 2013, 33.) Determining this can be particularly tricky if the fan operating point in is near a nonmonotonic fan curve's local maximum.

The following figure showcases curve shapes of most common centrifugal fans. The leftmost curve in the figure 14 showcases the performance of a forward-curved centrifugal fan. The power curve of these fans steadily increases with gas flow towards free delivery which makes proper driver selection essential to circumvent overloading the fan motor. Also, it can be seen that this blade type is not ideal for lower gas flow rates, as it tends to stall. This stall region is represented by the dip in the fan curve. (LBNL 2003, 20.) Radial blade type manages well at delivering lower air volumes at medium speed fans in medium to high pressure. (Aerovent 2018, 3.) As seen in the following figure 14, typical fan power curve for a radial-blade fan is well suited to model-based estimation due to its monotonic nature. Like it can be seen in the figure 14, the shaft power of a backward-inclined fan increases for most of the performance curve, but then drops drastically at higher gas flow rates. This non-overloading motor characteristic makes it attractive for applications where the system's behaviour at high gas flow rates is unreliable. (LBNL 2003, 21.) This characteristic can also hinder estimation accuracy if the operating point is located near the local maximum value of the power curve.

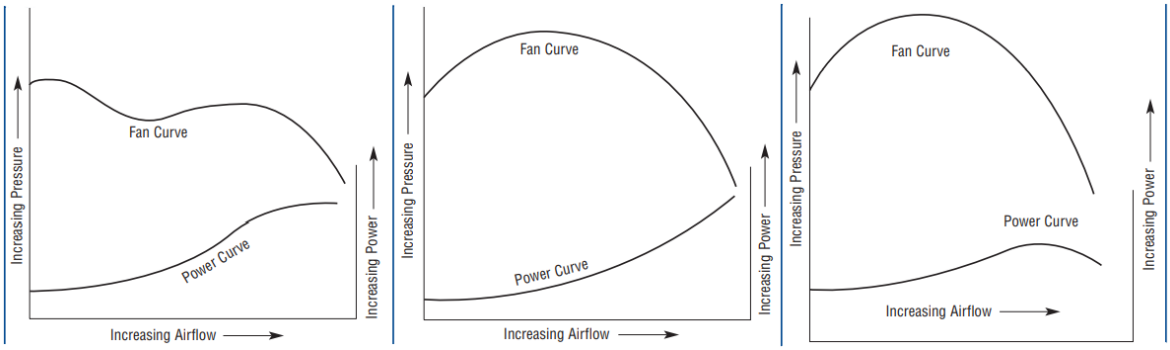

Figure 14. Performance and power curves of centrifugal fans. From left to right the blade types are forward-curved, radial fan, and backward-inclined centrifugal fans (LBNL 2003, 20–22).

3. Bioproduct mill

A bioproduct mill is a production facility which manufactures pulp from wood, which can then be further processed other products, such as cardboard or paper. Pulp manufacturing is conducted either chemically or mechanically, or as a combination of both. In this thesis, the focus is on the kraft process. It is the most globally prevalent form of chemical pulp production as it can generate a good pulp quality from multiple wood types. (Pinheiro and Quina 2020.) Typically, the kraft pulp process is divided into two parts, the fibre line and chemical recovery cycle. The fibre line includes the wood processing procedures, while the chemical recovery cycle covers the processes used to recover the cooking chemicals back for use. (Erikson and Hermansson 2010, 7.) The following subchapters showcase the operation of a bioproduct mill and their typical fluid handling systems. Sections of the first subchapter presents the different unit processes of a bioproduct mill, from both the fibre line and the chemical recovery cycle. The bioproduct mill concept and the generated emissions are also discussed. The second subchapter showcases the fluid handling systems of a bioproduct mill. Their power, energy consumption, and the procedures they are used for are showcased.

3.1 Bioproduct mill operation

First step in the fibre line, described in its entirety in the figure 15, is to transform the wooden logs into a usable form. Logs are first debarked in a barking drum and then reduced in size in a chipper. The generated wood chips are also heated to remove excess air. Bark and other unsuitable wood can be utilized in a boiler to produce heat for other unit processes. Then, the chips are mixed with white liquor in the cooking plant. (Erikson and Hermansson 2010, 7.) White liquor is an alkali consisting mostly of sodium hydroxide (NaOH) and sodium sulphide (Na_2S) (CNBM International 2022). The wood chips and white liquor are cooked in high-pressure conditions that break down the wood structure and separate the two main components, lignin, and cellulose fibres, from each other. (Pinheiro and Quina 2020.) In the cooking process, the depolymerized fibres and lignin detached from the wood get mixed with the cooking chemicals turning the white liquor into black liquor, which is then sent to

the chemical recovery cycle. After the component separation, the pulp mass is washed and screened. In the screening process, branches and other incompletely cooked fibres are separated from the pulp. To remove remaining lignin, the pulp is finally bleached with oxygen before sending it to further processing (Erikson and Hermansson 2010, 7.) Further processing includes procedures, such as sorting, drying, pressing, and coating, where the pulp is formed into the desired products (Piri 2017, 19–20).

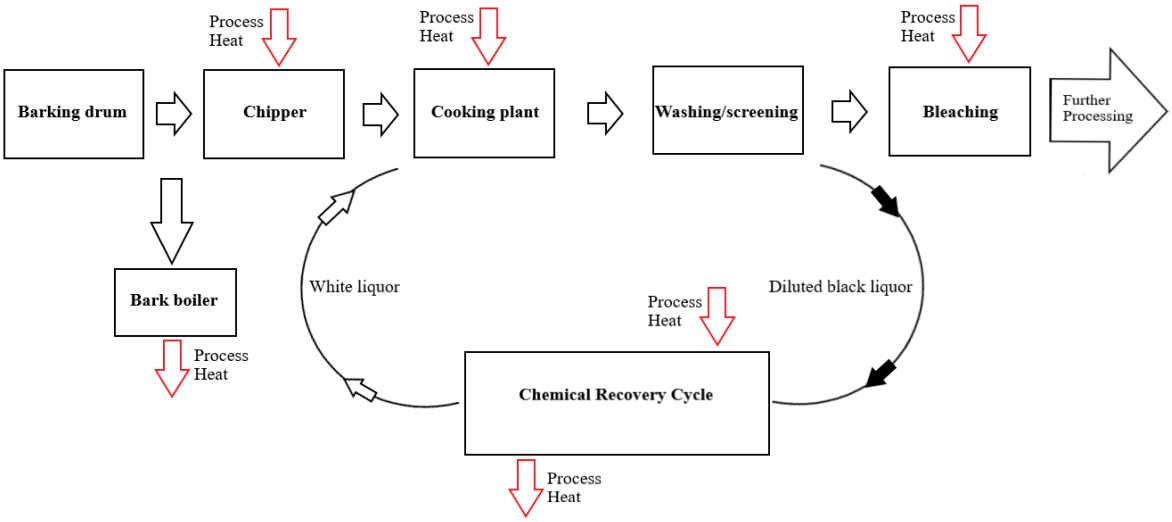

Figure 15. General outline of the fibre line unit processes and its connection to the chemical recovery cycle (modified from Erikson and Hermansson 2010, 7).

The harvested diluted black liquor exiting from the cooking plant possesses high levels of moisture and biomass, making it unsuitable for white liquor regeneration as such. Therefore, those values must be lowered. This is done in the chemical recovery cycle, which's unit processes are illustrated in more detail in the following figure 16. The different unit processes utilize heat, combustion, and chemical reactions to regenerate the diluted black liquor back to white liquor, which can then be used at the cooking process.

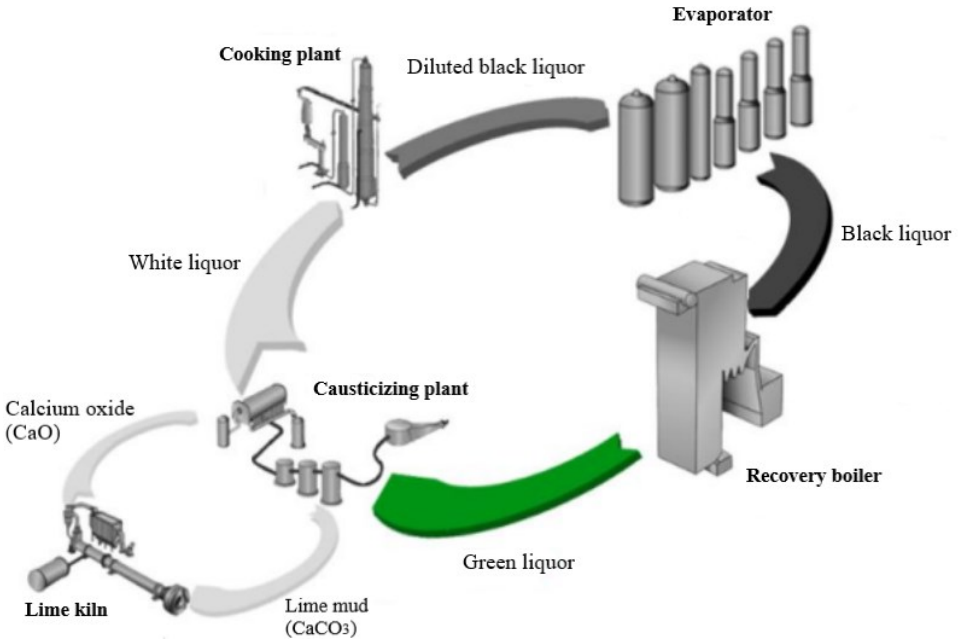

Figure 16. Kraft mill chemical recovery cycle (Hiltunen 2020, 15, modified in accordance with Vakkilainen 2005, 10).

The diluted black liquor is initially directed to the evaporator. In the evaporator, water is evaporated from the diluted liquor to lower its moisture content. The strong black liquor is then transferred to the recovery boiler, where the biomass is consumed in incineration to generate heat for the process, and spent chemicals are harvested. The process transforms the incoming black liquor into green liquor. (Pinheiro and Quina 2020.) Last step is the causticizing process, where lime is recycled and added to the green liquor to form white liquor. Before the green liquor enters the causticizing plant, insoluble substances, such as soot and metal oxides, are separated from it. After the added calcium oxide (CaO) has reacted, the resulting lime mud, which is mostly calcium carbonate ($CaCO_3$) (University of Georgia 2017), is removed from the white liquor, the liquor is ready to be reused at the cooking plant. The separated lime mud is directed to the lime kiln, where it is regenerated with the help of heat back to calcium oxide, which is then used again in the causticizing plant. This calcium oxide regeneration process is often referred to as the lime cycle. (Piri 2017, 15–16.)

The concept of the bioproduct mill is to utilize all the raw and generated material at the pulp mill facility, including the side-streams, as various bioproducts that can replace fossil fuels

and materials. For example, bark and sawdust can be utilized in energy production, ash and other solids in fertilizers and earthwork materials, and acids from sulphurous gases. This boost in resource efficiency is great both environmentally and financially as the generated pulp production side-streams can be turned into other valuable bioproducts such as biochemicals and energy. (Metsä Group 2022.)

The utilized kraft process generates emissions, the amount of which can be mitigated with different technologies, raw material choices, and treatment at the bioproduct factory itself. The utilized kraft process generates effluent that is often treated at the mill. Digestion and bleaching are cited as the generators of the most pollutant effluent. For example, the raw material treatment unit processes' effluent includes suspended solids, like bark, dirt, and sand. Pulping unit process effluent contains resin and fatty acids, dissolved inorganics, and volatile organic compounds (VOC). Bleaching effluent consist of dissolved lignin, inorganic chlorines, and different organic halogens. (Vidal et al. 2021, 2–3.)

Even though, the bioproduct mill can utilize its side-streams, the kraft mill industry still generates a variety of atmospheric pollution, including nitrogen oxides (NO_x), hydrogen sulphide (H_2S), and sulphur oxide (SO_2) emissions (Bordado and Gomes 2002, 3). In chemical pulp industry, most the carbon dioxide (CO_2) emissions are generated in the combustion processes. In a kraft process mill, the primary CO_2 sources include the recovery and cooking boilers, and the lime kiln. Other CO_2 sources of the mill, such as non-condensable gas destruction, are often considered inconsequential. (Kuparinen 2019, 29.)

These compounds must be processed and directed to the correct place, such as the recovery boiler or an exhaust pipe, which makes airflow management have a vital role in the kraft mill industry. Fans are required throughout the process to constantly supply and exhaust required amount of gas. The fan operations are susceptible to changing conditions, like the volume and pressure requirements, which can cause the fan's operating point to fluctuate. In some conditions, the fan may have to operate very inefficiently, which leads to unnecessary energy usage and increased costs.

3.2 Fluid handling systems of a bioproduct mill

Pulp mills are complex facilities with plenty of demand for fluid handling systems. A report by PTS München et al. (2007, 11) showcases typical consumption values of general mill services. According to the report, pumps utilized in effluent treatment, which includes mechanical, anaerobic, and aerobic stages, consume 5–10 kWh per tonnes of treated effluent. Fresh water treatment, raw water pumps and preparation requires 2–5 kWh tonnes of treated water. Compressors, which are required at multiple different stages of kraft process, consume 20–30 kWh per tonnes of treated gas. According to Pulp and Paper Research Institute of Canada (1999, 69), kraft process fans consume 8 kWh per tonnes of end-product, and HVAC fans consume 5 kWh per tonnes of end-product.

Pumps, fans, and compressors are utilized in both the fibre line and chemical cycle to move fluids and materials between unit processes. The following table 2 compiles examples of typical fluid handling systems in different bioproduct mill unit processes. The power scale presented in the table is a based on a thesis conducted at a Finnish kraft pulp mill by Piri (2017) and should be regarded more as indicative rather than exact values. When the thesis was conducted, the total annual pulp output of the was 460 000 tonnes (Piri 2017, 18), which was an average size of the time. As the production requirements increased, so have the production capacities. As of 2023, the same facility's capacity is 630 000 tonnes of pulp annually (Stora Enso 2023). Also, it is not known whether if the power value data is of the nominal value for the motor or the fluid handling device. Hence in reality, some power values can be smaller. While the table includes all three main types of fluid handling systems, it should not be regarded as definitive since other fluid handling applications and system approaches can surely be found. For example, applications utilized in moving materials between different unit processes are not separated in this table.

Table 2. Typical fluid handling systems of a kraft process bioproduct mill (Piri 2017, 51–58).

Process	Application	Power Scale
Bark boiler		
	Primary air fan	
	Feed water pump	
	Turbo compressor	
Cooking		
	White liquor pumps	
	Exhaust fan	
Washing, screening, and bleaching		
	Scrubber filter pump	
	Tank washer pressure booster pump	
	Seal water pumps	
	Seal water pressure booster pump	
	Bleaching air conditioning fans	
	Hydraulics room cooling fan	
	Oxygenated white liquor dosing pump	
	Hydrogen peroxide pump	
Evaporator		
	Waste condensate pumps	
Recovery boiler		
	Turbo compressor	
	Primary, secondary, and tertiary air fans	
	Flue gas fan	
Causticizing plant		
	ClO_2 water pumps	
	Pressure booster pump	
	Discharge pump	
	Air conditioning center	

	> 400 kW
	200 – 400 kW
	100 – 200 kW
	50 – 100 kW
	< 50 kW
	Undetermined

	Lime kiln primary air fan	

Effluent treatment		
	Aeration fans	

Further processing		
	Air condition fans	
	Collection tank mass pumps	
	Bleached pulp mass pump	

The bioproduct mill operation requires fluid handling at every unit process. As it can be seen in the table 2 above, processes in which combustion takes place require larger fans. The fans are utilized to feed air into and out of the process to enable the most efficient combustion process possible. Compressors are often utilized in capturing pressurised steam, which can then be utilized in other unit processes. For example, the sawdust for the chipper can be dried in tandem by flue gas, scrubber water, and compressed air. The sawdust is directed to lime kiln where it is used as combustion fuel in calcium oxide regeneration. (Piri 2017, 25.)

Pumping units are utilized in various tasks, cooling, and transporting fluids being the largest. Pumps are also used in many other tasks that are not showcased in the table separately. For example, water is pumped in many systems that are only utilized as accident prevention precautions, such as sprinkler and extinguishers systems. Water is also pumped in reserve and levelling basins for easier access. (Piri 2017, 29.) Pumps transfer materials between unit processes, like mentioned before. In the fibre line, pumps move the pulp from the super batch cooker, where the pulp manufacturing is done, to dump tanks, where the mass waits for the next process, to washing, oxygen bleaching, and sorting. The chemical cycle also utilizes many pumps not showcased in the table. The different liquor types are of course pumped between and inside the unit process. In the evaporator, for example, pumps cycle the liquor between tanks where the heat of the low-pressure steam is used to extract water vapour from it. The pumps then handle the condensate water and direct it to other uses. (Piri 2017, 20–22.) Likewise in the causticizing, pumps are used to direct the green liquor between tanks where the lime mud is extracted and then pumped to the lime kiln. (Piri 2017, 24.) In the

recovery boiler, pumps feed the black liquor in the furnace with spoon nozzles pumps that disperse it into small droplets (Piri 2017, 16).

The range of bioproduct mill fan operations is broad. Fans are utilized in basically all the buildings' HVAC applications. Proper HVAC functions ensure good working conditions in the premises, and prevent different damages, caused by moisture accumulation or overheating. Fans also play a vital part in the combustion processes where they often either insert or extract gases to make sure the procedure works in the best possible manner. Fans are also utilized in other essential tasks, such as aeration in the effluent treatment and managing the evaporator black liquor drying procedures. (Piri 2017, 20, 22, 29.)

4. Case study of the VSD monitoring applicability in a bioproduct mill

The case chapter study analyses fan systems of a bioproduct facility. After communication with the bioproduct mill contact persons, a few interesting fans were selected for the case study. This selection was based on the fan's power and suitability for the model-based estimation. In this thesis, the aim was to analyse as high-powered units as possible, while ensuring that the shape of the power curve is suitable for the model-based estimation. First fans analysed in the case study are 4 identical flue gas fans. They direct flue gas generated at the recovery boiler combustion process to a smokestack. The second analysed fan handles diluted odorous gases. It directs the gases to the recovery boiler or alternatively straight outside through a smokestack, if incinerating them in the recovery boiler is not possible. The following subchapters showcase the studied systems and their components. The content of the received data set utilized in the calculations are also outlined. Lastly, the applicability of VSD model-based calculations to monitor and recognize various phenomena in the studied systems is discussed.

4.1 Recovery boiler flue gas treatment

After communication contact persons of the bioproduct mill, the flue gas fans were selected to be one of the examined cases. Out of the reviewed fan unit options, these fans were the most high-powered and their fan curves are well suited for model-based estimation. Although guiding flue gas to a smokestack might not seem important on the surface, the flue gas fans are still very vital in guaranteeing best possible operation of the bioproduct mill chemical cycle. As they remove flue gas for the recovery boiler furnace, they can affect the prevailing pressure conditions, and ensure that the recovery boiler operates optimally. This makes them important adjustment tools that are controlled in accordance with the conditions of the recovery boiler combustion process.

The studied flue gas treatment system includes four fans that are all aimed to be operated as similarly as possible. The flue gas generated at the recovery boiler combustion process is divided into four different ductworks that each house an electrostatic precipitator (ESP), that cleans the incoming flue gas, a flue gas heat exchanger, which lowers the gas temperature, and a fan that directs the flue gas into a shared duct that leads to the smokestack. Each of these applications are showcased in the following subchapter that showcases the system components. Every individual duct also has dampers that can be used to stop gas flow from entering or leaving a certain duct. These dampers do not function as adjustment dampers, they are always either open or closed. The following figure 17 illustrates the configuration of the system.

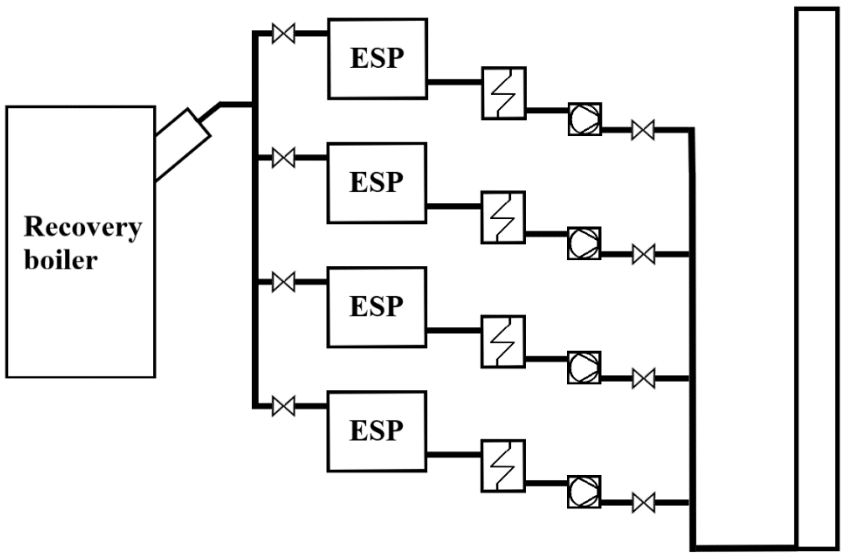

Figure 17. The studied flue gas fan system.

The flue gas fans are remotely controlled based on the pressure at the upper part of the recovery boiler furnace. The fans strive to maintain the boiler constantly under negative pressure to ensure controllability and appropriate gas flow of the combustion process. All four fans are uniformly controlled with the same remote controller, as they all are used to adjust the same factors. The uniform operation also promotes equal fouling and wear distribution across all four fans. Differences between fans do still occur, but for example when it comes to temperatures, the differences are typically in the scale of 5–10°C, which in this process is a negligible difference.

System maintenance is conducted once every 4 to 5 months. During the maintenance, the recovery boiler combustion process is halted. Different components in the ductwork and recovery boiler are cleaned and maintenance and possible repairs are all conducted to guarantee efficient operation of the system. If leaks or other deleterious phenomena are discovered, they are usually taken care of during the maintenance. As an example, removing fouling from the ESP and heat exchanger surfaces lowers the pressure drop generated by them, and re-improves their efficiency. This reduces the number of particles reaching the fan.

In a case of a malfunction, the dampers included in each fan ductworks can be used to direct the gas flow to other fans. This requires the remaining fans to increase their output, but it allows the process to operate even if one of the fans malfunctions. This generates redundancy and potentially high savings in making sure that chemical recovery cycle does not need to be ceased unnecessarily, even if a certain flue gas fan would malfunction.

4.1.1 System components

The following sections present the processes and components that affect the studied flue gas fans' operation. As the main objective of the fan operation is regulation of recovery boiler furnace conditions, the first examined process is the recovery boiler. Besides showcasing its components, the sections showcase the contents of the flue gas. Before reaching the fans at the end of the ducts, the flue gas first cleaned by an electrostatic precipitator, and cooled by a heat exchanger. These devices are examined in their own sections. As for ESPs, their operation principles and related maintenance are discussed. As the knowledge of the utilized flue gas heat exchangers is limited, the section focuses more on presenting a general overview of the different heat exchanger type categories, their operating principles, and maintenance related to them.

Recovery boiler

Recovery boiler is one of the most important parts in the whole bioproduct mill operation. It plays a major part in the chemical recovery as it is used to harvest spent chemicals from the black liquor. It also generates heat by burning organic material in the black liquor, which can then be used in steam and electricity generation at the mill facility. Recovery boilers are also used in minimizing discharges from other waste streams, such as incineration of odorous gases. (Vakkilainen 2005, 22.)

The process has undergone over a century of development and improvements. The development has been directed by the market's need for larger production quantities, improved energy efficiency, and firmer emission regulations. Nowadays, all modern recovery boilers, except small boilers, have transitioned to a single drum design, which allows for a larger size and better operational reliability. (Vakkilainen 2005, 15–17.) As a result of the development, the recovery boilers have almost quadrupled in size during the last 30 years (Salmenoja 2019, 4).

This thesis assesses the fan operation of the mill; thus, the chemical reactions of recovery boilers are not showcased. Also, only those components most relevant to the flue gas flow are discussed. More information about the operation and minutia on the recovery boilers can be found from Vakkilainen (2005), presented in the references. As seen in the following figure 18, multiple different heat transfer surfaces are employed in the process. The flue gas generated in the black liquor combustion travels through different super heaters, heat exchanger surfaces, which are often referred to as the boiler bank, and economizers (feed water preheaters), which cool the gas with their counter flow design before they are directed to the final treatment and flue gas fans.

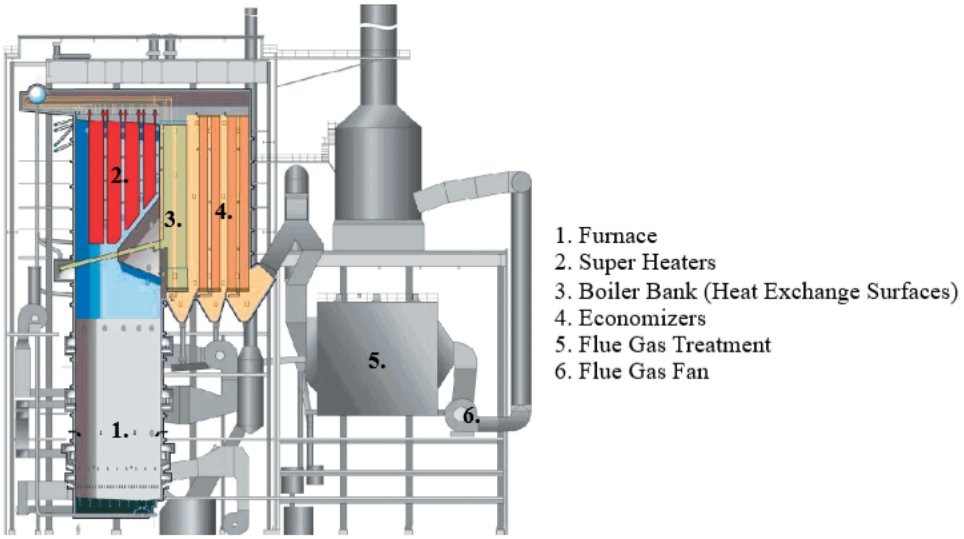

Figure 18. Modern recovery boiler design, with the flue gas pathway marked (Vakkilainen 2005, 11, modified in accordance with Korhonen and Ahola, 242).

According to Vakkilainen (2005, 198), recovery boiler is the largest producer of gaseous emission in the kraft process. Recovery boilers generates flue gas that that is a substantial source of particulate matter (dust). The particulate matter emission after the recovery boiler economizer is typically below 20 g/Nm^3 (N indicating standard conditions). 80 to 99% of these particulates belong in the PM2.5 category, which covers particles with diameter less than or equal to 2.5 micrometers. The dust generation is greatly related to the boiler load. It has also been detected that combusting black liquor droplets as small high velocity droplets increases dust production. Dust emission is reduced by electrostatic precipitator usage, which is showcased in the following section. (Vakkilainen 2005, 205–206.)

Pulp manufacturing used to generate large sulphur emissions, mostly at the recovery boiler. Since then, the correlation between boiler conditions, fuel composition and sulphur dioxide (SO_2) emissions has been studied, which has led to optimization in furnace temperatures and black liquor dry solids percentage. Cooler furnace temperatures and lower dry solids quantities increase the SO_2 emissions. (Vakkilainen 2005, 207–209.)

The level of nitrogen oxides (NO_x) generated at a kraft mill is below the mean value for an average energy production facility. Laboratory experiments have indicated that the release of nitrogen from black liquor seems to be dependent on the wood species and cooking method. For instance, liquor manufactured from a high nitrogen wood (hardwood) generates more NO_x than softwood-based liquors. Optimizing air and black liquor input in the combustion process, are examples of methods to reduce the NO_x generation. (Vakkilainen 2005, 198, 201.) The combustion process also generates small amounts of other compounds, such as carbon monoxide (CO), which are generated at all combustion processes. The CO formation increases drastically when black liquor is burnt in conditions where very low amount of excess oxygen is present. Thus, ensuring high furnace temperature and proper air ratio are key in decreasing CO formation. (Vakkilainen 2005, 199–200.)

The combustion process can also generate water vapour from the small amount of moisture possessed by the combusted black liquor it. This can lead to the water vapour reacting and forming different chemicals. For example, char can react with water vapour to form carbon monoxide. Water vapour reacting with sodium chloride (NaCl) generates sodium hydroxide and hydrochloric acid (HCl). It can be generally stated that in conditions where water vapour is present, sodium hydroxide is almost certainly formed. (Vakkilainen 2005, 50, 69, 76.) Whilst the flue gas can end up containing water vapour, in thesis the flue gas is examined a dry gas. This simplification was done since the moisture content of the flue gas is not known and the effect of humidity on the calculations performed in this thesis was deemed to be small.

Other potential emissions of the recovery boiler include sulfuric acid (H_2SO_4), fluorine, dioxins, and others. They are considered negligible as most factors related to them have been identified and thus preventatively negated. For example, H_2SO_4 emissions, which are highly connected with the SO_2 emissions, are anticipated to be virtually non-existent at modern recovery boilers. Same with fluorine emissions, which have been identified to be linked with the fluorine levels of the black liquor. As the black liquor fluorine level is very low, the recovery boiler fluorine emission is assumed to be insignificant. (Vakkilainen 2005, 210.) Kraft process is also often referred as producer of bad smells. However, the release of the

smelly component, reduced sulphur, from recovery boilers is small-scale (Vakkilainen 2005, 198). This is discussed more in the following case subchapters where odorous gas treatment is examined.

Electrostatic precipitator

Since the first installations in coal steam plants in the 1920s, electrostatic precipitator technology has emerged to be the prevalent technology in particulate emission control in the power generation industry (Parker 2003, 1). Nowadays, ESPs are utilized in a variety of applications and temperature ranges, such as dry collection of valuable materials or wet collection of fumes and mists. Their main advantages include their high efficiency, which can be over 99.5%, and low pressure drop, usually in the range of 200 to 300 Pa (Ohlström et al. 2005, 20, 33). ESPs are also able to handle very large gas volumes with heavy dust loads, while retaining a durable, long, service life with relatively little maintenance need. But like with everything, ESPs also have downsides, such as high capital costs, large space, and voltage requirements, that can make other options more fitting. It operates most efficiently in steady conditions, as it is not very flexible to changes in operating conditions, thus it should not be utilized in cases with highly variable conditions. Also, ESPs might not operate properly if the treated particulates possess exceptionally high electrical resistivity. (LUT University 2020.) In consequence of its versatile advantages in treating large quantities of flue gas with particulate, electrostatic precipitators are also applied in processing recovery boiler flue gas.

The ESP operation principle is based on electrically charging the flue gas particles, which can then be accumulated on to collecting surfaces. A typical ESP, shown in the figure 19, consists of thin wires, which operate as the negative discharge electrode, which are spaced between large, positively charged, collection electrode plates. (Neundorfer 2016, 1–2.) There is a strong electric field between the plates, through which the gas passes. The free electrons in the air accelerate quickly and attain a high velocity when encountering the strong field between the plates. If an electron then collides with a gas molecule, it possesses sufficient energy to knock one, or more, electrons loose, which ionizes the gas molecule. These detached electrons are similarly accelerated by the field, causing more and more electrons

to get knocked loose, until there are enough free electrons to form a steady corona discharge. The formed positive ions drift to the wire where they are discharged. As the electrons then flow towards the plate, they can engage with flue gas particles, capturing, and charging them. The electric field then propels the particles toward the plate. (LUT University 2020.) Neundorfer (2016), Hirvonen (2020) and Parker (2003), presented in the references, provide more meticulous information about ESP assembly, types, and operation, which are not showcased at length in this thesis, as the main aim is to present the potential effects of ESP on fan operation.

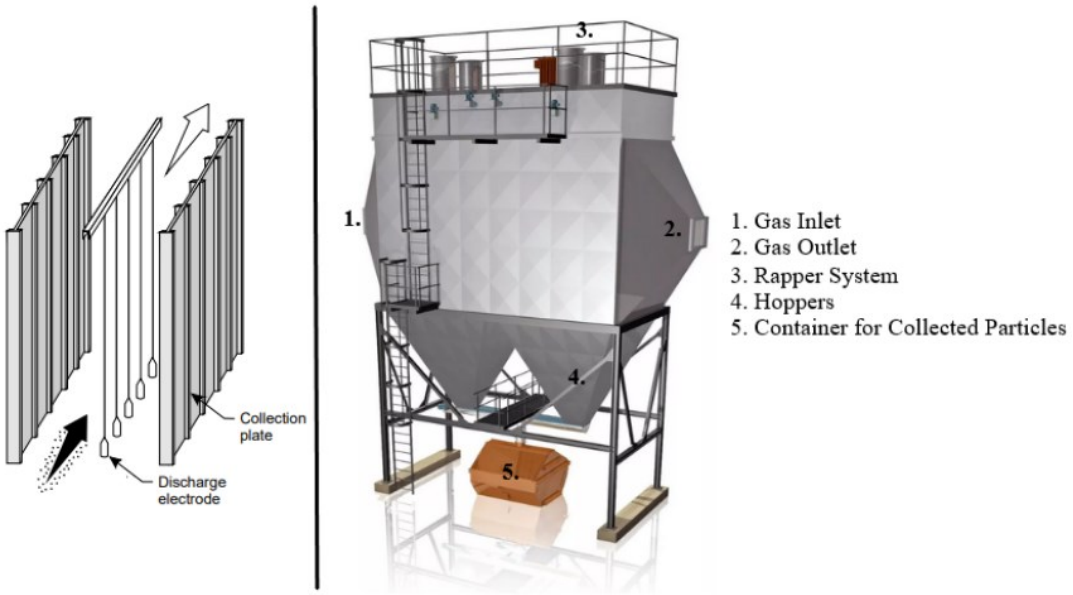

Figure 19. On left: flue gas flow direction through a plate-type ESP indicated by the arrows (Neundorfer 2016, 1–2). On right: ESP assembly with descriptions (Solarbiox 2022).

When the charged particles reach the grounded collector plates, their charge starts to slowly leak into the collector plates. Part of the charge remains and contributes to the forces holding the particles in the plates. Inter-molecular adhesive forces make the particles physically stick together due to their differing surfaces, while new incoming particles attach to the collected ones by cohesive forces. This means that the particles stick together and attract others. The formed dust layer must be then removed at certain intervals to ensure proper functioning of the ESP. (Neundorfer 2016, 7.) Cleaning the plates too infrequently weakens the process efficiency and causes to collected layer to become compact, making it very hard to clean.

The dust layer is still allowed to grow to a certain point before cleaning so that the process is not disturbed unnecessarily. Typically, the ESP functionality begins to deteriorate when the thickness of the dust layer exceeds 2.5 cm. (Hirvonen 2020, 13.)

The cleaning can be conducted via two different methods, utilization of water sprays or a process called rapping. In spray cleaning, the plates are cleaned periodically during the ESP use. Commonly, the utilized spraying liquid is water, but other liquids can also be utilized situationally if gaseous pollutant absorption is also desired. In the rapping process, the collected particles are removed for the plates by a shaking device that sends mechanical impulses, or vibrations, to the collection plates. The plates are rapped regularly during use, meaning that the flue gas flow does not have to be suspended, and the process can continue even during cleaning. Typically, the rapping takes place when the accumulated dust layer is relatively thick, 0.08 to 1.27 cm, which makes the layer fall of the plate as a large sheet to help reduce the chance of dust reattaching back to the plates during cleaning. Most modern-day ESPs have adjustable rappers that can vary the rapper intensity and frequency in accordance with the particle concentration of the flue gas. Regardless of the removal method, the removed dust falls from the plates into hoppers, which serve a ducting to system that directs the dust to a storage and to wait for further processing. (Neundorfer 2016, 78.)

ESPs are important in guaranteeing the best possible operation conditions for activities downstream from it. For example, if the particulate matter is not captured, it can start to accumulate onto the fan impeller and heat exchanger surfaces. The fan impeller mass will steadily increase, which decreases fan efficiency and potentially can cause the fan to vibrate. The vibration, or negligence in maintenance, can detach some of the particle mass, causing a mechanical imbalance on the fan impeller. If not detected, the phenomenon will cause a fan failure, leading to production interruptions and losses, and even compromises in employee safety. (Tamminen et al. 2013, 1.) Particulate accumulation on heat exchanger surfaces has also multiple negative consequences, such as decrease in effectiveness and increase in pressure drop (Kakaç et al. 2012, 237), which are discussed more in the next section.

Heat exchanger

Heat exchangers are used to transfer thermal energy in most fluid handling systems. They are utilized for both addition and removal of thermal energy, depending on system part's requirements. The transfer process can take place between two or more fluids, a solid surface and a fluid, or solid particulates and a fluid, the former being the most common. Traditionally, the heat transferring between fluids is conducted through a separating wall in a way that the heat transferring fluid does not mix with the system fluid. (Shah 1998, 1.) But in some heat exchanger types, the fluids come in direct contact with each other (Shah 1998, 1 and Kakaç et al. 2012, 3–4).

There are multiple heat exchanger types available on today's market. They are often designed for limited operating conditions, which emphasises the selection importance. Thus, certain knowledge on the system characteristics, such as temperature and pressure ranges, layout limitations, and fouling characteristics, should be known beforehand to ensure the selection of the most fitting heat exchanger for the system (Carotek 2022).

To facilitate this selection process, heat exchangers are categorized by their many attributes. Hewitt et al. (1994) categorized them into 4 groups, as Shah (1998) have utilized a 6-category division. Kakaç et al. (2012) have utilized a categorization method combining these factors, making the heat exchanger categorization be based on the following the main criteria:

- Type: recuperator or regenerator
- Construction geometry: tubular, plate-type, or extended surface
- Heat transfer process: indirect or direct contact
- Heat transfer mechanism: single-phase, two-phase, or combination
- Flow arrangements: parallel flow, counterflow, or crossflow (Kakaç et al. 2012, 1)

This categorization is by no means definite, as authors and publications have applied alternative categorization methods, such as categorization according to the process function, which are condensers, liquid-to-vapour phase-change exchangers, heaters, coolers, and chillers (Shah 1998, 3–4).

Recuperators are the most common heat exchanger type. In them, the heat transfer takes place between two flows through a separating wall or an interface between them. In regenerators, the same flow passage (matrix) is consecutively occupied by the two flows. First, the thermal energy of the hotter flow is stored in the passage. The energy then extracted from the passage when the colder fluid flows through it. The passage can either be rotated to make contact with the colder fluid, or the fluid pathway is changed to transfer the heat. (Kakaç et al. 2012, 1–3.) The difference in the principles is showcased in the following figure 20.

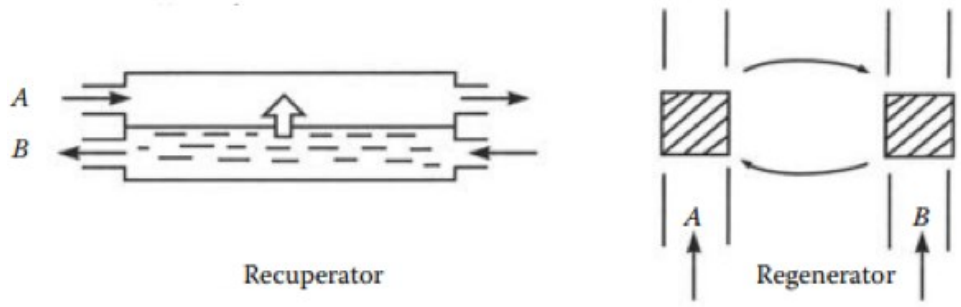

Figure 20. In recuperate heat exchangers (on left), hot flow, A, recovers some heat from flow, B. In regenerative heat exchangers, while the matrix (dashed square) is in the cold flow, A, it loses heat. While it is in the matrix hot stream B, it gains heat, thus the heat is regenerated. (Kakaç et al. 2012, 2.)

Depending on the heat transfer method, regenerators can be further categorized into fixed matrix and rotary regenerators, which can be subcategorized to disk- and drum-type regenerators. In the disk-type regenerators, the flow is axial, and the heat transfer surface is conducted via a disk. In the drum-type regenerators, the flow is radial, and the heat transfer is done through a hollow drum matrix. (Kakaç et al. 2012, 3)

Rotary regenerator heat exchangers are commonly applied as preheaters in power plants, where the two most utilized types are rotating-plate and the stationary-plate. In rotating-plate heat exchangers the rotor turns slowly, exposing the heating surface alternately to the flue gas and the entering air. As the heating surface is positioned in the flue gas stream it stores heat, and then when it is positioned into the gas flow, the stored heat is gets released which heats the gas flow. The stationary-plate heat exchanger has stationary heating plates and hoods that rotate across the heating plates. The heat transfer principle is the same as before, but instead of moving the heat plate, the gas flow is redirected. (Kakaç et al. 2012, 3–6.) The following figure, figure 21, shows a simplified version of these type of heat exchangers.

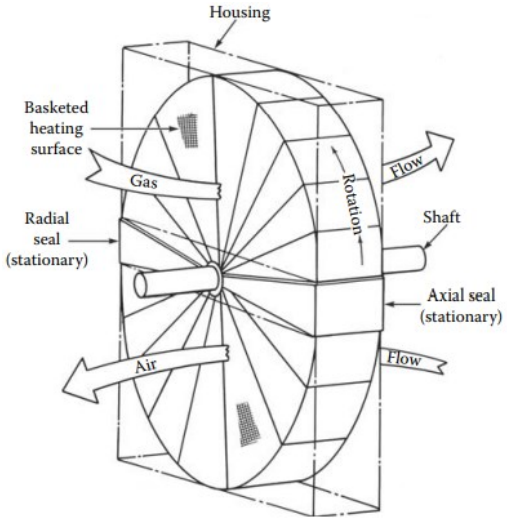

Figure 21. Rotary storage-type heat exchanger (Kakaç et al. 2012, 4).

Like mentioned before, the most common heat exchangers are recuperative. As going through all main and subcategories falls out the scope of the thesis, the following text showcases some of the most common heat exchanger types. Tubular heat exchangers are a widely used heat exchanger type. Their relatively low costs, in addition with the multiple available design and size options, has made them the first choice in countless industries. (Walker 1982, 45.) Types of tubular exchangers include single-, cluster, and double-pipe applications with tube-and-shell type being the most popular multitubular design (Walker 1982, 46–48).

The shell-and-tube heat exchangers consists of a large tubular enclosure, a shell, which houses carefully spaced tubing bundles inside it. The shell is manufactured from metal that can resist corrosion and endure high temperatures. The tubing of the heat exchanger, manufactured often from copper, stainless steel, or different alloys, holds in the fluid utilized in the heat transfer. (Industrial Quick Search 2022a.) Depending on the fluid flow layout, the fluid enters the exchanger through a front header and leaves through a rear header, or it recirculates back. Both layouts are available in various designs. Baffles are used to direct the flow along the tubes to attain higher heat transfer values and reduce fouling. (Brogan 2022.) Fouling is a particularly important factor to minimize, since accumulation of materials on the heat transfer surfaces increases thermal resistance, which then reduces the heat transfer rate and thus worsens the efficiency of the heat exchanger (Springer 2010, 80). An exemplary model of a shell-and-tube heat exchanger is presented in the following figure 22.

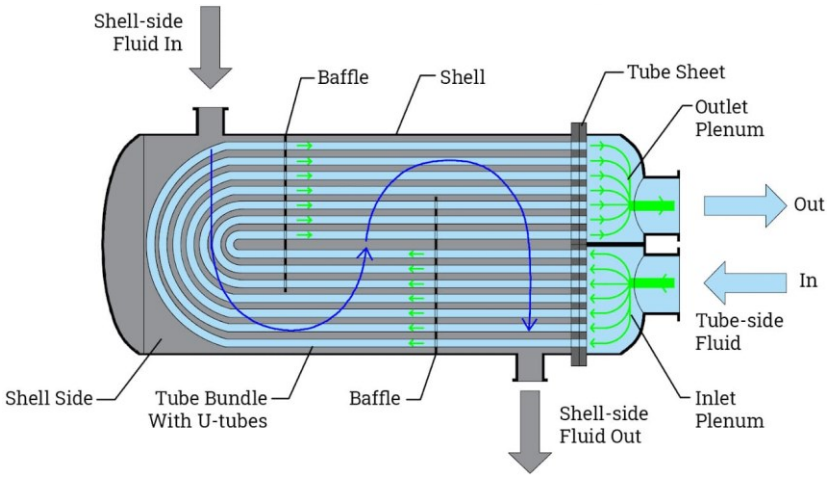

Figure 22. Cross-section of a U-type shell-and-tube heat exchanger (Industrial Quick Search 2022a).

Plate heat exchangers possess a lot of good characteristics which makes them a potential number one choice in various applications. According to Walker (1982), industrial plate heat exchangers can be divided in four designs categories, which are plate-and-frame, spiral, plate-coil, and plate-fin heat exchangers. Once again, there are other ways to conduct the categorization, for example Industrial Quick Search (2022b), and other sources and manufacturers, like Alfa Laval (2022), utilize other categorization methods.

The plate-and-frame heat exchangers have multiple advantages compared to the shell-and-tube heat exchangers (Walker 1982, 92–96). The main one is their more effective usage of space and smaller surface area requirements. This is achieved by their design that helps to reduce fouling, and to generate high turbulence and high thermal energy exchange, by grooved flow pathing and true counter current flow, in which the handled fluids flow in the opposite directions. (Walker 1982, 90.) A more effective system, with less material requirements, results in not only lower investment costs but also lower operating costs, as less energy is needed to be harnessed to generate the same heat transfer effect (Walker 1982, 90–92). The following figure 23 presents an example of a plate-and-frame heat exchanger.

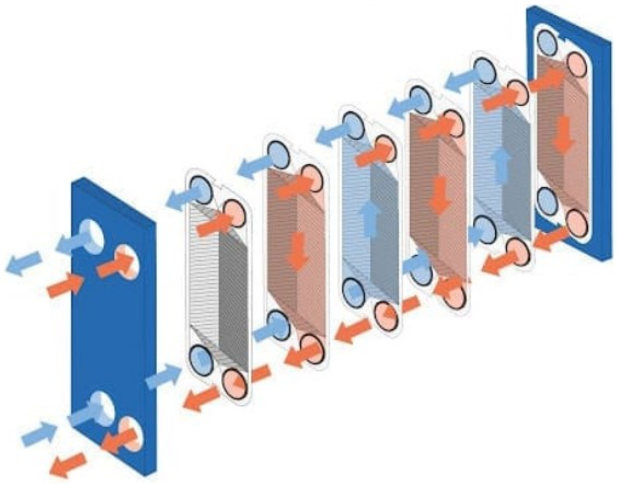

Figure 23. Cross-section of the parts of a plate heat exchanger (Industrial Quick Search 2022b).

Spiral heat exchangers include two circular metal plates rolled around each other to make two spiral flow passages for both inlet and outlet flows, which are shown in the figure 24. Originally developed to recover waste energy from contaminated water effluents in pulp mills in the 1930s (Walker 1982, 96), the spiral heat exchangers have a high efficiency, due to their ability to generate counter current flow. They are also known to be user-friendly, as the passages are self-cleaning and easy to access, and they require relatively small amount of space. (Gooch Thermal 2022.)

Plate-coil heat exchangers are often used in heating or cooling various chemical and other liquid containers, pools, and tanks, for example. They consist of two welded together metal plates which house the heating or cooling fluid. The surface of the plate-coil heat exchangers is regularly embossed with different patterns to better the efficiency of the heat transfer process. (Walker 1982, 102.) This type of a plate heat exchanger is also visualized in the following figure 24.

Plate-fin heat exchangers consist of metal fins brazed between flat metal plates. Whilst plain straight metal fins are often utilized, they can also be corrugated in various ways to enhance the heat transferring. For example, the herringbone pattern, in which the fins are placed at angle to generate a wavy gas flow path, can generate higher velocities and pressures. Plate-fin heat exchangers can be operated in a few different arrangements, counterflow arrangement being the most typical. Crossflow is often utilized in vehicle radiators, and cross-counterflow in liquid subcoolers. (Gregory 2022.) These different arrangements can be seen in the following figure 24.

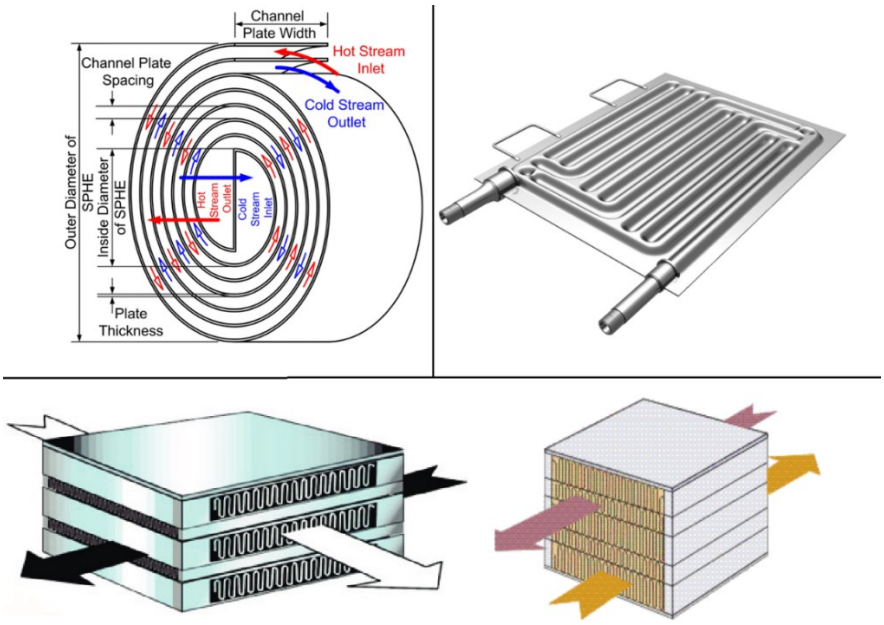

Figure 24. Left to right, on the upper row are a cross-section of a spiral heat exchanger (Sabouri Shirazi et al. 2020), and a 3-dimensional rendering of a plate-coil heat exchanger (Philippine Parkerizing, Inc. 2022). Crossflow and counterflow plate-fin heat exchangers are showcased on the lower row (Tu and Zhou 2015, and Gregory 2022).

Heat exchangers generate pressure drop, which Shah and Dušan (2003) conducts thorough analysis on by defining calculation formulas and identifying effects of different heat exchanger types on pressure drop amount. According to the book, pressure drop is considered to consist of two key components: pressure drop related to the heat exchanger surface, matrix, or core, and pressure drop stemming from the gas flow redirecting devices, for example manifolds, tanks, or inlet/outlet headers. Preferably, most the pressure drop should be generated by the former factor. The pressure drop in the heat exchanger is mostly generated by the core friction. If possible, this should account for over 80–90% of the pressure drop, as the generated turbulence can be utilized in the heat transfer location. Other contributors to pressure drop include the entrance, exit, and momentum change effects, and the effects of elevation changes. (Shah and Dušan 2003, 380, 419–420.)

If the heat exchanger malfunctions, and fails to cool the flue gas flow, the fan service life may shorten. Wheel, bearing, and shaft related failures typically occur in higher temperatures than the temperature of the flue gas when it enters the heat exchanger after the ESP. Consequently, the chance of fan failure resulting from insufficient cooling is small in regular bioproduct mill operation. (Saldanha 2020.)

Heat exchanger surfaces are susceptible to the accumulation of undesirable material, especially if the ESP cannot clean the incoming gas flow. While affecting the heat transfer ability and flow conditions of a heat exchanger, fouling can also corrode some materials that can ultimately lead to the heat exchanger failing. (Kakaç et al. 2012, 237.) Fouling generates an insulating coating on the heat transfer surface. This finite, sometimes thin, layer increases thermal resistance, decreases thermal conductivity, and causes changes in the flow field, which influences the pressure drop and power requirement (Kakaç et al. 2012, 240–241). In gaseous applications, fouling generally reduces heat transfer rate by only 5–10%, but it can have a huge effect on pressure drop and consequent power requirement, which can increase up to several hundred percent. (Shah and Dušan 2003, 865.) Thus, heat exchangers are more often cleaned due to excessive pressure drop than the failure to reach the heat transfer requirements (Kakaç et al. 2012, 241). In tubular heat exchangers for instance, the fouling

layer roughens the heat exchange surface, increases the outside and decreases the inside diameter the heating tubes (Kakaç et al. 2012, 241).

Fouling can also potentially cause production losses stemming from a shutdown or reduced capacity, and increase energy if cleaning is not conducted properly and excessive pressure drop, and reduced heat transfer are allowed to take place. (Shah and Dušan 2003, 863.) Most important factor in alleviating fouling related problems is a well-designed cleaning cycle. Depending on the fouling process, the cleaning cycles are often based on either ensuring reliability or minimizing costs. Cleaning is often conducted during shutdowns which are utilized to maintain and clean multiple components of the system. (Shah and Dušan 2003, 892–893.) Typical cleaning methods include washing, steaming, chemical washing, and mechanical removal, via blasting or stripping, much like with ESPs (Vahterus 2022).

4.1.2 Data sets

Data about the examined system was gathered from two different sources. Measurements conducted via physical instrumentation at the bioproduct mill were received from the contact person working at the bioproduct mill. These measurements utilized in the case analysis include:

- Flue gas pressure after the cooler [mbar]
- Flue gas temperature before the fan [°C]
- Total flue gas flow rate [Nm^3/s]

These measurements were recorded at the frequency of 10 seconds. They cover a one-year period from January 1st to the January 1st of the next year. The pressure and temperature data sets were unique for each fan, i.e., there were a total of four sets of both pressure and temperature data. The total flue gas flow rate measurement was conducted in the smokestack where the flue gas handled by the individual fans has been directed one common duct which

directs the gas outside. In the measurements, and consequently in this thesis, the normal conditions have been defined to be 101 325 Pa and 20 °C.

The VSD signal data was received from a contact person at ABB. ABB is the manufacturer of the variable-speed drives examined in the thesis. The received data sets include:

- Torque [% of nominal]
- Speed, without filter [rpm]

The signal data was recorded from January 1st to December 14th of the same year, at the frequency of one second. Only exception being an 8-week period from February 20th to April 17th, during which no VSD signals were recorded. All examined fans have their own VSDs, meaning the torque and speed data were recorded for all four fans separately.

Contact was also made with the fan manufacturer. This was done to gain access to the fan curves and to gather information on the specifications of the fans. They were able to provide a detailed catalogue that listed information about the examined fans and granted access to the fan curves. The fan curve information was then used to rule out fans whose fan curves were unsuitable for model-based estimation, and to model the fans selected for the case analysis.

4.1.3 Applicability of VSD-signal-based monitoring

This subchapter analyses the applicability of model-based estimation monitoring in the studied flue gas handling system. The phenomena examined by VSD-based methods are restricted to the ones discussed in the subchapter 2.1.1 and listed in the table 1. The following sections showcases the factors that can be monitored in the studied system, with the received data sets. Figures are used to visualize the model-based estimations and measured values. Differences between the two are also showcased. Reasons for the differing values are discussed, and the effect of a potential correction factors, introduced to decrease these

differences, is also visualized, and discussed. These findings of the applicability are then compiled in a table.

Operation point estimation can be conducted with the model-based calculation formulae presented in the subchapter 2.3. By examining the VSD data received from the contact person, it was noticed that all four flue gas fans operate in almost matching fashion. Thus, the operation point examination was conducted jointly by adding all the individual flow rate values together. This allows the estimated and measured values to be compared, since the flow rate measurement instrument resides in the smokestack, it generates a single value that is the total sum flow rate of all individual fans.

According to the bioproduct mill contact person, 3 maintenance breaks occurred during the studied period. Those breaks can be recognized from the estimation values, in the following figure 25. During start of January, the turn of May and June, and start of October the estimated flow rate declines as some of the fans are off and maintained. In the measured values, these breaks have resulted in an increase of flow rate. For example, during the maintenance in the summer, May/June, the measured flow rate increases up to the limit value of 670 Nm^3/s, which is not realistic according to the VSD data. The figure 25 visualizes the estimated and measured flow rate values during the studied period. The visualized model-based estimation values are calculated using the calculation formulae of subchapter 2.3, and data showcased in the subchapter 4.1.2.

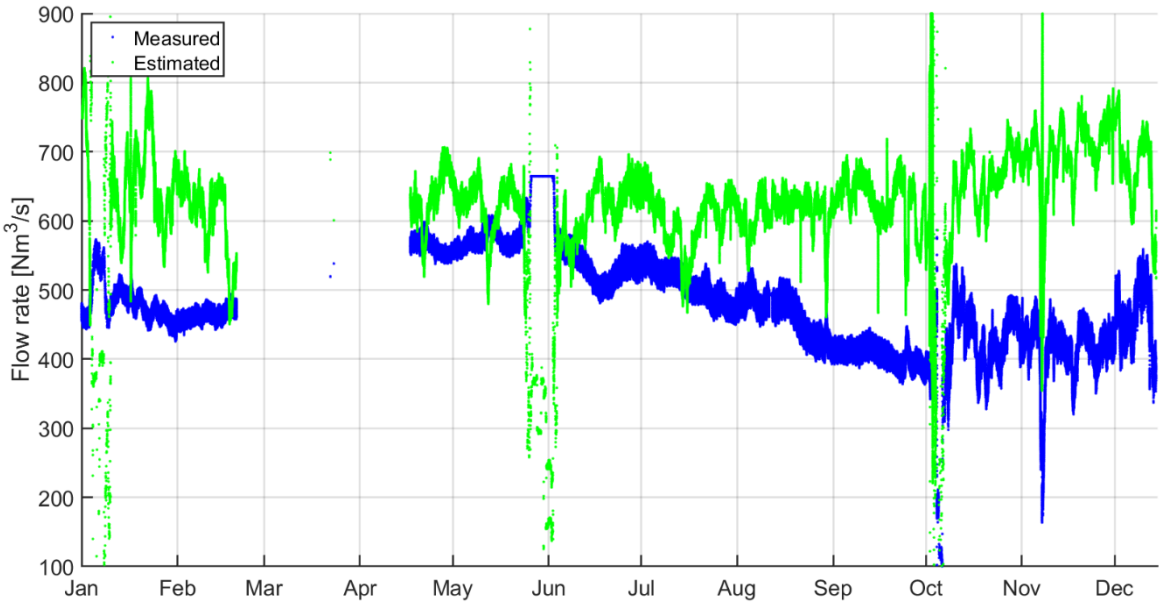

Figure 25. The measured and combined estimated flow rates of the four flue gas fans.

As seen in the figure 25 before, the model-based flow rate estimation seems to initially not be suitable for operation point estimation in a flue gas application of this type. But, after the October maintenance the behaviour of the measured values changes, and the trends of the model estimated values start to match with the measured values. It is not known what type of maintenance procedures occurred, but it can be speculated that some cleaning or calibration took place that influenced the measurement values. After the maintenance, estimated values imitate the trends of measured flow rate data in a great manner. But like mentioned in the literature section, model-based estimation possesses uncertainty, even if temperature and pressure data would be provided, and utilized, in density calculation. Like it can be observed from the prior figure 25, October onwards both trends are similar, but a certain estimation error is clearly constantly present. The relative difference between the estimated and measured values can be calculated with the following formula (10):

$$Relative\ error = \frac{Q_{est.} - Q_{meas.}}{Q_{meas.}} * 100\% \tag{10}$$

In the formula (10), Q represents to flow rate, while the subscripts “est.” and “meas.” refer to estimated and measured values, respectively. When the values generated by formula (10)

are positive, it indicates that the estimated values are greater than measured. And consequently, they are smaller when the generated values are negative. (Online Math Learning 2005.) The following figure 26 showcases the relative error as function of time. The months in which the measurement instrument is assumed to be providing faulty flow rate values are excluded from the figure. It instead focuses on the time after the October maintenance.

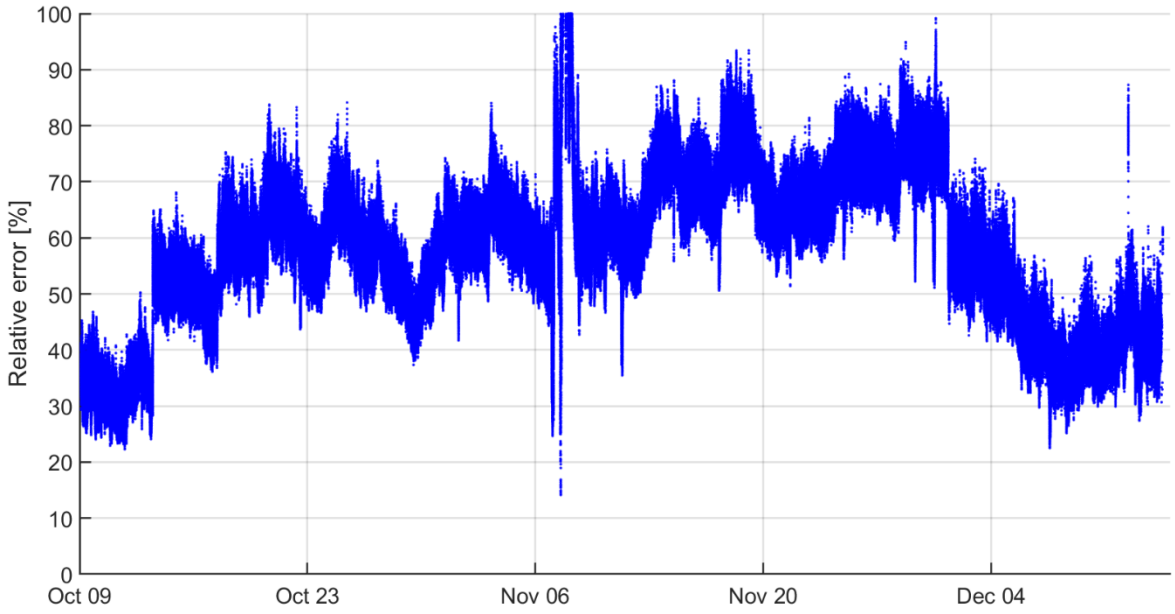

Figure 26. Relative error between the measured and estimated flow rates after the October maintenance.

Like it can be seen from the figure 26, the estimated values are generally 30 to 80 percent higher than the measured values. During the examined time from October 9th to December 14th, the average relative error was 58%. On November 7th, the error becomes vast as the estimated values suddenly rise to absurdly high values. Inspecting the VSD data reveals that during that date, the fans very run at significantly lower speeds and torque values, which caused the estimation to generate wavelike unrealistic values that rise and fall in rapid succession. This type of a phenomenon happens in the studied data only once, and thus it can be considered a calculation anomaly.

This difference between the values could potentially result from a difference in the realized and calculated gas properties. The estimation utilizes a theoretical value for gas density calculated with formula (6) that relies on pressure and temperature measurement provided by the contact person. The measurement instrumentation is positioned in differing locations of the ductwork. Whilst they are close to each other, pressure measurement being after the cooler and temperature being before the fan, this difference can still generate variability in density calculation. Also, the gas flow is assumed to be dry since relative humidity only has a trivial effect on density. But still, in real-life condition the humidity could affect the density. Used wood types, their quantity, pre-treatment, and moisture, and the consequent moisture of the combusted fuel, i.e., black liquor, are all aspects that could affect the recovery boiler process and flue gas fans' operation. Examining them could potentially provide insight on the gas composition and flow rate behaviour but their examination is outside the scope of this thesis, since the focus is on the monitoring. Furthermore, the differing location of the flow rate measurement could affect the values. The flow rate measurement is located further in the ductwork than the fans, which could generate difference in the estimated and measured values. But this location difference can also be regarded as a positive since it enables detection of negative events in that part of the system. This is discussed more on the following section.

Even though, uncertainty is associated with the generated estimations, the estimations can still be used in monitoring. Different phenomena, like fouling, leaks, and surplus flow, can be recognized from the estimated fan operation trends. Fouling is a phenomenon that can be recognized without additional instrumentation. Like mentioned before, fouling generates extra pressure drop by particulate accumulation and increasing flow resistance (Pöyhönen et al. 2021, 2). If the system is assumed to be a clean after a maintenance, the operation state and power requirements should be compared to it. Decreasing flow rate, without lowering rotational speed or torque, could result from fouling. In the studied system, this type of phenomenon does not find time to occur as the maintenance schedule is well designed, and strictly enforced, to ensure system cleaning before complications could arise. Leakage and surplus flow can also be monitored. This can be accomplished in conjunction with the physical measurement instrumentation. The fact that the estimations and measurements describe operation points at different points of the system, could be utilized as an advantage.

Vast differences in trends could indicate that there is a leak in the system. This requires the additional instrumentation to work properly, which in the studied system seems to be doing so only during the last 2 months. But still, during that period, unusual deviation in trends was not exhibited, like seen in the figure 28. Also, knowledge of the system operation is necessary in recognizing typical trend deviation from leakage and surplus flow in systems where changes in flow rate, at certain or random times, is a part of the system's regular operation.

The operation point estimation can also be used in calculations. The flow rate value can be utilized to calculate specific energy consumption of the system, as shown in following formula (11). Specific energy consumption outlines the total energy consumption per unit of output, which in this case is a normal cubic meter of gas.

$$e = \frac{\frac{P}{Q}}{3.6 * 10^6} \tag{11}$$

In the formula (11), P stands for power, Q for flow rate, and *e* for specific energy consumption. (Odyssee-Mure 2023.) A coefficient of $3.6*10^6$ has been used to convert the units to kWh/Nm^3. The power value has been calculated with the formula (8) with the VSD signal data, and it naturally stays the same for both estimated and measured flow rates. Like seen in the following figure 27, the trends of the two figures imitate each other well. Estimated operation points generate lower specific energy consumption values than the corresponding measured values. This happens due to the estimated flow rate values being greater than the measured ones, and the calculated power value remaining the same for both cases. Thus, with the estimated operation points, same energy is consumed to generate a larger flow rate, which results in lower energy consumption per cubic meter of gas. Once again, the figure 27 is restricted to the time after the maintenance in October to simplify the comparison in the figure.

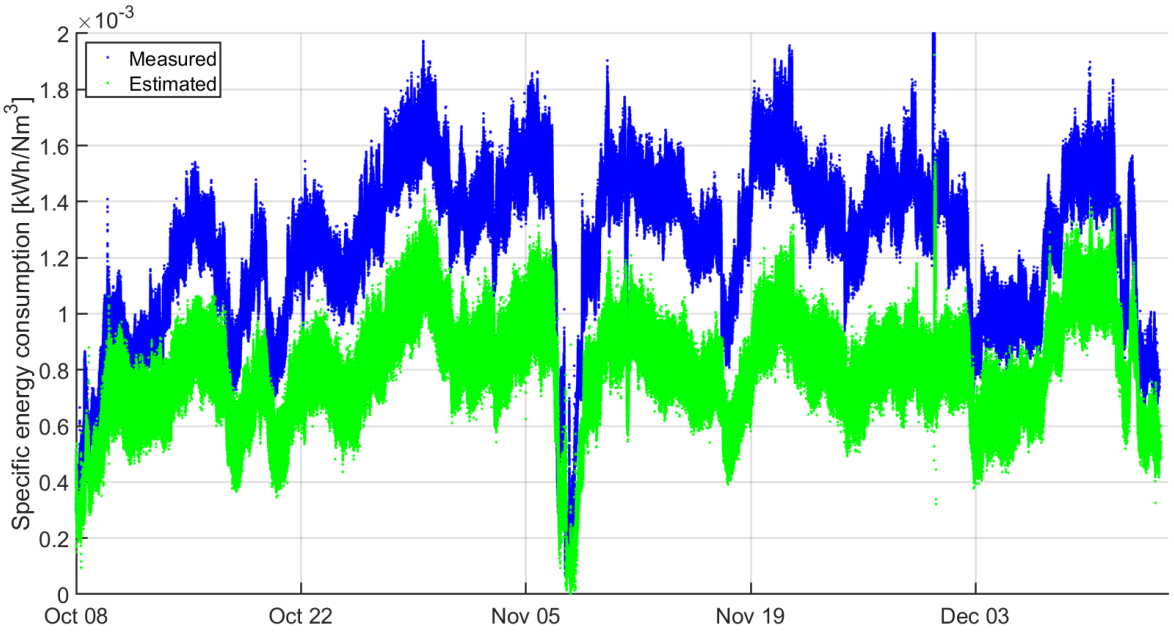

Figure 27. Specific energy consumption per of cubic meter of moved gas for measured and estimated flow rates.

As the main cause for differing values was identified as probable density change, a correction factor can be applied to the earlier presented formula (6), to negate its effects, and to generate estimated with a lower relative error. This improves the visualisation of trend deviation, as the curves are now presented closer to each other. The following formula (12) presents the corrected density that is then subsequently used in the formulae (7) to (9) in generating corrected flow rate estimations. The process was conducted iteratively multiple times to generate a factor which reaches a minimal relative error between the estimated and measured values.

$$\rho = \left(\left(\frac{p_d}{R_d * T} \right) + \left(\frac{p_v}{R_v * T} \right) \right) * Correction\ Factor \tag{12}$$

In formula (12), all the characters remain the same as in the formula (6), except the addition of the *Correction Factor* that multiplies the calculated density with a factor that has been determined to generate the lowest relative error. This relative error examination as conducted on the time span after the October maintenance, since the relative error values before that

could not be regarded as reliable and including them would generate a different factor. The following figure 28, visualizes the measured, estimated, and corrected estimated flow rate. After iterative investigation, the correction factor with the lowest relative error was determined to be 1.142. By utilizing this factor, the average relative error for the values from October onwards fell from 58% to 6.4%. The factor and relative error reduction were calculated by excluding the anomaly of November 7th when the relative error rose to more than 100%.

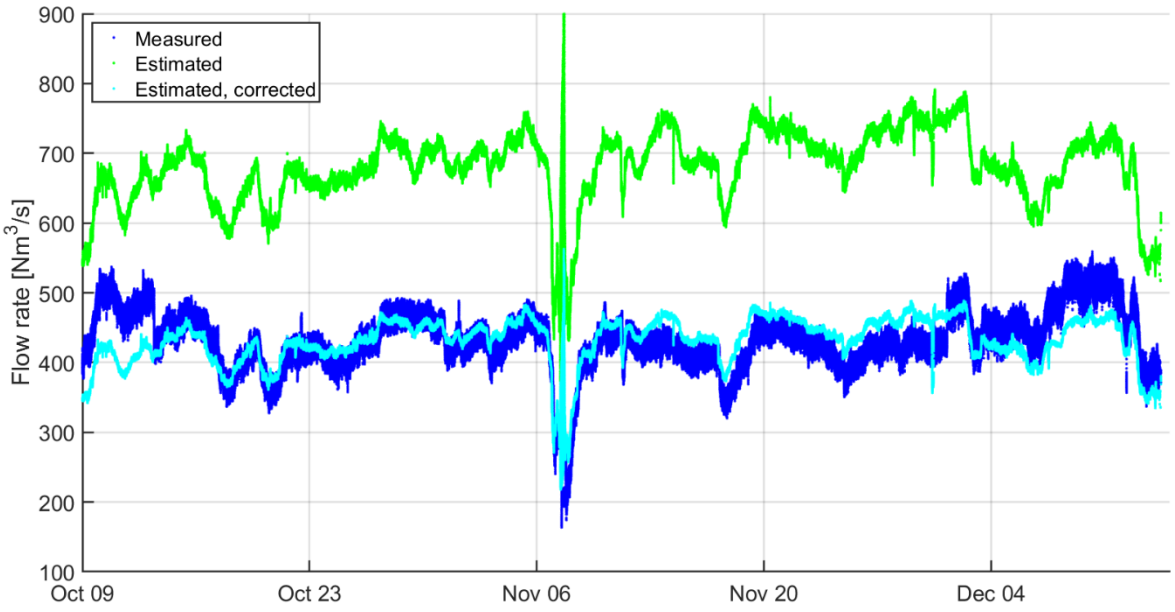

Figure 28. The measured, estimated, and corrected estimated flow rates of the four flue gas fans combined.

Like visualized well by the corrected curve in the figure 28, the trends of both estimated and measured values represent each other well. Leakage or surplus flow can be concluded to not be present in the system. Other inexplicable phenomena, such as fan impeller wear, might not be visible in such a short period of time as two months. But like it can be seen in the figure 28, such anomalies are not present in the operation. The following table 3 concludes which phenomena monitoring this data set of the bioproduct mill flue gas system could be applicable to.

Table 3. VSD monitoring applicability in bioproduct mill flue gas fans.

VSD monitoring applicability in: bioproduct flue gas fans	
Phenomena monitoring via standalone calculations:	
Fan surge	
Fan or pump rotation direction	
Impeller contamination build-up	
Phenomena monitoring via operation point monitoring:	
Specific energy consumption	Calculation
Leakage or surplus flow	Redundancy
Fouling	Operation point examination

Specific energy consumption can be calculated via a calculation using the model-based estimation operation point values. Operation point examination can be utilized in recognizing fouling. Leakage or surplus flow can be monitored in tandem with redundancy provided physical measurement instrumentation and model-based estimation. Whilst glaring issues in the studied system were not discovered, the model-based operation point estimation, and its utilization in monitoring, was conducted successfully. The aspects related to the VSD-based monitoring are discussed more in detail in subchapter 4.3.

4.2 Odorous gas treatment

As mentioned before, the kraft process generates various chemical compounds of which some are odorous. This odour results from different sulphur compounds, which are often referred as total reduced sulphur (TRS). The odorous gases are often referred to as non-condensable gases (NCG), which are usually divided into concentrated and diluted non-condensable gases (CNCG and DNCG) in accordance with their sulphur concentration. NCG are generated at almost all phases of the kraft process. Main CNCG sources are the cooking and evaporation plants. Also, pulping from hardwood typically generates more CNCG compared to softwood pulping. DNCG are generated at different phases of the kraft process, such as the evaporation plant, causticizing, and recovery boiler are sources in the chemical cycle, while in the fibre line, the sources include screening, pulp washing, and storage tanks. (Suhr et al. 2015, 244–245.)

There are various ways to dispose NCG, such as thermal oxidation, absorption using scrubbing, or combustion in the lime kiln or a dedicated burner (Suhr et al. 2015, 244). The gases can also be directed outside, but to avoid causing nuisance to the residents of the surrounding area, and generating additional atmospheric emissions unnecessarily, this is done only when none of the above methods are available. Also, Finnish legislation has set guide values to different sulphur emissions, including TRS. The legislation specifies that a facility's second highest daily emission value during a month should be limited to 10 $\mu g/Nm^3$. (480/1996.) This encourages facilities to be aware of their TRS emissions which are monitored nationally by the Finnish meteorological institute (Finnish meteorological institute 2020).

While processing NCG, it is important to note that it's TRS content can form an explosive compound if mixed with air at certain concentrations. Therefore, the dilute and concentrated gases are processed at their own lines which prevents the concentrations from getting between the explosive limits. Explosive limits present limit value for NCG concentrations where interaction with air causes an explosion. In practice, the DNCG are handled below their lower explosive limit, while correspondingly, CNCG are processed above the upper

explosive limit. Thus, the concentration of the DNCG can be kept so weak that the compound does not ignite, and the concentration of the CNCG is so high, that it does not cause an explosion. These limits are illustrated in the following figure 29. Due to their many sources, the volumes of DNCG generated in a kraft process mill are high, while CNCG generation is typically lower. (Lipponen 2016, 12.) Still exceptions can exist as the amount of CNCG may fluctuate extensively (Suhr et al. 2015, 245).

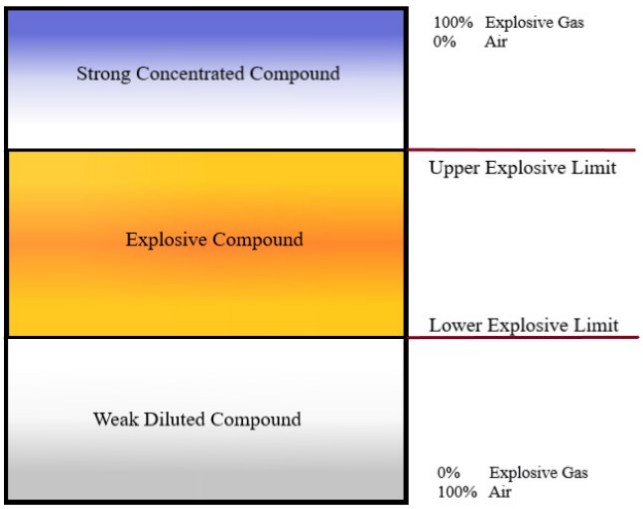

Figure 29. Explosive limits (modified from Tolvanen 2022, 17).

Odorous gas treatment fan was selected as the second studied fluid handling device. It possesses fan curves suitable for the model-based modelling, and appropriate measurement and VSD signal data of the fan operation has been recorded, like with the flue gas fans. The studied fan is utilized in directing the DNCG to incineration in the recovery boiler. The gases can also be guided straight outside through a smokestack, if incinerating them is not possible. The gas flow route and the system components are showcased in the following figure 30. Due to its typically high level of water vapour DNCG needs to be treated before entering the fan and combustion. The DNCG are first washed with diluted white liquor in a scrubber. After that, the gas flows through a condenser. Its main function is to cool the gas flow, but it also can be utilized in removing water vapour from it. From the condenser the gas flows to a droplet separator, which removes the final excess particles and water vapour before the gases arrive to the studied fan. The fan is controlled based on the negative pressure of the odorous gases. The fan directs the gases to the recovery boiler from incineration. The duct

leading to the recovery boiler also includes a heat exchanger, which used to preheat the gas before incineration. If the incineration is not possible, a damper closes the duct, and the gas is directed to a smokestack leading directly outside.

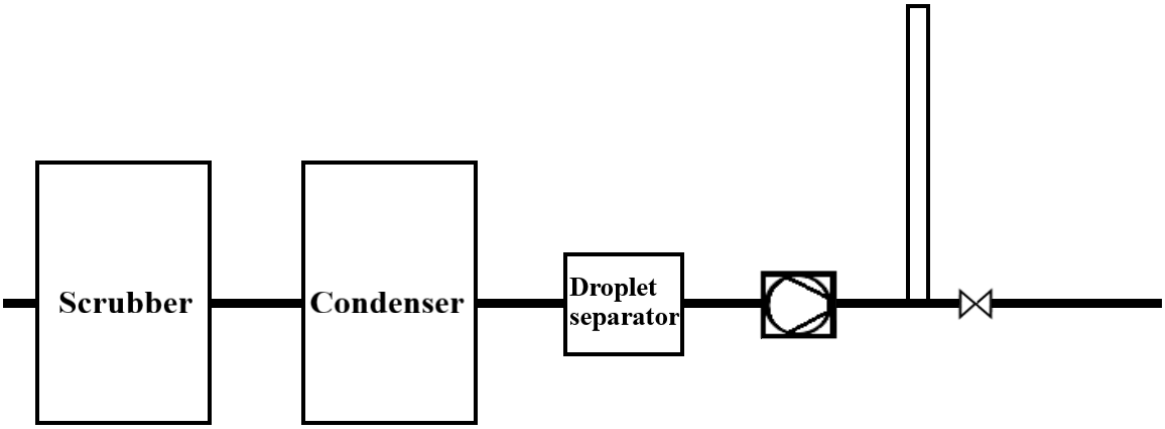

Figure 30. The studied diluted odorous gas handling fan system.

The diluted odorous gas treatment system also includes complex condensate ducting, which may have their own effects to the flow rate. But after communication with the contact person, their effect on the operation was deemed to be insignificant. Thus, they are not depicted in the figure 30. These ductworks are utilized in automatically directing different compounds out of the system, into tanks with water locks, for example.

Maintenance of the odorous gas system is takes place during the same time as the recovery boiler maintenance, once in 4 to 5 months. Like with other fluid handling systems, leaks and other problems are resolved. As an example, maintenance of the condenser and droplet separator systems removes excess particles and condensate, ensuring that the excess water vapour removal stays effective, so that the gas flow moisture is kept at a level suitable for the recovery boiler incineration.

4.2.1 System components

The following sections describes the components utilized in the diluted odorous gas fan system operation. Although the major DNCG sources were listed in the formed subchapter, they are not examined in this subchapter. While the odorous gas generating unit processes influence some aspects of the studied fan operation, such as the volume of handled gas, they are still deemed to not have enough of a direct impact on the everyday fan operation to warrant their thorough examination in this subchapter. The unit processes of a bioproduct mill were also already showcased in the 3rd chapter, which has been considered to provide sufficient knowledge of their operations. As per the scope, the sections focus on the components affecting the studied fan. These components include the scrubber, condenser, and droplet separator, which are all located in the same ductwork before the studied fan. All these components are reviewed in their own sections. Scrubbers are used as air pollution control devices to capture certain particles from the flow and prevent them from moving further in the system. The section showcases advantages, and weaknesses of scrubbers, their unique configurations and efficiencies. Condensers are a type of a heat exchanger used in processes where moisture collection and cooling of flow are desired. Heat exchangers operating in two-phase and multiphase flow conditions are categorized as condensers and vaporizers. (Shah 1998, 120.) As the variety of condenser geometry, phase-change, and operation conditions is so vast, along with the fact that the most common heat exchanger types were meticulously examined in the subchapter 4.1.1 before, the section focuses on showcasing the condensing principles, most common condenser types and applications, and potential problems related to the condenser examined in this thesis. Droplet separators are used to capture the final moisture before the gas flow enters the fan and recovery boiler. Since the utilized droplet separator type is unknown, the section showcases the four most common types, conditions they are most suitable for, and characteristic pressure loss generation.

Scrubber

Scrubbers are air pollution control devices in which a gas flow is subjected to contact with a wet or dry absorber that aims to force certain particles to defect from the gas to the absorber. The absorber is sprayed into the entering gas flow as fine droplets. Like the electrons in an

ESP, they attach onto particulate in the flow. The size and mass of the particulates to grows, which causes them to be either collected by subsequent filtration more easily, or they flow with the sorbent into a collection container. (Cooper and Alley 2011, 231.)

The two main methodologies of scrubbing are wet and dry scrubbers, former of which being the popular. In dry scrubbers, dry sorbent is sprayed into the gas flow, which mitigates the sludge problems related to wet scrubbing. Dry scrubbing has been applied to remove acidic gases from boilers, and incinerators. (GlobalSpec 2023.) As the studied scrubber utilizes white lye liquid, dry scrubbers are not analysed in this thesis. Some of the key advantages and disadvantages of wet scrubbers compiled by Cooper and Alley (2011, 237–238) include:

Advantages

- Ability to treat flammable and explosive dusts
- Provides gas absorption and dust collection in a single unit
- Neutralizes corrosive gases and dusts
- Provides additional cooling of the gas flow

Disadvantages

- High likelihood of corrosion related issues
- Effluent can generate water pollution
- Collected particulate can contaminate, and not be recyclable
    - Waste sludge disposal potentially expensive

Nowadays, there are several different types of scrubbers available that vary in both function and performance. In spray-chamber scrubbers, showcased in the figure 31, gas flow passes through a circular or rectangular chamber while making contact with the liquid sprayed in the chamber by nozzles. Droplet size, nozzles geometry, and gas flow path can be modified and varied to enhance the separation efficiency. Spray-chamber scrubbers can reach a collection efficiency of 90% particles larger than 8 μm. Despite their relatively low

particulate collection efficiency, they are utilized in various industrial tasks, such as controlling paper dust in paper towel manufacturing, and latex aerosol in fiberglass manufacturing. Their power consumption is also comparatively low, which makes it a viable option for many facilities. (Cooper and Alley 2011, 231–232.)

Scrubber's collection efficiency can be improved by modifying a typical spray-chamber scrubber by installing the inlet to the side of the chamber, as seen in the figure 31. The gas flow enters the chamber tangentially, which enables it to reach higher velocities. This allows cyclone spray-chamber scrubbers to utilize smaller droplet size, which in conjunction with added centrifugal force, improves its particle collection efficiency. Cyclone spray-chamber scrubbers provide a collection efficiency 95% for particles larger than 5 μm. Their operation requires more energy, but less water, compared to the spray-chamber scrubbers. (Cooper and Alley 2011, 233.) According to the United States Environmental Protection Agency (EPA 2003a, 2), cyclonic and regular spray-chamber scrubbers are a popular choice in wet scrubber applications where the gas flow is forced into contact with a sorbent to absorb and react with the contained SO_2.

Venturi scrubbers consist of a venturi-shaped chamber, showcased in the figure 31, to which a liquid is added at low pressure through which the treated gas flows in a high speed. Gas atomizes the liquid, entraining particles and pollutants in the droplets. Venturi scrubbers take advantage of the fact that the wet scrubber efficiency is strongly related with the relative velocity between the liquid droplet and particulate to collect 98% of particles larger than 0.5 μm. This requires high throat velocity which leads to high energy consumption and high pressure drop, which has been tried to be negated by venturi jet design. In it, the liquid travels at high speed, instead of the gas. As a result, they have a lower pressure drop, but a lower efficiency as well. Their collection efficiency is 92% for particles larger than 1.0 μm. (Cooper and Alley 2011, 235.) Venturi scrubbers used in controlling particulate matter emissions from industries, like chemical, pulp and paper, mineral, and metal production industries (EPA 2003b, 1).

Other scrubber types include orifice and impingement scrubbers, latter being a further developed model from the former. In orifice scrubbers the gas flow collides with the liquid and a series of baffles. In impingement scrubbers, seen in the figure 31, the gas-liquid mixture moves through a perforated bed containing a liquid and foam layers, followed by a plate directly above the perforations. Advantages of these type of scrubbers are their low energy consumption and liquid requirements. Both types also have a relatively good collection rate of 97% for 5 µm particles. Industrial use cases of orifice scrubbers include food and pharmaceutical processing and packaging, and manufacturing of chemicals, ceramics, and plastics (EPA 2003c, 1). Impingement scrubbers are typically utilized in food and agriculture industries, and iron foundries (EPA 2003d, 1).

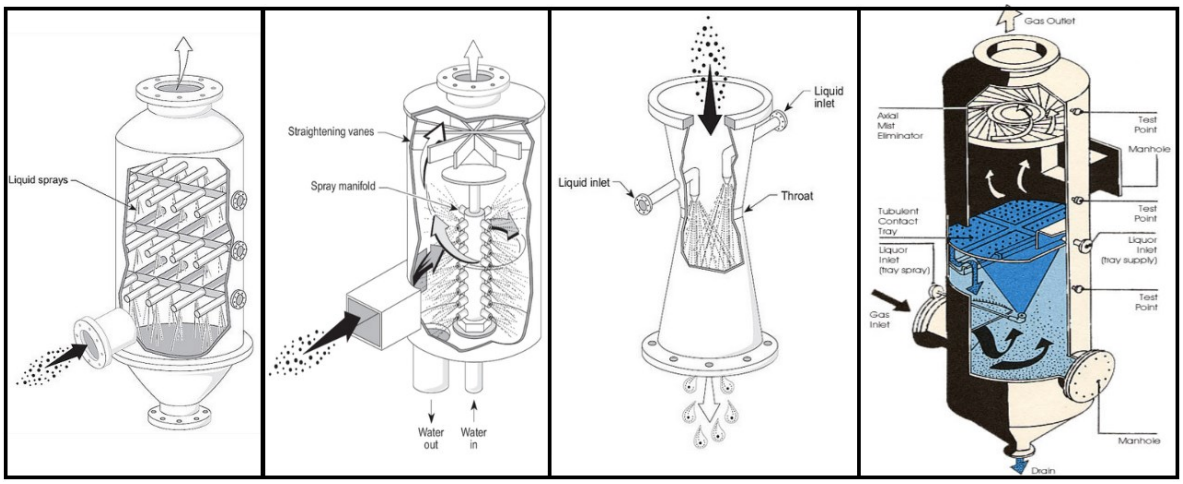

Figure 31. Scrubber types from left to right are spray-chamber, cyclone spray-chamber, venturi, and impingement scrubber (GlobalSpec 2023).

All scrubber types have similar maintenance related to them, with some types being more prone to some phenomena than others. Nozzle plugging and erosion, and consequent cleaning and replacement are important with all types. Especially, with spray-chamber scrubbers, this process makes up most of the maintenance. The liquid recycled in the scrubber must be filtered or settled adequately to avoid nozzle from clogging. (Cooper and Alley 2011, 232.) Since orifice scrubber design is rather simple, and it includes only few moving elements, its key maintenance interest is removing the sludge that accumulates at

the scrubber's bottom. (EPA 2003c, 3). Impingement scrubbers are designed with user access to the compartments, making them clean and maintain (EPA 2003d, 3).

Condenser

When fluid in a vapour phase makes contact with a cold surface, thermal energy is transferred from the vapour to the surface. The fluid temperature decreases, and the density increases. If the temperature of the wall is less than the saturation temperature of the vapour, the vapour condenses on the surface. The saturation temperature is the temperature in which a fluid transforms from liquid into vapour at a corresponding saturation pressure (Wärtsilä 2023). The temperature where this phase change takes place depends on the vapour pressure. The saturation temperature increases as the pressure rises. When multiple gases or vapour are present, the saturation temperature of a particular component primarily depends on the components partial pressure but is affected also by other factors. (Walker 1982, 40.)

Like mentioned before condensers are a heat exchanger category that try to reduce the moisture level in the treated gas flow. They also can be categorized similarly to the division seen in the subchapter 4.1.1 by Kakaç et al. (2012), with some categories being more favoured than others. Indirect condensing is the most common method, with a shell-and-tube condenser being one of the most common types (Shah 1998, 120). As examples, shell-and-tube heat exchangers are widely used as condensers in power plants, various fields of the chemical industry, petroleum refineries, and air-conditioning and refrigeration applications (Shah and Dušan 2003, 16). Tube-fin heat exchangers, which utilize finned tubing between plates, are another commonly used condenser type in electric power plants, air-conditioning and refrigeration industries. (Shah and Dušan 2003, 43.) Welded and other plate heat exchanger are utilized as condensers in the refrigeration industry too (Shah and Dušan 2003, 30). Spiral exchangers are also well suited as condensers. They are cited to be used in pulping industry for cleaning relief vapours in kraft pulp mills. (Shah and Dušan 2003, 32.)

Indirect condensation process occurs in two main ways: dropwise or filmwise. In dropwise condensation, the liquid condensate congeals into droplets, leaving most of the heat

exchanging surface void of liquid. The droplets are removed from the surface by gravity. In filmwise condensation, the liquid condensate wets the entire heat exchanging surface, isolating it from the incoming vapour. (Walker 1982, 40.) Difference between the condensation methods is show in the following figure 32.

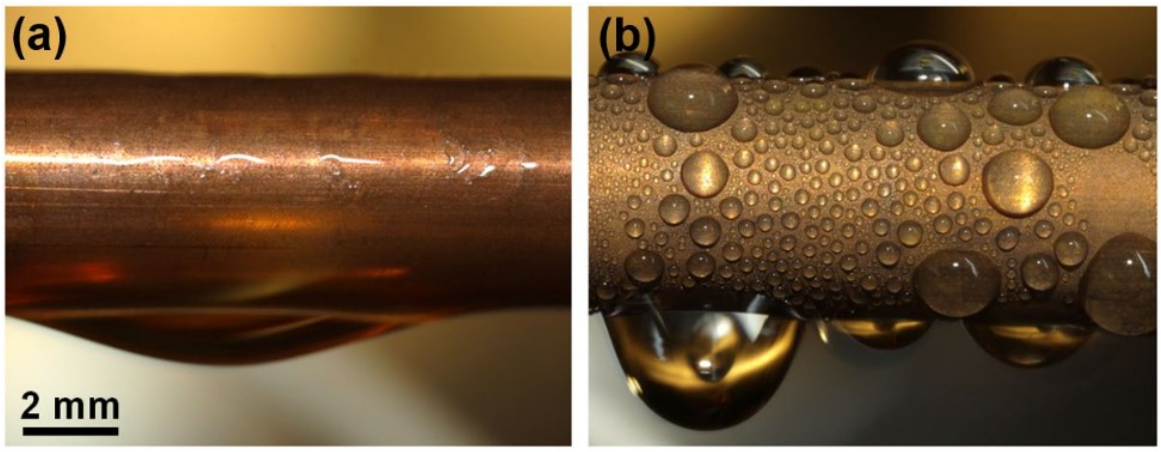

Figure 32. Filmwise condensation on a smooth hydrophilic copper pipe (a), and dropwise condensation on a silane coated smooth copper pipe (b) (Zhao 2018, 11 and Miljkovic 2013, 24.)

Since part of the heat exchanging surface remains exposed in the dropwise condensation, it has been quoted to be up to 10 times more effective than filmwise condensation. In use, depending on the application, the condenser surfaces become contaminated to varying degrees or degrade to filmwise condensation. Efforts are made in researching and developing surfaces that promotes dropwise condensation. Different additives, such as silane or oils, are added to the surfaces to prevent the condensate from generating a film. However, these methods cannot permanently prevent filmwise condensation from occurring, thus condensers capable of dropwise condensation are invariably also designed from filmwise condensation. (Walker 1982, 40.)

NCG are present in the studied system. Condensation of a fluid that includes NCG is referred to as partial condensation (Shah 1998, 120). Communication with the bioproduct mill contact person revealed that the applied condenser's main task is to cool the gas flow, while the main part of moisture retention is handled by the droplet separator. This simplifies the process since condensing is not the focal point of the process, but instead a useful by-product.

If the aim would be to condense the gas flow, shell-and-tube heat exchangers would be recommended as they are suitable for partial condensation with NCG (Shah 1998, 123).

Presence of non-condensable gases causes changes in the saturation temperature and pressure. Flow maldistribution is one the potential deleterious effects of partial condensation. However, this issue can be mitigated with good ventilation and condensate drainage. (Shah 1998, 145.) As mentioned before, the studied system includes sophisticated condensate systems, thus flow maldistribution is unlikely to take place. Considering this, along with the fact that the condenser aims to act as a cooling heat exchanger, harmful effects typically related to partial condensation are not likely to take place in the studied system.

Same procedures are performed in condenser maintenance as with any other heat exchanger. Accumulated fouling and condensate are removed from the heat exchanger surfaces, which enhances its cooling efficiency and reduces energy consumption. It is essential to maintain the condenser's cooling capability at a maximum level to guarantee optimal operation of the droplet separator. If the treated gas temperature is too high, the water vapour included in the gas flow does not saturate. This decreases the droplet separator efficiency as it might not be able to capture typical levels of moisture. If the gas flow is too moist, it can be determined to be unfit for incineration and directed outside. The recovery boiler is designed with the NCG incineration in mind, hence directing it outside is not optimal. Also, Finnish legislation limits the amount of sulphur, included in the NCG, a facility can emit outside, so the smokestack utilization should be tried to be minimized.

Droplet separator

Droplet separator dehumidifies the gas flow to reduce the moisture accumulation on the fan surface and decrease the amount of moisture content ending up in the recovery boiler combustion. Since liquid separation from the gas flow can be done in various ways, multiple separator solutions have immerged. The separators can be divided into four general categories based on their structure: wire mesh, fibre, vane, and cyclone. Once again, the

design phase has an immeasurable importance in assuring optimal system performance as all types have their preferred operation temperatures, pressures, and droplet sizes.

Wire mesh separators, shown in the figure 33, consist of finely woven stainless steel or polymer pads that into a tightly packed cylinder with stainless steel wires. Their effectiveness is mostly contingent on the gas flow velocity. In too high velocities, the separated droplets re-enter the flow. Correspondingly in low velocities, the water vapour just flows through the mesh without the droplets colliding with the mesh and amalgamating. Also, wire mesh utilization is not advised in conditions with high fouling rates and humidity as they have a tendency to get clogged easily. Wire mesh separators are best suited for moderate gas flow applications that contain droplets in the range of 3–10 μm. Also, the advantage of this technology is its low pressure drop, which in range of >250 Pa. (Chandranegara 2016, 3–4.)

Fibre separators utilize pads made of thin fibres. These dozen centimeters thick pads are typically used in cylindrical form, as seen in the figure 33, but flat panel applications are also available. The fibres are mostly manufactured from metal, plastic, or cellulose. Fibre separators can capture liquid droplets that are 0.1 micrometers in length, or even less, that common in nearly invisible haze or smoke. Depending on the conditions it can generate substantial pressure drop, 500–5000 Pa, which makes it suitable for only very low moderate flow rate and humidity cases. Fibre separator efficiency improves as the time the gas spends in the separator is prolonged and the system temperature is increased. The efficiency decreases in conjunction with increase in droplet size and pressure. (Chandranegara 2016, 3–4.)

Vane droplet separators utilize corrugated parallel plates, showcased in the figure 33, to change the gas flow direction to cause liquid droplets to crash and accumulate the plate surface where they are drained either using gravitation or mechanical equipment. Vanes are manufactured from a variety of materials, like stainless steel, polypropylene, and fiberglass reinforced polymer. In high humidity conditions, vane separator tends to suffer from low efficiency as the droplets tend to flow through the system along with the gas. Also, the

efficiency drops as pressure increases or gas velocity decreases. Vanes are still a popular choice in industrial applications due to their versatility, simple maintenance, and ability to handle medium to high gas flow levels. They generate 100–900 Pa of pressure drop and perform best in the droplet range of 10–40 µm. (Chandranegara 2016, 3, 5–6.)

Cyclone separators utilize centrifugal force to merge smaller droplets into a larger film that does not easily get removed or re-enter the gas flow. Cyclones can be divided into two main categories, tangential and axial, which contain many different subcategories and layouts, some of which are shown in the figure 33. Main advantage in cyclone separators is their ability to handle very high gas flow capacities while maintaining high droplet removal efficiency, even at higher pressures. Rise in temperatures causes a decrease in removal efficiency, while lower gas velocities cause an increase. Cyclones are made for 7–10 µm diameter droplet separation, but in proper conditions, all droplets with a diameter above 10 µm can be feasibly separated. This has made it a viable option, even though they generate quite a lot of pressure drop, 2000–2400 Pa. (Chandranegara 2016, 3, 7–8.)

Figure 33. Droplet separator technologies. Left to right, on the upper row are pictures of a wire mesh separator (Alino 2022) and a cylindrical fibre separator (Ningbo T.C.I Company 2022a). General depictions of vane (Ningbo T.C.I Company 2022b) and cyclone separators (Ganga Reddy and Kuppuraj 2015) are seen on the lower row.

If the droplet separator malfunctions, or it has been designed poorly, it becomes incapable of handling the required gas flow or droplet size. The water vapour can then pass through to the fan and recovery boiler. This could affect the incineration process and its efficiency negatively. In cases like this, the damper can be utilized to guide the odorous gases to the smokestack and consequently outside.

4.2.2 Data sets

Like with the data sets examined in the flue gas system, the odorous gas treatment data sets were gathered from two different sources. Measurements done with physical instrumentation at the bioproduct mill were received from the same bioproduct mill contact person. The utilized measurements include:

- Odorous gas pressure after the fan [mbar]
- Odorous gas temperature before the droplet separator [°C]
- Total odorous gas flow rate after the heat exchanger [Nm^3/s]

The measurements span over a period of one year, from January 1 to January 1 of next year. And they were recorded 10 seconds apart from each other, similar to the flue gas fans' measurements.

The VSD signal data received from the ABB contact person included:

- Torque [% of nominal]
- Speed, without filter [rpm]

The signal data recorded on January 31, 2022– December 14, 2022, at the frequency of one second. Contact with the fan manufacturer yielded the same information for this studied fan as for the flue gas fans. The catalogue provided the fan curves utilized in the model-based operation point estimation.

4.2.3 Applicability of VSD-signal-based monitoring

This subchapter analyses the applicability of VSD monitoring in the studied odorous gas handling system. Like the subchapter 4.1.3, figures are used to visualize calculated estimates and measured values. The differences between the two are also presented. The reasons for the deviating values are considered, and a possible correction factor is calculated.

Estimation of the operating point is performed with the calculation formulas presented in chapter 2.3. As seen in the following figure 34, the model-based flow rate estimation values imitate the trends of measured flow rate data in an excellent manner, especially during the latter half. The estimated and measured trends differ throughout the maintenance breaks of June and October. According to the VSD signals, the fan generates a high flow rate during the June maintenance, but the measured data shows the flow rate to be close to zero. This was originally speculated to results from the measurement device being turned off, or the VSD providing unreliable signals, during maintenance. Communication with the bioproduct mill contact person revealed that this resulted from the damper being closed, in which case no gas flow reached the measuring device. The fan generated a high flow rate as a part of the maintenance procedures. Same during the October maintenance, the damper was shut, and the fan was run at minimal speeds.

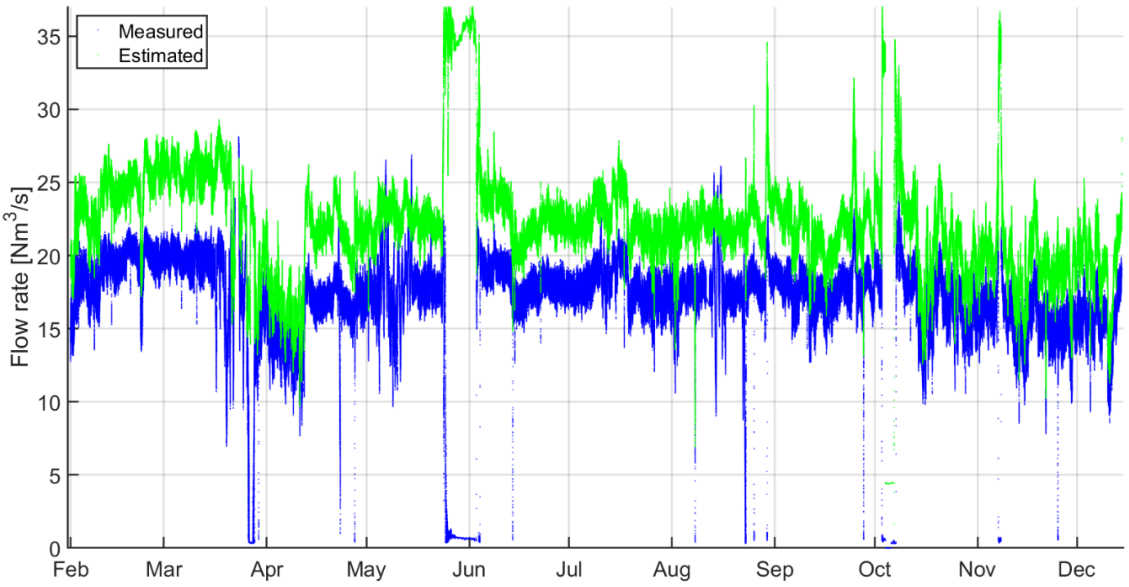

Figure 34. The measured and estimated flow rates.

But much like with the earlier studied flue gas fans, the estimates are not able to coincide with the measured values. But they mimic the trends well throughout the year. This information can be used in monitoring harmful occurrences and perform calculations. By utilizing the operation points and formula (10), the relative error between the measure and estimated values can be calculated. On average, the relative error through the studied period was 25%. This indicates that on average the estimated values were a quarter higher greater than the measured, which can be seen in the figure 35 below.

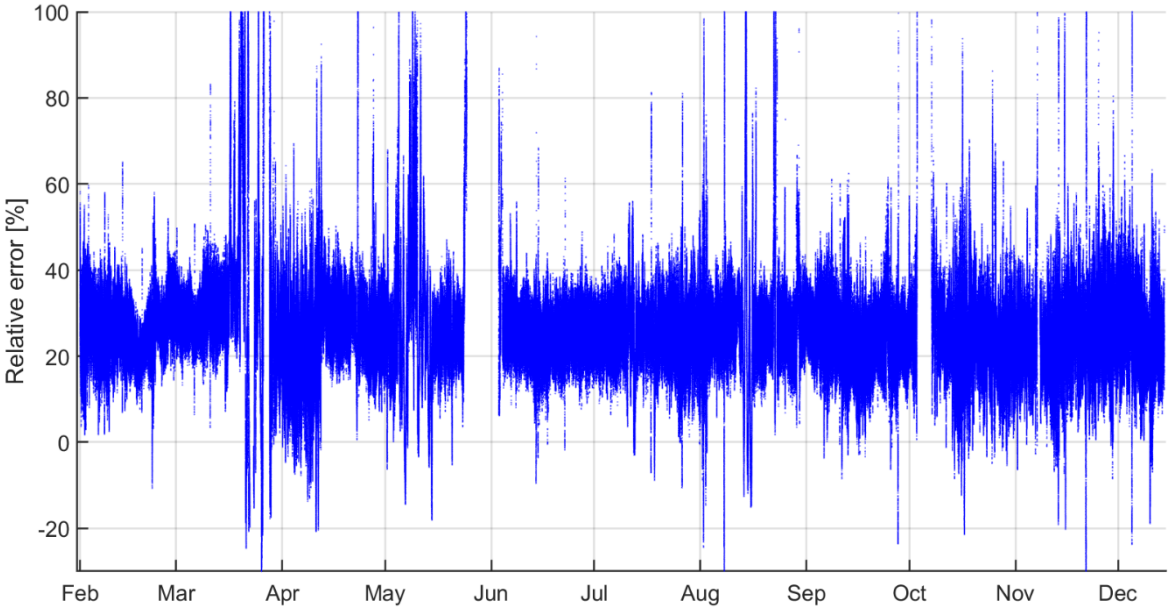

Figure 35. Relative error between the measured and estimated flow rates throughout the studied period.

It is important to note, that if the relative error was over 100%, like it was during the maintenance periods, those values were disregarded from the average relative error calculation to maintain the focus on periods where both methods were presumably in working order. Like seen in the figure 35, the relative error does explicably rise and fall additionally during other months when operation is assumed to be stable. This phenomenon is covered more in the following section. Again, the gas properties can generate relative error. The data utilized in the density calculation can be prone to making erroneous estimations, since the utilized pressure is collected after the fan, which generates a pressure difference, while the temperature measurement was done before the droplet separator.

Using the formula (12), a correction factor for density associated with the least relative error can be determined. After iteration, that correction factor turned out to be 1.131, that lowered the relative error to 5.2%, excluding the maintenance periods. This allows for easier visual inspection of the data, during the time periods when the relative error behaviour was deemed to be strange. Manual inspection of the studied data revealed six instances, during which the flow rate inexplicably either decreases or increases without the change being reflected in the model-based estimations. These instances are showcased in the following figure 36.

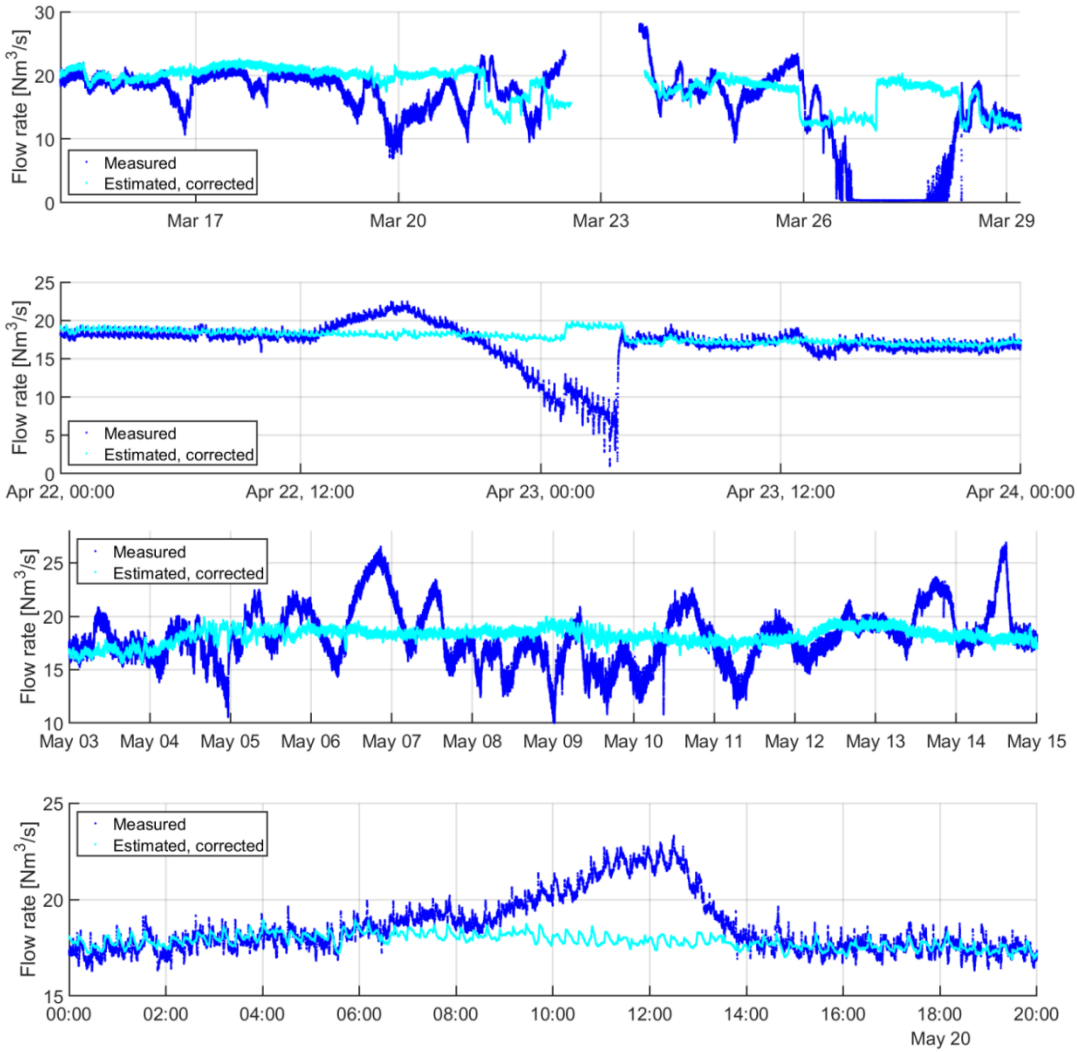

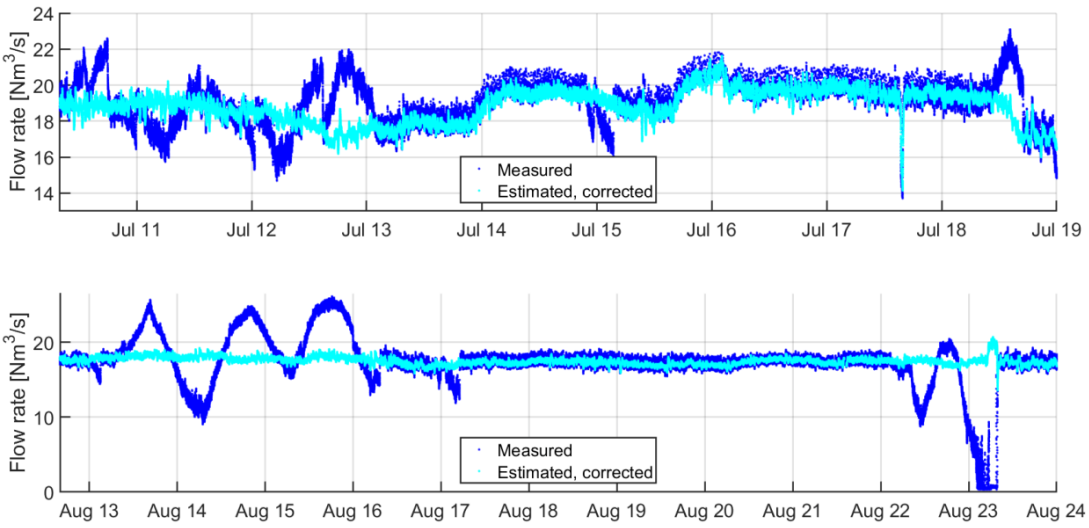

Figure 36. The sudden increases and decreases in the measured flow rates, which do not correlate with the estimated values.

The characteristics of these events is not the same in all instances. Like seen in the figure 36, sometimes the measured flow rate can change a lot, up to 50%, like in the 3rd and 6th instances. Other times the changes are more minor, in the range of 20–30%, but those changes are still very much noticeable, like in the 4th and 5th curves. Furthermore, the duration of these effects varies. Occasionally, the measured flow rate increases and decreases successively for several days, or even over a week. This can be seen in the 1st, 3rd, and 6th figures within the figure 36. While in some instances, the flow changes only once or twice before reverting to similar behaviour as the model-based estimation values, like in the 2nd and 4th figures. This seemingly random nature of the occurrences suggested that the events depicted either leaks or excess flow. Hence, contact was made with the bioproduct mill contact person once more to inform them about the findings. After some additional communication with personnel working closely with the process, they were able to clarify that these cases were not a cause for concern. They deduced that these differences were most likely caused by the complex condensate ducting contained by the system. Although no abnormal operation conditions were discovered, these instances proved model-based monitoring in conjunction with physical measurements to be the applicable in monitoring these types of phenomena flow in the system.

Additionally, operation point data can be used in calculating the specific energy consumption of the system with the formula (11). Showcasing these values visually is not deemed necessary since the figure 27, about the specific energy consumption of the flue gas fans, has already considered the effects of this calculation. In the studied odorous gas fan, the estimated values generate smaller specific energy consumption per cubic meter of gas than the measured values. Similar to the flue gas fans, this difference results from the estimated flow rate values being greater. The following table 4 summarizes the monitoring applicability of the studied bioproduct mill odorous gas handling fan data set.

Table 4. VSD monitoring applicability in odorous gas handling fans, in a bioproduct mill.

VSD monitoring applicability in: bioproduct mill odorous gas fans	
Phenomena monitoring via standalone calculations:	
Fan surge	
Fan or pump rotation direction	
Impeller contamination build-up	
Phenomena monitoring via operation point monitoring:	
Specific energy consumption	Calculation
Leakage or surplus flow	Redundancy
Fouling	Operation point examination

At first, the leaks or surplus flow were thought to occur in the studied odorous gas treatment fan system but contact with the industry contact person revealed that the phenomenon was caused by a condensate ducting within the system. Model-based operation point estimation can be conducted, as well as the calculation of specific energy consumption and detection of fouling from the operation points. While the VSD-signal-based monitoring did not locate failures in the studied system, model-based estimation of the operating point and its consequent utilization in monitoring has been recognized to be applicable.

4.3 Potential changes to enable testing the applicability of phenomena monitoring

This subchapter goes through the phenomena whose monitoring applicability could not be tested in the studied system. Reasons why these monitoring methods cannot be applied to the studied data sets are discussed, while potential changes to enable monitoring are considered. Only phenomenon not considered in the following sections is cavitation, which is not relevant in fan operations that handle gases.

Like touched on in the subchapter 2.1.1, fan surge monitoring can be enabled by calculating the root mean square value for the low-frequency variation of both rotational speed and torque estimates. In the paper by Tamminen et al. (2012, 3.), on the novel detection method for fan surge detection, the frequency band for the fluctuation in the measurement system was determined to be from 0 to 2 Hz. Like said in subchapter 4.1.2 and 4.2.2, the utilized VSD signals were recorded once per second. This would not be a sufficient frequency to utilize such monitoring with the utilized data sets. Still, this monitoring method could be applied in this type of a system, with higher VSD signal frequency availability. This could be done by implementing the calculation process directly in the VSD. Since VSDs can reach signal frequencies of 500 Hz, implementing the monitoring directly to the VSD could conducted (Tamminen et al. 2012, 4). Additionally, this can be a very user-friendly solution, since it could inform the user about its findings instantly and time that would be spent on data processing afterwards could be shortened.

Fan impeller rotation direction recognition is also conducted by calculating the low-frequency fluctuation. Like before, the data set signal frequency presents a problem since fluctuations related to this phenomenon are present in a 0–4 Hz band. Beside the frequency, the monitoring relies on a test period in which the fan has be operated in both rotation directions. Such a test was not performed during the studied period, but it could be done in the future during a maintenance break. The test should only be done once, which then serves as the reference values, thus implementing this could be conducted in the studied system. (Tamminen 2013, 62.)

Like the impeller rotational direction detection, the impeller contamination build-up relies on a test conducted during a controlled start-up. First, the rotational speed is increased with a constant torque reference. Those signals are then saved and used to calculate the angular acceleration from a selected rotational speed range. (Tamminen 2013, 58.) While the flue gas fans were off during maintenance, the start-ups were not conducted with constant torque values. However, these trial runs could be implemented during maintenance when regulating the recovery boiler combustion process with the fan operation is not required. The following table 5 compiles the discussed constraints set by data related to VSD-based monitoring. The methods that rely on the VSD signals, and the low-frequency fluctuation detected within them, do not require knowledge of the operation point to operate properly.

Table 5. Data set qualities required to facilitate VSD-based fan monitoring.

Aspect VSD monitoring requires to operate (**Yes**/No)		
Phenomena	Frequent VSD signals	Controlled start-up test
Surge detection	**Yes**	No
Rotational direction detection	**Yes**	**Yes**
Impeller contamination build-up detection	No	**Yes**

5. Conclusions

Monitoring and recognizing phenomena from fluid handling system operation is important in ensuring reliable performance of the system. Model-based monitoring, utilizing fan curves and VSD signals, was proven to be applicable in this type of systems and sites, according to the two studied case fan systems. In both cases, model-based operation point estimation provided values that corresponded with the trends of the measured values. With the relative error being 30–80% and 10–40% for flue gas system and odorous gas system, respectively, uncertainty was concluded present in the model-based estimations. But with a density correction, the relative errors could be dropped to significantly, from 58% to 6.4% in flue gas system, and from 25% to 5.2 % odorous gas system. Therefore, proving that the model-based estimates were able to mimic the trends of the occurred gas flow. The difference between the measured and estimated values could have been generated by uncertainty in the applied gas density values. Since the values were calculated with a simplified dry gas density formula, the values could be generating uncertainty in the calculations. Also, the utilized pressure and temperature values are prone to uncertainty, especially when the measurements take place further away or after the fan.

The operation point values were able to be used in calculating the specific energy consumption of the system and to also monitor leaks, surplus flow, and fouling. Monitoring the deleterious phenomena in the system can be conducted by comparing the estimates with other values. These other values can be obtained via installed physical instrumentation, or calculations that approximate the realized flow rate. In the flue gas fan case, the amount of consumed fuel could be used to derive the realized flue gas flow rate. If it is known that combusting a certain amount fuel generates a certain amount of flue gas, the generated flue gas flow rate can be calculated with the realized fuel consumption. In the industrial sector, the combustion processes are often very closely monitored, and thus, the fuel consumption value is often known. Even if the correlation between the realized fuel consumption and flue gas generation is not known, non-invasive measurement methods, such as doppler and transit time, could be utilized to conduct a short-term measurement to determine it. Both popular methods measure the passing flow with ultrasonic sensors that are attached to the outside of

a duct. Therefore, no interruptions to the operation are required. (Manufacturing.net 2012.) Despite the deviation in the values, this thesis concludes that the model-based estimation methods are applicable as monitoring tools in the future, especially in facilities with no physical instrumentation installed. While determining the realized flow rate without instrumentation can require a few extra steps, information on aspects that could have a correlation with the gas flow generations, like end-product generation or fuel consumption, in conjunction with short-term measurements, could be rather effortlessly used to generate a reliable foundation for future VSD model-based monitoring.

Applicability of monitoring other phenomena which requires more frequent VSD signals or controlled test scenarios, for instance during start-up, could not be tested with the received data sets. Therefore, the thesis focused, in subchapter 4.3, on outlining the aspects that could allow for the applicability testing. These methods could be most efficiently utilized by implementing them directly to the VSD to notify the user if the monitored limit values are exceeded during operation or start-up. By doing this, transferring the high-frequency VSD estimation data from the database to an external computer for the calculations would not be required. This could save time and processing power as handling the large files could take a lot of time. In future studies, analysing the applicability of VSD-based phenomena monitoring and recognition systems and sites like this would be facilitated by differing data sets. The calculations could initially be conducted with past data, after which the calculations could be applied directly to the VSD. Working in conjunction with the VSD manufacturer could provide this opportunity, which would allow to monitor the phenomena throughout a longer time span.

6. Summary

Human-caused climate change has generated global key climatic changes, which have resulted in several policies and studies on greenhouse gas emissions of the energy system, utilization of renewable energy sources and energy efficiency of different processes. Since fluid handling systems are a large electricity consumer in both the industrial and service sectors, they have developed to be a well-studied field. Their emissions are known to be closely knit with their energy consumption during use, which has been indicated to amount for around 90 percent of an electric motor's life cycle carbon emissions. (Zawya 2023.) Harmful events in fluid handling systems impact the system's energy efficiency, and potentially generates additional LCC which could be avoided. The thesis investigates the applicability of VSD-based estimation methods as monitoring tools. VSD monitoring can help to lower LCC and better the system's efficiency by detecting phenomena that can then be addressed before they damage the system or cause large losses.

VSDs can be used in estimating the system operation and recognizing different phenomena from the system. Model-based estimation utilizes the manufacturer-provided fluid handling device characteristics curves to model the application. Those values are then used together with the VSD signals to estimate the operation point. VSD signals, and the estimated rotational speed, torque, and shaft power values formed from them, can also be used in standalone methods, which can detect different phenomena, such as surge and impeller contamination build-up, from the system. These methods showcased in table 1 often rely on low-frequency fluctuations in the signals, or a controlled baseline test that the values gathered during use are compared with. Estimations conducted based on VSD signals are a viable alternative in systems where physical measurement instruments are prone to break, malfunction, or produce unreliable results. But still, the use of VSD-based monitoring does not mean that traditional measuring devices should not be used. Especially if metering infrastructure already exists, utilization of multiple monitoring methods in conjunction with each other can corroborate the achieved results, and verify their applicability, or non-applicability. (Tamminen et al. 2014, 1.) Since the estimations calculation utilizes different simplifications, they will always be prone to making erroneous estimations under certain

conditions. Potential factors influencing estimation accuracy showcased in this thesis included initial data suitability, i.e., curve accuracy and shape, changes in the gas flow conditions, such as temperature, pressure, density, and humidity variation, system wear over time, and accuracy of the VSD signals and numerical methods applied in converting visual data into numerical data sets.

Bioproduct mills are facilities that manufacture pulp from wood, while utilizing side-streams to generate various bioproducts that can replace fossil fuels and materials. For example, bark and sawdust can be utilized in energy production, and ash and other solids in fertilizers and earthwork materials. (Metsä Group 2022.) The thesis' focus was on kraft process mills, which are the most common chemical pulp production facilities globally (Pinheiro and Quina 2020). Typically, the kraft pulp process is divided into two parts, the fibre line and chemical recovery cycle. The fibre line includes the wood processing procedures, while the chemical recovery cycle covers the processes used to recover the cooking chemicals back for use. (Erikson and Hermansson 2010, 7.) Pulping is complex process with lots of demand for fluid handling systems. The table 2 compiled examples of typical fluid handling systems in different bioproduct mill unit processes. Common tasks for compressors included capturing pressurised steam, which can then be utilized in other unit processes. Fans are utilized in a variety of HVAC applications, but also in combustion, evaporator, and effluent treatment processes. Pumps are used in transferring materials between unit processes and cooling, for instance. (Piri 2017, 22, 25, 29.)

The applicability of the model-based methods and VSD-based phenomena monitoring was studied in two case systems. Real-life data received from a bioproduct mill contact person and information about the system components were showcased in their individual subchapters. The chapter 4 presented the findings of the applicability in the studied case systems. The following sections presents the case studies and summaries conclusions.

The first studied case was a flue gas treatment system that included four identical fans that aimed to be operated as similarly as possible. They are utilized in controlling the recovery boiler combustion process by generating negative pressure in the furnace. Therefore, they

are very vital in assuring optimal performance of the chemical recovery. The flue gas generated at the recovery boiler combustion process was divided into four ducts that each housed an ESP, which cleaned the incoming flue gas, a heat exchanger, which lowered the gas temperature, and the fan that directed the flue gas into a shared duct leading to the smokestack. The fans were controlled according to the recovery boiler conditions; hence they are not always operated at their best efficiency.

Studying the first case concluded the model-based monitoring to be applicable in this system category. The model-based operation point estimation generated values that matched with the trends in the measured values. Additionally, it was concluded that the estimations were not able to generate correct absolute values. Even though the gas flow density was calculated using the available temperature and pressure data, the estimated values were 30–80% larger than the measured ones. The nature of the difference between the values and the measured values suggested that it was the resulted of a density calculation. Thus, approaches to level out the difference between these values was discussed. Physical instrumentation or calculations that approximate the realized flow rate were identified as means to perform this operation. In this case, the amount of combusted black liquor could be used to derive the level of realized flow rate, if relation between the two is known. If the generated flue gas volume per a combusted fuel unit is known, the relation can be determined. If not, a short-term measurement of the gas flow could be compared with the fuel flow to find out this correlation. This type of testing could be conducted in future a study. Regardless of the characteristic uncertainty, the model-based estimation has value as a monitoring tool. The operation point estimations can be utilized in calculating the specific energy consumption of the system with the formula (11). Besides recognizing trends of the operation, the values can be utilized in recognition of different phenomena. The increased friction resistance resulting from fouling, and leakage, and surplus flow scenarios can be recognized from the estimations. The latter two phenomena recognition requires knowledge of the system and additional instrumentation at different part of the ductwork that the estimates can be compared with. In this system, no phenomena were observed that appeared to indicate of these problems. The maintenance schedule was well designed and strictly followed, which ensured reliable system operation.

The second chapter of the case study examined an odorous gas treatment system, which handled diluted non-condensable gases. The ductworks of the system included first a scrubber, from where the gas flows into a condenser, which cools the gas flow removing water vapour. From there the gas advances to a droplet separator, which removes the final excess particles and water vapour before the gases arrive to the examined fan. The fan directs the gases to the recovery boiler from incineration, or alternative directly outside if incineration is not possible.

Model-based estimation proved to be applicable in this case, and consequently in other similar systems as well. Furthermore, the operation point data can be used in calculating the specific energy consumption, like in the flue gas system. The trends of the estimated and measured operation points mimicked each other well, with a relative error of 10–40%. Additionally, unusual operation point behaviour was discovered in the odorous gas treatment system. The measured flow rates seemed to rise and fall unexpectedly, leading to thinking that the system was suffering from unwanted leaks or surplus flow, like shown in the figure 36. After further communication with personnel working closely with the process, it was found that these phenomena are not cause for concern. It was determined that these differences most likely resulted from complex condensate ducting contained by the system. Although no abnormal operating conditions were detected, these cases demonstrated model-based monitoring in combination with physical measurements to be applicable for monitoring these phenomena in these types of systems.

Testing the applicability of VSD-based phenomena monitoring was not successfully implementable to the received data sets. The monitoring methods examined in the subchapter 2.1.1 required additional aspects, such as more frequent VSD signals or controlled test scenarios, to operate. Hence, the thesis focused on outlining these requirements to allow for the applicability testing in future studies. They were investigated in the subchapter 4.3 and listed in the table 5. To expand the extent of this study in the future, communication with the case site management could make it possible to influence the operation and implement the desired testing protocols, for instance during maintenance breaks. If the prerequisite tests are conducted properly and monitoring is proved applicable, the monitoring calculation

processes could be implemented directly to the VSD. This could save time and processing power since transferring the high-frequency VSD estimation data from a database to an external computer for the calculations would not be required. Furthermore, the VSD could then notify the operators if the monitored limit values are exceeded during operation or start-up.

References

480/1996. Valtioneuvoston päätös ilmanlaadun ohjearvoista ja rikkilaskeuman tavoitearvosta (The Finnish Government's decision on the guideline values for air quality and the target value for sulphur deposition).

ABB. 2011. Technical Guide No. 1, Direct Torque Control. [e-document]. [Accessed: 26.10.2022]. Available: https://eee.sairam.edu.in/wp-content/uploads/sites/6/2019/07/Modern_power_electronics_and_AC_drives.pdf

ABB. 2022. What is a variable speed drive? [website]. [Accessed: 26.10.2022]. Available: https://new.abb.com/drives/what-is-a-variable-speed-drive

ABB. 2023. Driving down industrial energy consumption. [website]. [Accessed: 8.4.2022]. Available: https://new.abb.com/drives/highlights-and-references/driving-down-industrial-energy-consumption

Aerotech Fans. 2019. Centrifugal Fans. [website]. [Accessed: 23.7.2022]. Available: https://www.aerotechfans.com.au/products/custom-built-fans/centrifugal-fans/

Aerovent. 2022. Tubeaxial Commercial Fan, Direct Drive. [website]. [Accessed: 23.7.2022]. Available: https://www.aerovent.com/products/axial-fans/bsta-tubeaxial-fan/

Aerovent. 2018. Fan engineering – Information and Recommendations for the Engineer – Fan Performance Characteristics of Centrifugal Fans. [e-document]. [Accessed: 21.7.2022]. Available: https://irp.cdn-website.com/92cd82c9/files/uploaded/Fan-Performance-Characteristics-of-Centrifugal-Fans-FE-2400.pdf

Ahonen Tero, Pöyhönen Santeri, and Ahola Jero. 2017. Remote Monitoring of Fluid Handling Systems with Variable-Speed Drive. 19th European Conference on Power Electronics and Applications. 400 pages. ISBN: 9789075815276

Air Control Industries. 2015. Guide to Industrial Fan Selection. [website]. [Accessed: 1.7.2022]. Available: https://www.aircontrolindustries.com/technical-us/industrial-fan-selection-guide/

Alfa Laval. 2022. GPHE selection guide. [website]. [Accessed: 12.8.2022]. Available: https://www.alfalaval.com/microsites/gphe/tools/selectionguide/

Alino. 2022. Wire Mesh Droplet Separators (Demisters). [website]. [Accessed: 15.12.2022]. Available: http://www.alino-is.de/wire-mesh-droplet-separators.html

Almeida Anibal, Ferreira Fernando, and Fong João. 2023. Perspectives on Electric Motor Market Transformation for a Net Zero Carbon Economy. Basel: MDPI. 16 pages.

Almeida Anibal, Fonseca Paula, Falkner Hugh and Bertoldi Paolo. 2003. Market transformation of energy efficient motor technologies in the EU. Energy Policy; vol. 31. Pages: 563–575.

Awati Rahul. 2022. Definition – Extrapolation and Interpolation. [website]. [Accessed: 20.3.2023]. Available: https://www.techtarget.com/whatis/definition/extrapolation-and-interpolation

Blauberg Motoren. 2022. AC centrifugal fans (forward curved). [website]. [Accessed: 1.7.2022]. Available: https://blauberg-motoren.com/centrifugal-fans-forward-ac/isolation-class/2873

Bordado João and Gomes João. 2002. Atmospheric emissions of Kraft pulp mills. [e-document]. [Accessed: 21.10.2022]. Available: https://www.researchgate.net/publication/223221247_Atmospheric_emissions_of_Kraft_pulp_mills

Britannica. 2023. Cavitation – Physics. [website]. [Accessed: 3.3.2023]. Available: https://www.britannica.com/science/cavitation

Brogan R.J. 2022. Shell and Tube Heat Exchangers. [website]. [Accessed: 11.8.2022]. Available: https://www.thermopedia.com/content/1121/

Bureau of Energy Efficiency – A statutory body of Ministry of Power, Government of India (BEE). 2015. Energy Efficiency in Electrical Utilities. 301 pages.

Carotek. 2022. Guide: How to Select and Size a Heat Exchanger. [website]. [Accessed: 3.8.2022]. Available: https://www.carotek.com/heat-exchanger-selection-guide

Chandranegara Anang Satria. 2016. Improving Mist Eliminator Performance in Gas-Liquid Separators. [e-document]. [Accessed: 14.12.2022]. Available: https://www.researchgate.net/publication/305209725_Review_Improving_Mist_Eliminator_Performance_in_Gas-Liquid_Separators

Cibse Journal. 2011. Module 35: Fans for ducted ventilation systems. [website]. [Accessed: 24.7.2022]. Available: https://www.cibsejournal.com/cpd/modules/2011-12/

CNBM International. 2022. Introduction to Liquor of Paper Pulping. [website]. [Accessed: 6.2.2023]. Available: https://www.paperpulpingmachine.com/introduction-to-liquor-of-paper-pulping/

Cooper C. and Alley F. 2011. Air pollution control – A design approach. Fourth edition. Long Grove: Waveland Press. 839 pages. ISBN: 1-57766-678-X

Czernia Dominik and Szyk Bogna. 2022. Air Density Calculator. [website]. [Accessed: 24.5.2022]. Available: https://www.omnicalculator.com/physics/air-density

Dongguan Wanhang Electronic Technology Co. 2022. Type And Classification of Fans. [website]. [Accessed: 1.7.2022]. Available: https://www.wheecoolingfan.com/type-and-classification-of-fans.html

European Commission. 2011. Frequently Asked Questions on the Industrial Fans Regulation 2009/125/EC. [e-document]. [Accessed: 30.6.2022]. Available: https://ec.europa.eu/energy/sites/ener/files/documents/faq-ecodesign-requirements_fans.pdf

European Commission. 2021. 2030 climate & energy framework. [website]. [Accessed: 4.4.2023]. Available: https://climate.ec.europa.eu/eu-action/climate-strategies-targets/2030-climate-energy-framework_en

Erikson Lina and Hermansson Simon. 2010. Pinch analysis of Billerud Karlsborg, a partly integrated pulp and paper mill. Thesis for the degree of Master of Science (Technology). Chalmers University of Technology, Department of Sustainable Energy Systems. 52 pages.

Finnish meteorological institute. 2020. Ilmanlaatumittausten laatujärjestelmien kuvaus (Description of quality systems for air quality measurements). [e-document]. [Accessed: 9.3.2023]. Available: https://expo.fmi.fi/aqes/public/Ilmatieteen_laitoksen_ilmanlaatumittausten_laatujarjestelmien_kuvaus.pdf

Framework convention on Climate Change (FCCC 2021). 2021. Nationally determined contributions under the Paris Agreement. [Accessed: 4.4.2023]. Available: https://unfccc.int/sites/default/files/resource/cma2021_08_adv_1.pdf

Funkhouser Jack (Funkhouser 2021a). 2021. Know the Difference Between Fans and Blowers. [blog]. [Accessed: 30.6.2022]. Available: https://sofasco.com/blogs/article/know-the-difference-between-fans-and-blowers

Funkhouser Jack (Funkhouser 2021b). 2021. Tangential Fans: Introduction and Working Principle Discussed. [blog]. [Accessed: 1.7.2022]. Available: https://sofasco.com/blogs/article/tangential-fans-introduction-and-working-principle-discussed

Ganga Reddy C. and Kuppuraj Umesh. 2015. Numerical Study of Flue Gas Flow in A Multi Cyclone Separator. [e-document]. [Accessed: 15.12.2022]. Available: https://www.ijera.com/papers/Vol5_issue1/Part%20-%202/H501024853.pdf

GlobalSpec. 2023. Scrubbers Information. [website]. [Accessed: 19.3.2023]. Available: https://www.globalspec.com/learnmore/manufacturing_process_equipment/air_quality/scrubbers

Gooch Thermal. 2022. Spirals – Design Features & Benefits. [website]. [Accessed: 15.8.2022]. Available: https://www.goochthermal.com/spiral-heat-exchanger/design

Gregory, E.J. 2022. Plate fin heat exchangers. [website]. [Accessed: 17.8.2022]. Available: https://www.thermopedia.com/content/1036/

Grundfos. 2023. Lifecycle cost equation for pump systems. [website]. [Accessed: 6.4.2023]. Available: https://www.grundfos.com/solutions/learn/research-and-insights/lifecycle-cost-equation-for-pump-systems

Hewitt Geoffrey, Shires George, and Bott Theodore. 1994. Process Heat Transfer. CRC Press. 1017 pages. ISBN: 0-8493-9918-1

Hiltunen Juho. 2020. Performance evaluation for flue gas cooler in recovery boiler. Master's thesis. Lappeenranta–Lahti University of Technology LUT, Degree Program in Energy Technology, School of Energy Systems. 108 pages.

Hirvonen Sami. 2020. Sähkösuodattimen käyttö ja kunnossapito (The operation and maintenance of an electrostatic precipitator). Bachelor of Engineering. Metropolia University of Applied Sciences. Degree Program in Energy and Environmental Technology. 72 pages.

Industrial Quick Search (Industrial Quick Search 2022a). 2022. Shell and Tube Heat Exchangers. [website]. [Accessed: 11.8.2022]. Available: https://www.iqsdirectory.com/articles/heat-exchanger/shell-and-tube-heat-exchangers.html

Industrial Quick Search (Industrial Quick Search 2022b). 2022. Plate Heat Exchanger. [website]. [Accessed: 11.8.2022]. Available: https://www.iqsdirectory.com/articles/heat-exchanger/plate-heat-exchangers.html

Intergovernmental Panel on Climate Change (IPCC). 2023. AR6 Synthesis Report – Climate Change 2023. [e-document]. [Accessed: 4.4.2023]. Available: https://report.ipcc.ch/ar6syr/pdf/IPCC_AR6_SYR_SPM.pdf

International Electrotechnical Commission (IEC). 2007. Rotating Electrical Machines, Part 2, Section 1: Standard Methods for Determining Losses and Efficiency from Tests (Excluding Machines for Traction Vehicles).

International Energy Agency (IEA). 2022. World electricity final consumption by sector, 1974–2019. [website]. [Accessed: 5.4.2023]. Available: https://www.iea.org/data-and-statistics/charts/world-electricity-final-consumption-by-sector-1974-2019

International Energy Agency (IEA). 2017. World Energy Outlook 2017. [e-document]. [Accessed: 5.4.2023]. Available: https://iea.blob.core.windows.net/assets/4a50d774-5e8c-457e-bcc9-513357f9b2fb/World_Energy_Outlook_2017.pdf

International Energy Agency (IEA). 2016. World Energy Outlook 2016. [e-document]. [Accessed: 27.4.2023]. Available: https://iea.blob.core.windows.net/assets/680c05c8-1d6e-42ae-b953-68e0420d46d5/WEO2016.pdf

International Organization for Standardization (ISO). 2007. ISO 13348:2007, Industrial fans – Tolerances, methods of conversion and technical data presentation.

Kakaç Sadik, Liu Hontang, and Pramuanjaroenkij Anchasa. 2012. Heat Exchangers: Selection, Rating, and Thermal Design. Third edition. CRC Press. 605 pages. ISBN: 978-1-4398-4991-0

Korhonen Ilkka and Ahola Jero. 2017. Microwave attenuation in kraft recovery boiler. The Institution of Engineering and Technology Journal. Pages: 241–245.

Kuparinen Katja. 2019. Transforming the chemical pulp industry – from an emitter to a source of negative CO_2 emissions. Thesis for the degree of Doctor of Science (Technology). Lappeenranta–Lahti University of Technology LUT, Department of Electrical Engineering, LUT School of Technology. 177 pages. ISBN: 978-952-335-423-4

Kurganov Vladimir and Ibragimov Marat. 2011. Hydraulic Resistance. [website]. [Accessed: 31.3.2023]. Available: https://www.thermopedia.com/content/857/

Lappeenranta–Lahti University of Technology LUT (LUT University). 2022. Fan curves as a third-degree polynomial model. [e-document]. [Accessed: 20.5.2022].

Lappeenranta–Lahti University of Technology LUT (LUT University). 2020. Air Pollution Control – Control of particulates. [e-document]. [Accessed: 27.7.2022].

Lawrence Berkeley National Laboratory (LBNL). 2003. Improving Fan System Performance – a sourcebook for industry. 92 pages. DOE/GO-102003-1294.

Lendenmann Heinz, Moghaddam Heinz, Tammi Ari, and Thand Lars-Erik. 2011. ABB review 1|11 – Motoring ahead. [e-document]. [Accessed: 14.3.2023]. Available: https://lead-central.com/AssetManager/02427e68-6f15-4f3a-9749-

d37abf613741/Documents/APW2012/Low%20Voltage%20Drives%20Motors/ABB-136_WPO_Motoring%20ahead.pdf

Lipponen Torsti. 2016. Sulfaattisellutehtaan hajukaasujen keräily ja käsittely (Collection and handling of kraft pulp mill's odorous gases). Master's thesis. Lappeenranta–Lahti University of Technology LUT, Degree Program in Energy Technology, School of Energy Systems. 84 pages.

LTG. 2022. Functionality of tangential fans/application solutions. [website]. [Accessed: 23.7.2022]. Available: https://www.ltg.de/us/products-and-services/ltg-process-air-technology/fans/tangential-fans/functionality-of-tangential-fans/

Manufacturing.net. 2012. Outside Pipe Flow Measurement Technologies. [website]. [Accessed: 11.4.2022]. Available: https://www.manufacturing.net/home/article/13216898/outside-pipe-flow-measurement-technologies

Metsä Group. 2023. Kemin biotuotetehdasprojekti (Kemi bioproduct mill project). [website]. [Accessed: 8.4.2023]. Available: https://www.metsagroup.com/fi/metsafibre/metsafibre/sellun-tuotanto/kemin-biotuotetehdas/

Metsä Group. 2022. Ainutlaatuinen biotuotetehdaskonseptimme (Our unique bioproduct factory concept). [website]. [Accessed: 19.10.2022]. Available: https://www.metsagroup.com/fi/metsafibre/metsafibre/biotuotetehdaskonsepti/

Miljkovic Nenad, Enright Ryan, Nam Youngsuk, Lopez Ken, Dou Nicholas, Sack Jean, and Wang Evelyn. 2013. Jumping-Droplet-Enhanced Condensation on Scalable

Superhydrophobic Nanostructured Surfaces. [e-document]. [Accessed: 15.3.2023]. Available: https://www.researchgate.net/publication/233796977_Jumping-Droplet-Enhanced_Condensation_on_Scalable_Superhydrophobic_Nanostructured_Surfaces

Ministry of Environment. 2021. Suomen kansallinen ilmasto-politiikka (Finland's national climate policy). [website]. [Accessed: 4.4.2023]. Available: https://ym.fi/suomen-kansallinen-ilmastopolitiikka

Mitchell Mark, Muftakhidinov Baurzhan and Winchen Tobias. 2022. Engauge Digitizer Software. [website]. [Accessed: 11.5.2022]. Available: http://markummitchell.github.io/engauge-digitizer

Neundorfer. 2016. Lesson 1 – Electrostatic Precipitator Operation. [e-document]. [Accessed: 27.10.2022]. Available: https://www.neundorfer.com/wp-content/uploads/2016/05/ESP-KnowledgeBase-01-Operation.pdf

Ningbo T.C.I Company (Ningbo T.C.I Company. 2022a). 2022. Fiber bed demister. [website]. [Accessed: 15.12.2022]. Available: https://www.mist-eliminator-demister.com/mist-eliminator-demister/goods-881--Fiber+mist+eliminator+remover-Fiber+bed+demister.html

Ningbo T.C.I Company (Ningbo T.C.I Company. 2022b). 2022. Chevron Vane type mist eliminator. [website]. [Accessed: 15.12.2022]. Available: https://www.mist-eliminator-demister.com/mist-eliminator-demister/goods-882--Knitted+Wire+mesh+Mist+Eliminator-Vane+type+mist+eliminator-Chevron+Vane+type+mist+eliminator.html

Odyssee-Mure. 2023. Q&A – Result – Selected tag(s): Specific consumption. [website]. [Accessed: 28.3.2023]. Available: https://www.odyssee-mure.eu/faq/result/43/

Ohlström Mikael, Tsupari Eemeli, Lehtilä Antti and Raunemaa Taisto. 2005. Pienhiukkaspäästöt ja niiden vähentämismahdollisuudet Suomessa – Kasvihuonekaasupäästöjen rajoittamisen vaikutukset (Fine particle emissions and their reduction potentials in Finland – The effects of greenhouse gas emission reduction). Espoo: VTT (Technical Research Centre of Finland). 91 pages.

Online Math Learning. 2005. Relative and Percent Error Formula. [website]. [Accessed: 27.3.2023]. Available: https://www.onlinemathlearning.com/relative-error-formula.html

Parker Ken. 2003. Electrical Operation of Electrostatic Precipitators. London. The Institution of Engineering and Technology. 284 pages. ISBN: 978-0852961377

Philippine Parkerizing, Inc. 2022. Plate Coil Heat Exchangers. [website]. [Accessed: 17.8.2022]. Available: https://philparkerizing.com/products/powder-coating-industrial-equipment/plate-coil-heat-exchanger/

Pinheiro Carolina and Quina Margarida. 2020. Kraft Pulp Mill Process. [website]. [Accessed: 18.10.2022]. Available: https://encyclopedia.pub/entry/602

Process Barron. 2016. Flow Control Devices for Mechanical Draft Fans. [website]. [Accessed: 8.4.202]. Available: https://processbarron.com/learning_center/flow-control-devices-mechanical-draft-fans/

PTS München. 2007. Revision of best available technique reference document for the pulp & paper industry. München: Federal Environmental Agency Germany (UBA Germany), Dessau TU Darmstadt. 56 pages.

Pulp and Paper Research Institute of Canada. 1999. Energy Cost Reduction in the Pulp and Paper Industry – A Monograph. Quebec. 234 pages.

Pöyhönen Santeri, Ahola Jero, Niemelä Markku, Hammo Simo, and Punnonen Pekka. 2021. Variable-speed-drive-based method for the cost optimization of air filter replacement timing. Lappeenranta. 10 pages.

Radgen Peter and Oberschmidt Julia. 2008. EuP Lot 11: Fans for ventilation in non-residential buildings. Fraunhofer Institute Systems and Innovation Research, Karlsruhe, Germany. [e-document]. [Accessed: 23.7.2022]. Available: https://www.eup-network.de/fileadmin/user_upload/Produktgruppen/Lots/Final_Documents/Lot11_Fans_FinalReport.pdf

Rao Prakash, Sheaffer Paul, Chen Yuting, Goldberg Miriam, Jones Benjamin, Crop Jeff, and Hester Jordan. 2021. U.S. Industrial and Commercial Motor System Market Assessment Report – Volume 1: Characteristics of the Installed Base. Berkeley. 130 pages.

Robinson Keith. 2018. The System Curve, the Fan Curve, and the Operating Point. [e-document]. [Accessed: 21.3.2023]. Available: https://www.aiha-rms.org/assets/2018/2018_FTC/2018_Presentations/System%20Curve%20Fan%20Curve%20Operating%20Point%20BW.pdf

Sabouri Shirazi Amir, Jafari Nasr Mohammed, and Ghodrat Maryam. 2020. Effects of Temperature Differences in Optimization of Spiral Plate Heat Exchangers. [website]. [Accessed: 17.8.2022]. Available: https://link.springer.com/article/10.1007/s41660-020-00128-5

Saldanha Aaron. 2020. Specifying High-Temperature Industrial Fans. [website]. [Accessed: 15.11.2022]. Available: https://www.amca.org/educate/articles-and-technical-papers/amca-inmotion-articles/specifying-high-temperature-industrial-fans.html

Salmenoja Keijo. 2019. Development of Kraft Recovery Boilers –What have been the Main Development Steps? [e-document]. [Accessed: 11.5.2022]. Available: https://www.tappi.org/content/Events/19PEERS/19PEE59.pdf

Shah Ramesh. 1998. Heat Exchangers. In: Handbook of Heat Transfer. New York: McGraw Hill. Chapter 17.

Shah Ramesh and Sekulić Dušan. 2003. Fundamentals of Heat Exchanger Design. New Jersey: John Wiley & Sons Inc. 941 pages. ISBN: 0-471-32171-0

Solarbiox. 2022. Savukaasujen puhdistus (Flue gas cleaning). [website]. [Accessed: 6.11.2022]. Available: https://www.solarbiox.fi/tuotteet/savukaasujen-puhdistus

Springer. 2010. VDI Heat Atlas. Second English edition. Berlin: Springer-Verlag Berlin Heidelberg. 1585 pages. ISBN: 978-3-540-77876-9

Stora Enso. 2023. Enocellin tehdas (Enocell Factory). [website]. [Accessed: 21.2.2023]. Available: https://www.storaenso.com/fi-fi/about-stora-enso/stora-enso-locations/enocell-mill

Suhr Michael, Klein Gabriele, Kourti Ioanna, Rodrigo Gonzalo Miguel, Giner Santonja Germán, Roudier Serge, and Delgado Sanch Luis. 2015. Best Available Techniques (BAT) – Reference Document for the Production of Pulp, Paper and Board. Luxembourg: European Commission. 901 pages. ISBN: 978-92-79-48167-3

Tamminen Jussi. 2013. Variable speed drive in fan system monitoring. Thesis for the degree of Doctor of Science (Technology). Lappeenranta-Lahti University of Technology LUT, Department of Electrical Engineering, LUT School of Technology. 81 pages. ISBN: 978-952-265-532-5

Tamminen Jussi, Viholainen Juha, Ahonen Tero, Ahola Jero, Hammo Simo, and Vakkilainen Esa. 2014. Comparison of Model-Based Flow Rate Estimation Methods in Frequency-Converter-Driven Pumps and Fans. Springer Energy Efficiency Journal. 16 pages.

Tamminen Jussi, Ahonen Tero, Ahola Jero, Niemelä Markku, Tahvanainen Arto, and Potinkara Ari. 2013. Detection of Mass Increase in a Fan Impeller with a Frequency Converter. IEEE Transactions on Industrial Electronics, vol. 60 no. 9. Pages: 3968–3975

Tamminen Jussi, Ahonen Tero, Ahola Jero, Jaatinen Ahti and Röyttä Pekka. 2012. Sensorless Method for Detecting Surge in Variable-Speed-Driven Fan Systems. 9th International Conference on Condition Monitoring and Machinery Failure Prevention Technologies (CM & MFPT). 10 pages.

Tolvanen Tarja. 2022. Soodakattilan liuotinhönkäjärjestelmän mittaukset, säädöt ja toiminnan tarkastelu (Measurements and controls of the dissolving tank vent system of the recovery boiler). Master's thesis. Lappeenranta–Lahti University of Technology LUT, Degree Program in Energy Technology, School of Energy Systems. 67 pages.

Trocel David. 2021 Vibration Analysis of Centrifugal Fans. [website]. [Accessed: 16.12.2022]. Available: https://power-mi.com/content/vibration-analysis-centrifugal-fans

Tu Shan-Tung and Zhou Guo-Yan. 2015. Compact Heat Exchangers in Clean Energy Systems. [e-document]. [Accessed: 17.8.2022]. Available: https://www.researchgate.net/publication/283325770_Compact_Heat_Exchangers_in_Clean_Energy_Systems_in_the_Handbook_of_Clean_Energy_Systems_in_2015_by_John_Wiley_Sons_Ltd_DOI_10100297811189919 78hces119

Twin City Fan. 2020. Heavy duty centrifugal fans. [website]. [Accessed: 5.7.2022]. Available: https://tcf.eu/products/heavy-duty-centrifugal-fans/

United Nations. 2022. Net-zero-coalition. [website]. [Accessed: 5.4.2023]. Available: https://www.un.org/en/climatechange/net-zero-coalition

United Nations. 2015. Paris Agreement. [e-document]. [Accessed: 4.4.2023]. Available: https://unfccc.int/files/essential_background/convention/application/pdf/english_paris_agreement.pdf

United States Environmental Protection Agency (EPA 2003a). 2003. Air Pollution Control Technology Fact Sheet: Spray-Chamber/Spray-Tower Wet Scrubber. [website]. [Accessed: 19.3.2023]. Available: https://www.epa.gov/catc/clean-air-technology-center-products

United States Environmental Protection Agency (EPA 2003b). 2003. Air Pollution Control Technology Fact Sheet: Venturi Scrubber. [website]. [Accessed: 19.3.2023]. Available: https://www.epa.gov/catc/clean-air-technology-center-products

United States Environmental Protection Agency (EPA 2003c). 2003. Air Pollution Control Technology Fact Sheet: Orifice Scrubber. [website]. [Accessed: 19.3.2023]. Available: https://www.epa.gov/catc/clean-air-technology-center-products

United States Environmental Protection Agency (EPA 2003d). 2003. Air Pollution Control Technology Fact Sheet: Impingement-Plate/Tray-Tower Scrubber. [website]. [Accessed: 19.3.2023]. Available: https://www.epa.gov/catc/clean-air-technology-center-products

University of Georgia. 2020. Poultry Housing Tips – High Humidity Improves Fan Performance. [e-document]. [Accessed: 29.1.2023]. Available: https://www.poultryventilation.com/wp-content/uploads/vol32n8.pdf

University of Georgia. 2017. Land Application of Pulp Mill Lime Mud. [website]. [Accessed: 28.4.2023]. Available: https://extension.uga.edu/publications/detail.html?number=B1249&title=land-application-of-pulp-mill-lime-mud

Vahterus. 2022. Cleaning Methods for Vahterus Plate & Shell Heat Exchangers. [website]. [Accessed: 25.11.2022]. Available: https://vahterus.com/company/vahterus-service/cleaning-methods/

Vakkilainen Esa. 2005. Kraft recovery boilers – Principles and practice. Helsinki. Suomen Soodakattilayhdistys ry (Recovery Boiler Association of Finland). ISBN: 952-91-8603-7

Van Holsteijn en Kemna B.V. 2015. Ecodesign Fan Review – Review study of Commission Regulation (EU) No 327/2011 – Final report. [e-document]. [Accessed: 29.6.2022]. Available:https://www.fanreview.eu/downloads/FINAL%20REPORT%20FAN%20REVIEW%20-%2016%20Mar%202015.pdf

Venti Oelde (Venti Oelde 2023a). 2023. Impeller repairs. [website]. [Accessed: 16.2.2023]. Available: https://www.venti-oelde.de/produkte/reparaturen-laufraeder

Venti Oelde (Venti Oelde 2023b). 2023. Wear protection for centrifugal fans. [e-document]. [Accessed: 16.2.2023]. Available: https://www.venti-oelde.com/fileadmin/_sbdownloader/Verschleissschutz-18-en_01.pdf

Vidal Gladys, González Yenifer, Piña Benjamín, Jarpa Mayra, and Gómez Gloria. 2021. Minimization of Environmental Impact of Kraft Pulp Mill Effluents Current Practices and Future Perspectives towards Sustainability. [e-document]. [Accessed: 14.3.2023]. Available: https://digital.csic.es/bitstream/10261/251483/1/sustainability-13-09288.pdf

Walker Graham. 1982. Industrial heat exchangers: A basic guide. Hemisphere Publishing Corporation. 408 pages. ISBN: 0-89116-259-3

Wärtsilä. 2023. Saturation temperature. [website]. [Accessed: 16.3.2023]. Available: https://www.wartsila.com/encyclopedia/term/saturation-temperature

Zawya. 2023. INTERVIEW: ‘Energy efficiency is the 'first fuel' for a decarbonised future’ – ABB official. [interview]. [Accessed: 14.3.2023]. Available: https://www.zawya.com/en/projects/industry/interview-energy-efficiency-is-the-first-fuel-for-a-decarbonised-future-abb-official-bbvwbec9

Zhao Yajing. 2018. Dropwise Condensation of Water and Low Surface Tension Fluids on Structured Surfaces. [e-document]. [Accessed: 15.3.2023]. Available: https://dspace.mit.edu/bitstream/handle/1721.1/118679/1056711228-MIT.pdf?sequence=1